

DOCKET NO. **SA- 516**

EXHIBIT NO. **9B**

**NATIONAL TRANSPORTATION SAFETY BOARD
WASHINGTON, D.C.**

Contracted Laboratory Documentation

9B -339 pages

CONTRACTED LABORATORY DOCUMENTATION INDEX

DCA-96-MA-070

A. <u>Switch Analysis</u> WL/MLS 97-074	1
B. <u>Scavenge Pump Relay</u> WL/MLS 97-078	33
C. <u>Scavenge Pump Relay and Reserve Transfer Valve Circuit Breakers</u> WL/MLS 97-086	51
D. <u>Analysis of a Submitted Wire</u> WL/MLS 97-091	72
E. <u>Electrostatic Charge Generation from Turbine Fuels</u> WL/MLS 97-097	81
F. <u>Analysis of Hot Stamped Wiring</u> WL/MSL 97-101	167
G. <u>747 Fuel Probe Evaluation</u> WL/MLS 97-102	183
H. <u>Electrostatic Charging of Fuel System Components</u>	249

ERRATA NOTICE: Airplane N93 105 (serial number 19671) was a B-747 airplane that had been retired from service by TWA, prior to the accident involving N93119. The TWA fleet identification for N93 105 was “airplane number 17105.” A mistake in the record of a Systems Group activity wrongly identified the N93 105 airplane as N17105. This mistaken identification was used by subsequent activities, such as at Wright Laboratory and is referenced in their reports.

TWA 800 Switch Analysis
(Failure Analysis)

1 October 1997

Evaluation Report
(4349LABR/NTSB)

Report No. WL/MLS 97-074

AUTHOR

Edward L. White
Materials Integrity Branch (WL/MLSA)
2179 12th Street Room 56
Wright-Patterson Air Force Base, Ohio 45433-7718

REQUESTER

Robert Swaim
National Transportation Safety Board
4900 L'Enfant Plaza, East, SW
Washington DC 20594-5000

DISTRIBUTION STATEMENT F: Further dissemination only as directed by the National Transportation Safety Board/NTSB; 1 October 1997 or DoD higher authority.

000002

ACKNOWLEDGEMENTS

As is usual for this type of investigation, the efforts of others are critical to its success. The author would like to thank the following individuals from The University of Dayton Research Institute: Messrs . Dale Hart for his SEM analysis, Richard Reibel and Tom Dusz for their advice, analysis, and photographic expertise. The author would also like to thank Messrs . Russell Henderson and J. Edward Porter, Universal Technologies Corporation for their expert advice and X-ray analysis. The author would also like to thank Ms. Marianne Ramsey for expert manuscript preparation and formatting.

TABLE OF CONTENTS

	Page
LIST OF FIGURES	iv
LIST OF TABLES	v
PURPOSE	1
BACKGROUND . .	1
FACTUAL DATA .	1
CONCLUSION(S) .	5
RECOMMENDATION (S)	5

LIST OF FIGURES

Figure		Page
1	Side 1 of the three switches received for analysis.	8
2	Side 2 of the three switches received for analysis .	8
3	Face side of flight engineer's fuel control panel as received.	3
4	Back side of flight engineer's fuel control panel as received.	3
5	Left jettison switch screw terminals exhibiting corrosion from salt water exposure. Note the exposed copper from the solder lug (arrow) .	10
6	The environmental seal of the left jettison switch exhibiting corrosion and salt water-like deposits.	10
7	Gouge found on the left side of the scavenge pump switch knob 15 degrees forward of the knob center line.	11
8	Close-up of the gouge. Note the metal displacement used to determine the gouge direction.	11
9	SEM view of the gouge found on the scavenge pump switch knob (arrow) .	12
10	Overall view of scavenge pump switch knob showing the impact gouge (white arrow) , the knob center line, the direction of the impact, and the displacement of the knob in the cam groove.	13
11	The areas (1, 2, and 3) of the gouge analyzed using energy dispersive spectroscopy and the resultant spectra.	14
12	Scavenge pump knob exhibiting displacement towards the right side of the locking cam (left in the photograph).	

Figure		Page
13	Close-up showing the lip shaped metal displacement of the locking cam (arrow) .	15
14	The left side of the scavenge pump switch indicating the knob had been displaced towards the right.	16
15	The environmental seal sleeve was displaced from the knob towards the "on" position.	16
16	Scavenge pump switch plunger guide exhibiting surface cracks from the mold runner (arrow) .	17
17	Right jettison switch plunger guide exhibiting typical mold runner marks (arrow) .	17
18	Evidence of internal salt water-like deposits on the scavenge pump switch case near the contact.	18
19	Internal view of the scavenge pump switch mechanism. The arrow indicates the lubricant material on the rocker arm which was chemically analyzed.	18
20	Internal view of the switch mechanism of the left -jettison switch. The track is apparent as indicated between the arrows.	19
21	Internal view of the switch mechanism of the right jettison switch.	19
22	Internal view of the plunger and guide, red lubricant, (at white arrow, chemically analyzed) and rocker arm of switch S11. The mold runner mark on the plunger is apparent at the black arrow. The larger black arrow indicates the typical black marks on the plunger resulting from actuation impact with the plunger stop.	20
23	Normally open contact surface from the left jettison switch exhibiting typical wear.	21
24	Normally open stationary contact surface of the right jettison switch exhibiting salt water-like residues.	21

Figure		Page
25	Normally closed stationary contact surface of the right jettison switch which exhibited little or no salt water-like residues.	22
26	Normally open stationary contact surface of the scavenge pump exhibiting some salt water-like residues.	22
27	Exploded view of switch S-11 following disassembly.	23
28	FTIR spectrum of the red lubricant in S-11 switch which was similar to the reference spectrum of ester-based lithium stearate.	23

LIST OF TABLES

Table		Page
1	Insulation and Contact Resistance Measurements	24
2	Actuation Forces	24

TWA 800 Switch Analysis**PURPOSE**

Examine and electrically characterize switches for any anomalies and witness marks.

BACKGROUND

The three switches, scavenge, right, and left jettison switches, had been previously examined by personnel at NASA. The scavenge pump switch was reported to be in the "off" position and volt meter tests confirmed this conclusion. The contacts exhibited a high resistance of 400 ohms when the scavenge pump switch was in the "on" position. Both jettison switches were observed and confirmed with the volt meter to be in the "off" position. The S-16 (left -jettison switch) switch had 0.3 ohm contact resistance, while S-17 (right jettison switch) had 0.28 ohm contact resistance in the "on" position. The left jettison pump switch toggle was observed to be smashed downward toward the "off" position. The toggle seal was damaged. The toggle of the right jettison switch was observed to be in the "off" position. The seal was also damaged.

FACTUAL DATA

As part of the TWA 800 mishap investigation, three environmentally sealed switches were analyzed as requested by NTSB. Another like design switch (S-11) was examined for comparison. The three switches consisted of the Right and Left Jettison Switches and Scavenge Pump Switch. The one of similar construction to the Right and Left Jettison Switches examined for comparison was the S-11 switch from the flight engineer's fuel control panel. All three switches were photographed as received (Figures 1 and 2). The flight engineer's fuel control panel from which the switches had been removed was also received (Figures 3 and 4).

Initially, the three switches were examined using real time X-ray'- The results were documented on video tape. No anomalies were noted.

The right and left jettison switches were the same model (1TL-3) and date code 7042. The switches had been labeled with a black marker to indicate the switch functions and terminal positions.

000003

The left jettison switch knob was bent towards the "off" position (bottom) 50 degrees beyond normal. The markings and the bent knob are shown in Figures 1 and 2. Corrosion was noted around the three contact screws (designated as top, left, and bottom) (Figure 5). The terminal wire was attached to the bottom screw terminal. The left screw terminal contact was in place but the wire had broken away at the lug terminal. There was no wire attached to the top terminal. There was green-colored corrosion around the terminal attachment. The exposed copper was also green colored. The copper was partly shiny on the broken solderless terminal connector (see arrow, Figure 5) . The top terminal appears to have been unused. Corrosion was noted on top of the switch and around the securing threads and inside the top one. There was a deep gouge in the securing thread. The case exhibited some corrosion and the blue colored case material was flaking off. The corrosion was primarily white in color with some green coloration- The metal surrounding the environmental seal had corrosion and salt water-like and sand deposits (Figure 6).

The right jettison switch had a similar appearance. It was received in the "off" position. There were gouges in the securing bushing. The screw terminals (labeled top, right, and bottom) were similar in appearance to the left jettison switch. The metal surrounding the environmental seal had corrosion and salt water-like deposits. There was green and white colored corrosion on the screws and threads. The right and bottom screw terminals had wires attached.

The scavenge pump switch had a locking feature (MS24658-23G) in the "off" position. By design the knob would have to be pulled out and over the stop to move to the "on" position. It was received in the "off" position. The date code on the switch was 7038. The screw terminals were intact and connected to the center and bottom positions. They exhibited green-colored and white-colored corrosion and salt water-like residues. A gouge was found on the forward side (as installed) of the switch knob, 15° above the knob center line (Figures 7 and 8) . This gouge was examined in the scanning electron microscope (SEM) and analyzed using energy dispersive spectroscopy (EDS) (Figure 9) . The metal displacement in the gouge was consistent with a tangential impact to the switch knob in the direction as diagramed in Figure 10. The EDS analysis of the gouge area (Figure 11) indicates the knob construction materials are a nickel plated brass (zinc and copper) . No foreign materials were identified in the areas analyzed to reveal the makeup of the object that impacted the knob. The knob locking cam exhibited rust-colored corrosion and salt water-like residues around the base and along the back side of the knob. Examination of the switch knob placement while in the locked "off" position revealed evidence it had been displaced

toward the right side of the switch. Optical inspection also showed evidence the knob was displaced towards the right side of the locking cam (Figure 12) . The locking cam groove for the "off" position on the right side had metal displacement in the shape of a lip (Figures 13 and 14) . The environmental seal sleeve around the knob was stretched away from the knob towards the "on" position (Figure 15) . The locking cam surface was examined for any witness marks which would indicate a blow to the knob and none were found. The wear pattern appeared normal.

Electrical measurements consisting of insulation resistance and contact resistance were made on the three switches. Insulation resistance measurements were made using an HP 4329A high resistance meter at 500 VDC after one minute stabilization at 23°C and 62% RH. Contact resistance measurements were made at 10 mA, using the four point probe method. A Keithley 2001 was used to measure the voltage. The constant current was supplied by an HP6227B and measured by an HP3478A. A Tektronix 576 curve tracer was used to make the initial measurements on the scavenge pump switch so as not to destroy any failure evidence. The resistance exceeded the internal resistance of the instrument. The results are compiled in Table 1.

Actuation forces were determined for the three switches using a Chatillon digital force gauge (DFG100) . The results are compiled in Table 2.

The switches were opened for internal inspection by the following process. Each plastic case was thinned on both sides by sanding with 240 grit sand paper. The thinned cases were then cut and pried open using a knife. The internal switching mechanisms could then be examined in detail. All three switch plunger guides showed evidence of removal from an injection mold runner (Figures 16 and 17) . All three switches had various amounts of salt-like deposits on most of the internal part surfaces (Figure 18) . Inside the switches, there is a rocker arm that contains a moving contact on each end and pivots at the center when the switch is activated or deactivated (Figures 19-21) . A plunger attached to the external knob moves laterally along this rocker arm along a track (Figure 17) . The plungers all exhibited black marks resulting from actuation impact with the plunger stop (Figure 22) . Along the track of the plunger, there is a red colored lubricant, applied during manufacture (Figure 22). Residues from this brown and red colored lubricant were found outside the normal plunger track marks and on the plunger in all four switches examined. The change in color found in the right and left jettison and scavenge pump switches is consistent with sea water exposure based on chemical analysis.

The contact surfaces of all three switches were examined and only the normal wear pattern was found (Figure 23) . The normally open contact surfaces in right jettison pump switch were covered with salt water-like residues (Figure 24) . Contact resistance for the normally open contacts when actuated was 825 m Ω . The normally closed contact surfaces did not exhibit any salt water-like residues (Figure 25) . The contact resistance as expected was much lower at 2.7 m Ω . There appeared to be little or no salt water-like residues on the contact surfaces of the left jettison switch. The contact resistances for the normally open and normally closed were 17.3 m Ω and 20 m Ω , respectively. The normally closed contact surfaces of the scavenge pump switch were clean with a contact resistance reading of 3.8 m Ω . There were slight salt water-like residues on the normally open contact surfaces resulting in a 22.2 k Ω contact resistance (Figure 26) .

Switch number S11 was removed as a test specimen to ascertain the effects of a static 25 pound side thrust on the actuator knob. This value was the maximum specified in the military specification MS24523 for this switch design. Sideways displacement of the knob was measured at 5 pound increments up to the 25 pound maximum. This was done to both sides of the switch. The maximum knob displacement was 0.085 inch one direction and 0.066 inch in the other direction. Internal parts would be displaced approximately seven eighths of this amount. This value was determined from the ratio of the distance from the pivot axis to the internal plunger (0.7 inch) to the distance from the pivot axis to the actuating knob end (0.8 inch) .

Switch number S11 was also used as a test specimen to observe the effects of impacts on the actuator knob. The test apparatus was a Universal Impact Tester Model #172. This tester consists of a set of weights and a drop tube. One of the weights of this tester had a threaded hole on one end. A large bolt was installed in this hole and the bolt head was used as the contacting surface that collided against the switch knob. This assembly weighed 2.15 pounds and was dropped from a height of 1, 2, 4, and 8 inches. The bolt head height below the bottom stop of the tester drop tube was adjusted to the thickness of the switch knob of 0.24 inch. This produced an overtravel of less than 0.24 inch for the knob and guaranteed most of the drop energy was transferred into the switch. The impacts from four different heights were applied in the "on" to "off" direction of knob travel. The switch was set to "on" position for each impact . Then the impacts were repeated at right angles to the previous impact direction and parallel to the pivot pin of the knob. This test produced nicks in the actuator knob metal at the area of impact. Internal inspection found additional black residue on the white plunger guide where it would contact the

000012

switch front faceplate during overtravel. The side impacts loosened the knob pivot pin from one side of the mounting bushing. The test scraped off-center tracks into the contact rocker arm. The switch was disassembled and is shown in exploded view in Figure 27.

The S-11, left and right jettison, and the scavenge pump switches were submitted for chemical analysis. The areas of interest were deposits found on the rocker arms and inside the casings of the switch samples. The rocker arm refers to the silver-colored metal plate that moves when the switch is operated. The samples were examined by means of low power optical microscopy and portions of the deposits were removed and analyzed by means of microscopic Fourier transform infrared spectrometry (FTIR). The results are as follows. FTIR spectra were obtained for the semi-solid red deposit on the S-11 rocker. The spectra obtained were consistent with references that suggested the deposit was an ester based lubricant with lithium stearate (Figure 28). Spectra for deposits on the rocker of the left jettison switch indicated the presence of the same lubricant. Various deposits were observed inside the casings of the left, right, and scavenge switches. These included methyl silicone materials, phthalate ester based materials, polyamide or urea type resins, hydrated inorganic oxides or hydroxides, inorganic carbonates and an unidentified material that exhibits absorption in a spectral region expected for inorganic nitrates and organic nitro compounds.

Summary of Findings

All three switches were received in the "off" position. The worst external damage, a bent knob, occurred on the left jettison switch.

Salt water-like residues and contamination on the contact surfaces of the switches indicate the contacts were received in the same position as they were in when recovered from the mishap site. Residues and contamination prevented accurate contact resistance measurements and resulted in higher readings. The right jettison switch contained the most contamination.

No discernible witness marks were found on any of the switches to indicate switch position during the initial stages of the mishap. Mechanical operation and contact appearance of all three switches were normal.

The metal displacement in the gouge found on the scavenge pump switch knob was consistent with an impact to the switch knob in the direction as diagramed in Figure 10. Since the impact was forward of the knob center line, the resultant force on the

000013

knob would be towards the "off" position. The EDS analysis was unable to determine the makeup of the material that caused the gouge. This was due to insufficient amount of material for analysis or because the impact object was constructed from the same material as the knob.

There was no evidence to support any forced movement to the "off" position by impact or some other means from the mishap breakup energy.

RECOMMENDATION(S)

None. Data submitted as requested.

PREPARED BY

Edward L. White

EDWARD L. WHITE
Structural Failure Analysis
Materials Integrity Branch
System Support Division
Materials Directorate

PUBLICATION REVIEW: This report has been reviewed and approved.

George Slenki

GEORGE SLENSKI, Acting Branch Chief
Materials Integrity Branch
Systems Support Division
Materials Directorate

000015

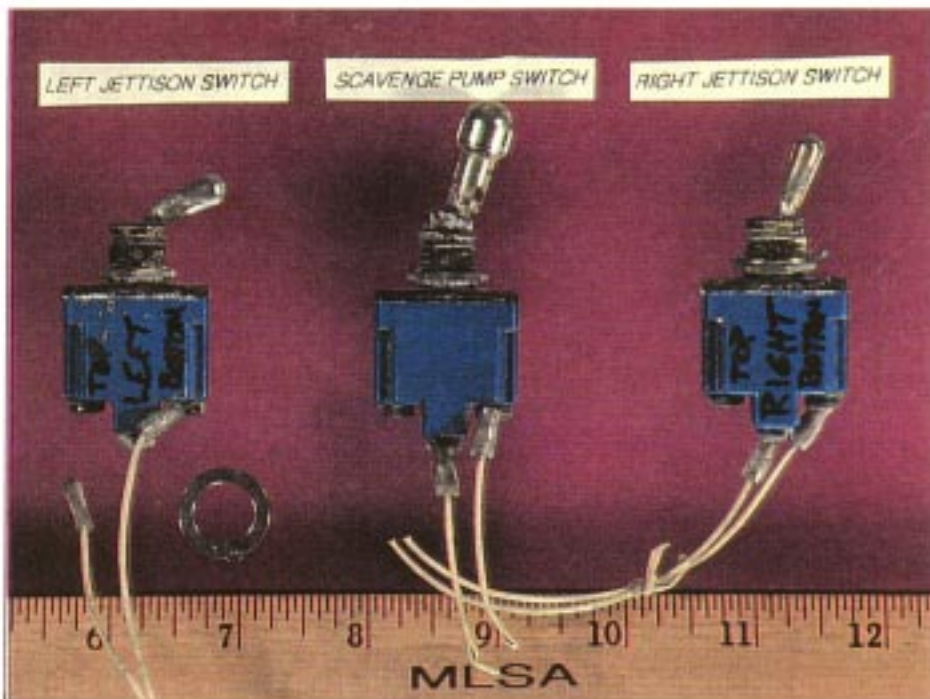


Figure 1. Side 1 of the three switches received for analysis.

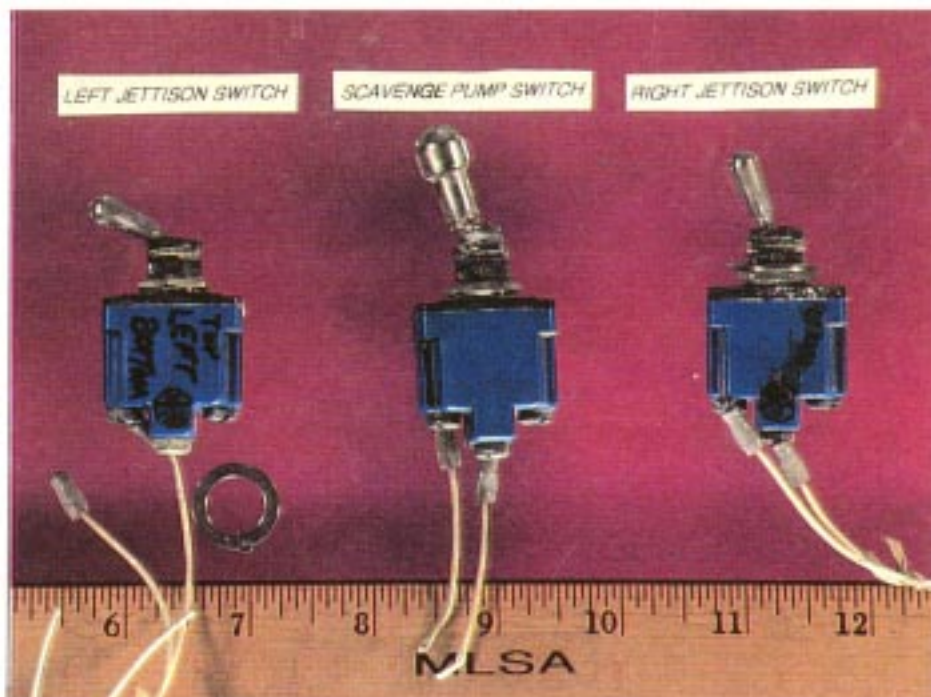


Figure 2. Side 2 of the three switches received for analysis.

000016

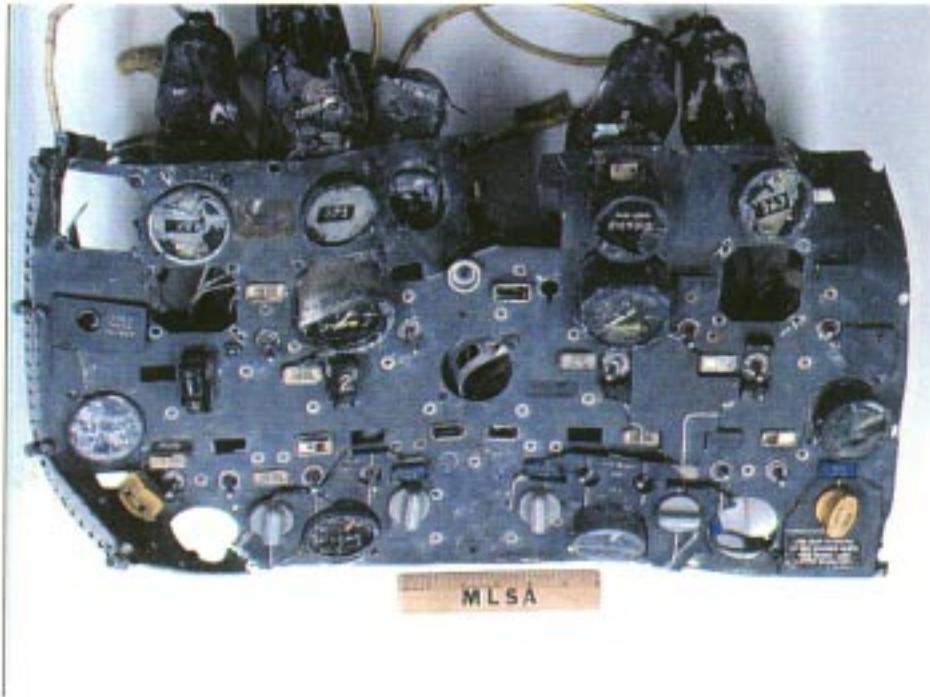


Figure 3. Face side of flight engineer's fuel control panel as received.

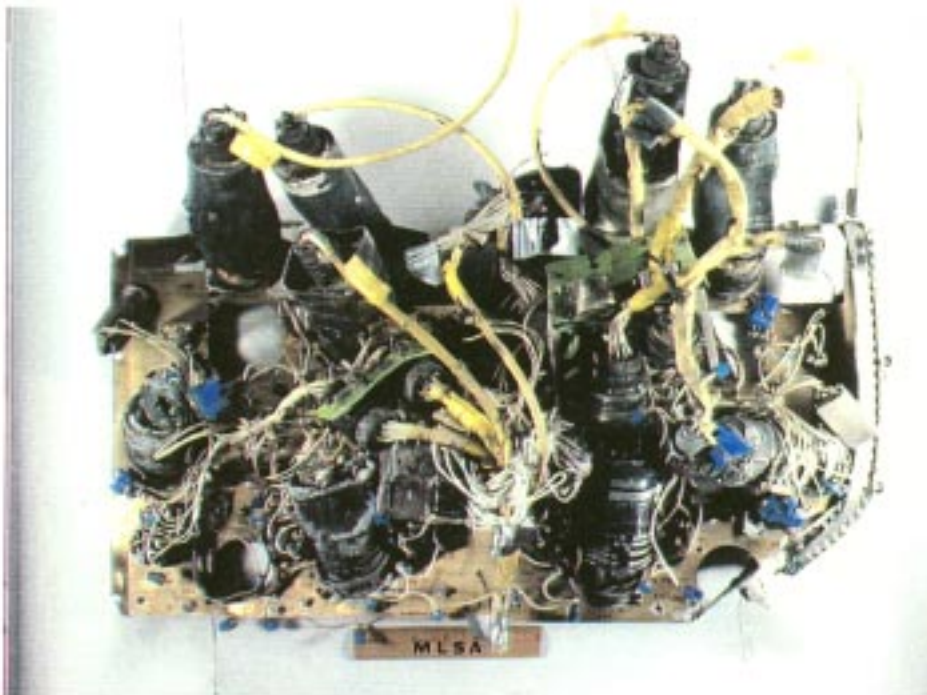


Figure 4. Back side of flight engineer's fuel control panel as received.

000017

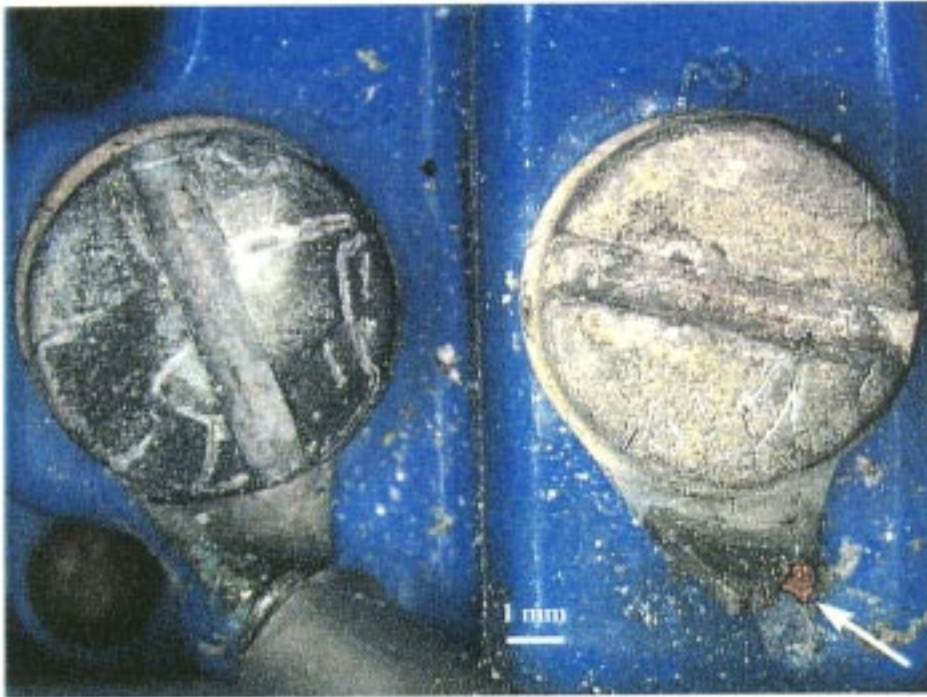


Figure 5. Left jettison switch screw terminals exhibiting corrosion from salt water exposure. Note the exposed copper from the solder lug (arrow).



Figure 6. The environmental seal of the left jettison switch exhibiting corrosion and salt water-like deposits.

000018

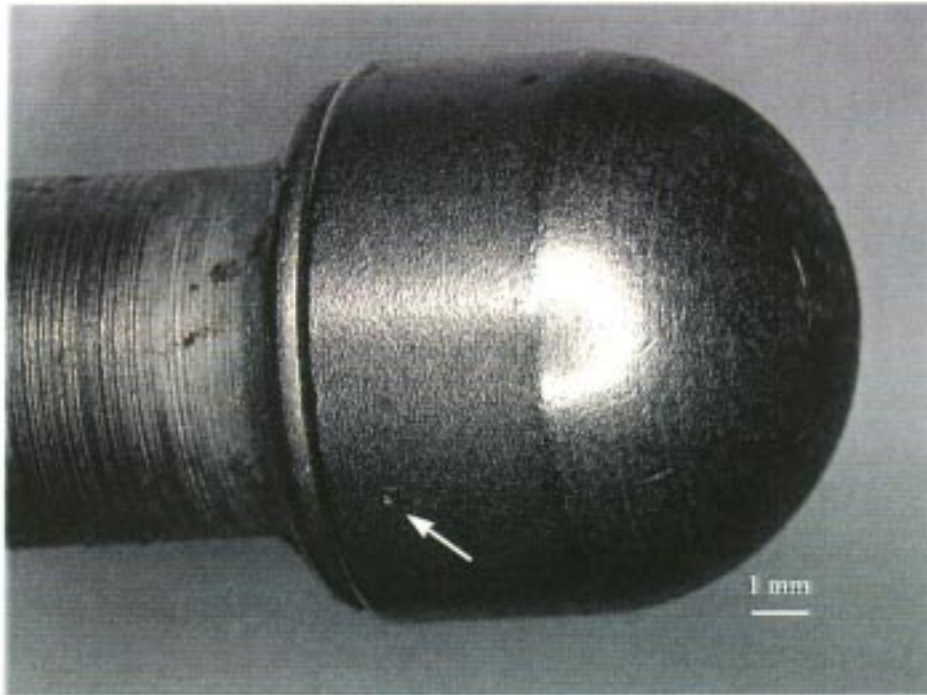


Figure 7. Gouge found on the left side of the scavenge pump switch knob 15 degrees forward of the knob center line.

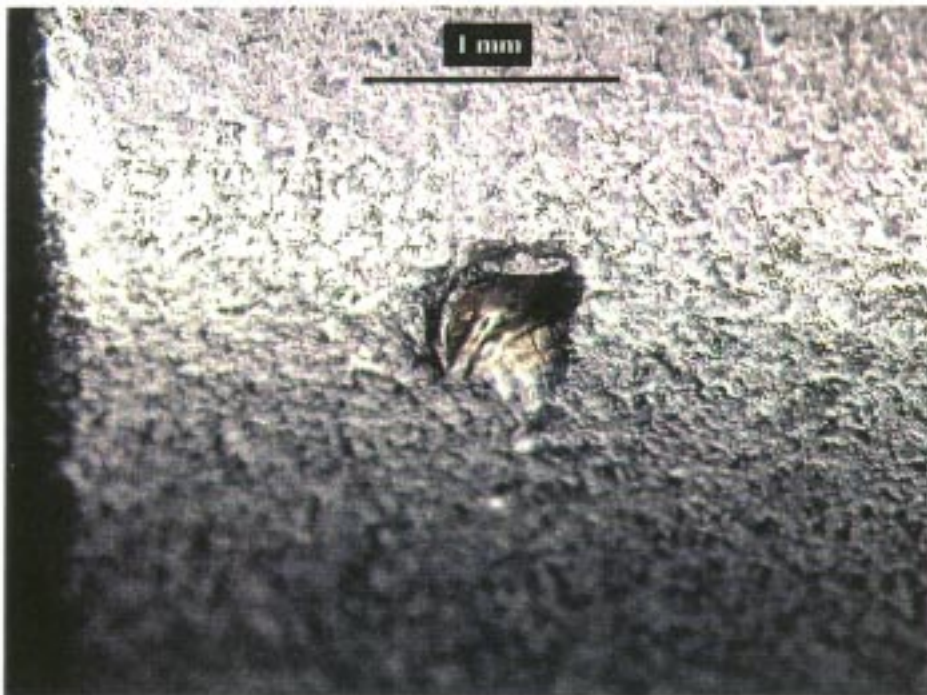


Figure 8. Close-up of the gouge. Note the metal displacement used to determine the gouge direction.

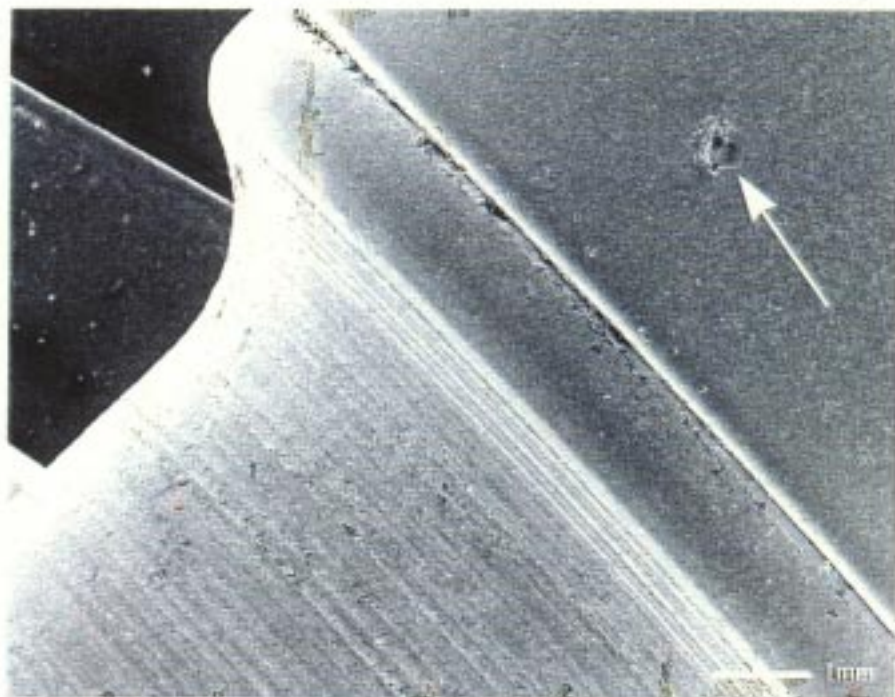


Figure 9. SEM view of the gouge found on the scavenge pump switch knob (arrow).

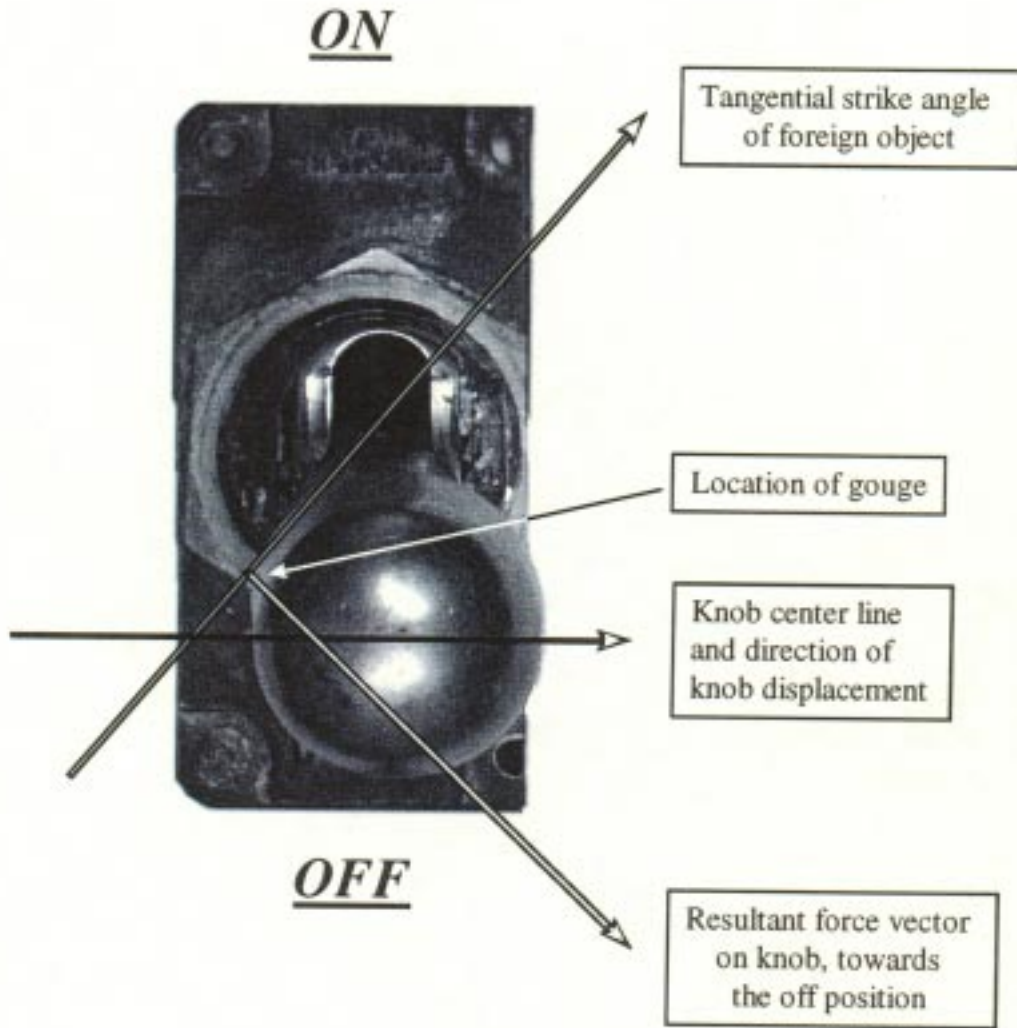
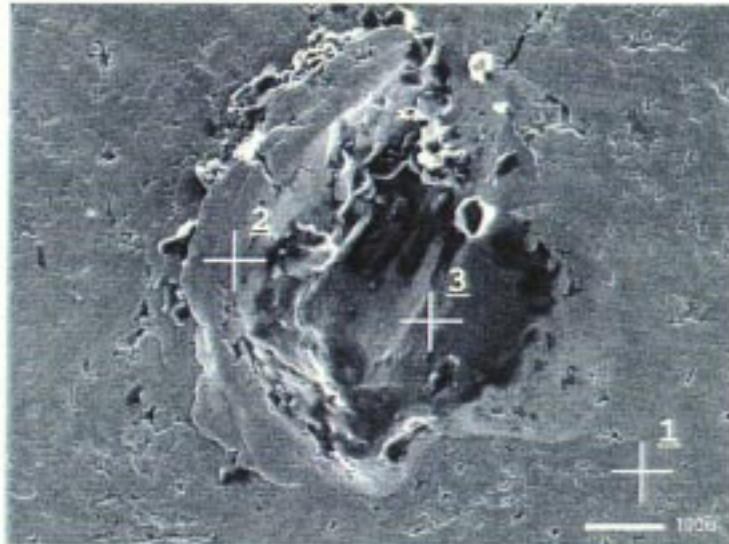
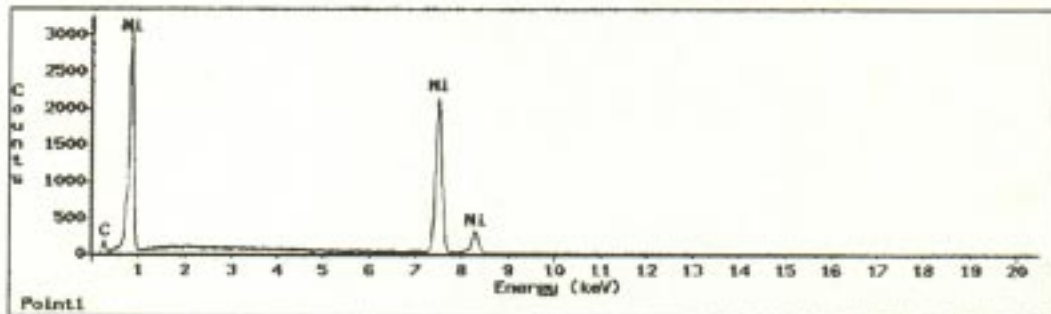


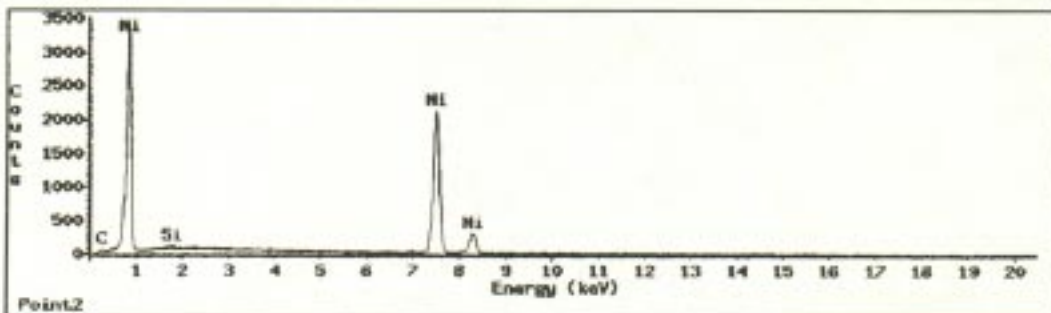
Figure 10. Overall view of scavenger pump switch knob showing the impact gouge (white arrow), the knob center line, the direction of the impact, and the displacement of the knob in the cam groove.



1



2



3

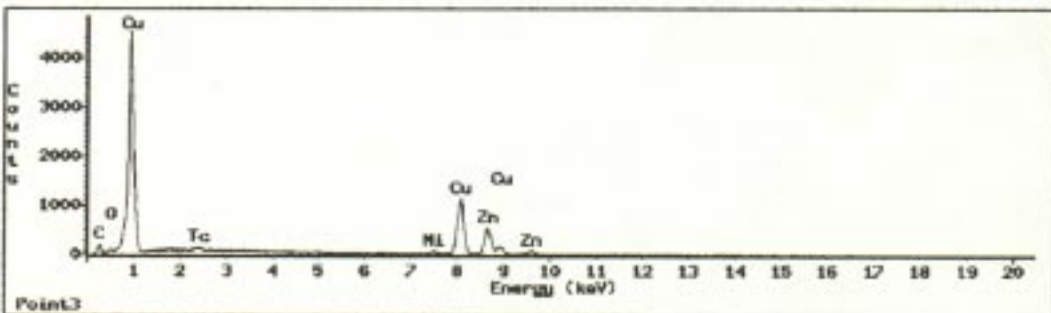


Figure 11. The areas (1, 2, and 3) of the gouge analyzed using energy dispersive spectroscopy and the resultant spectra.

000022

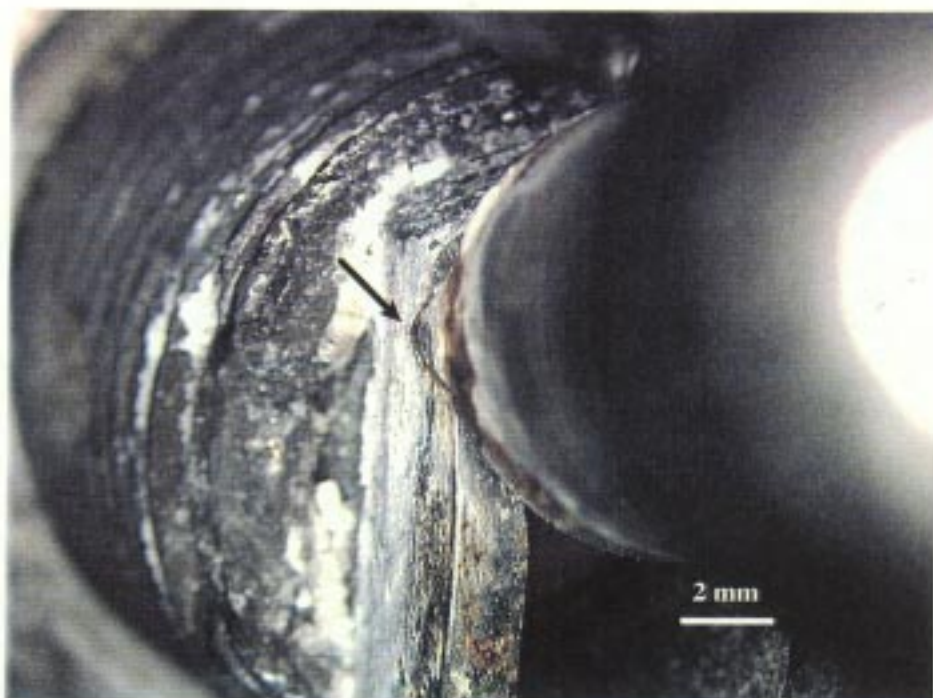


Figure 12. Scavenge pump knob exhibiting displacement towards the right side of the locking cam (left in the photograph).

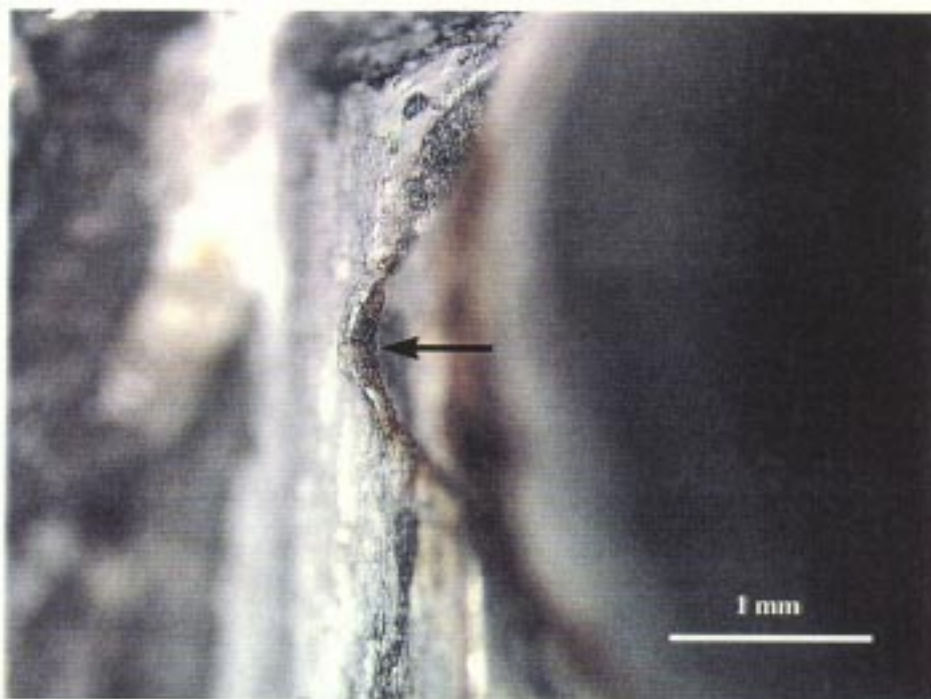


Figure 13. Close-up showing the lip shaped metal displacement of the locking cam (arrow).

000023



Figure 14. The left side of the scavenge pump switch indicating the knob had been displaced towards the right.

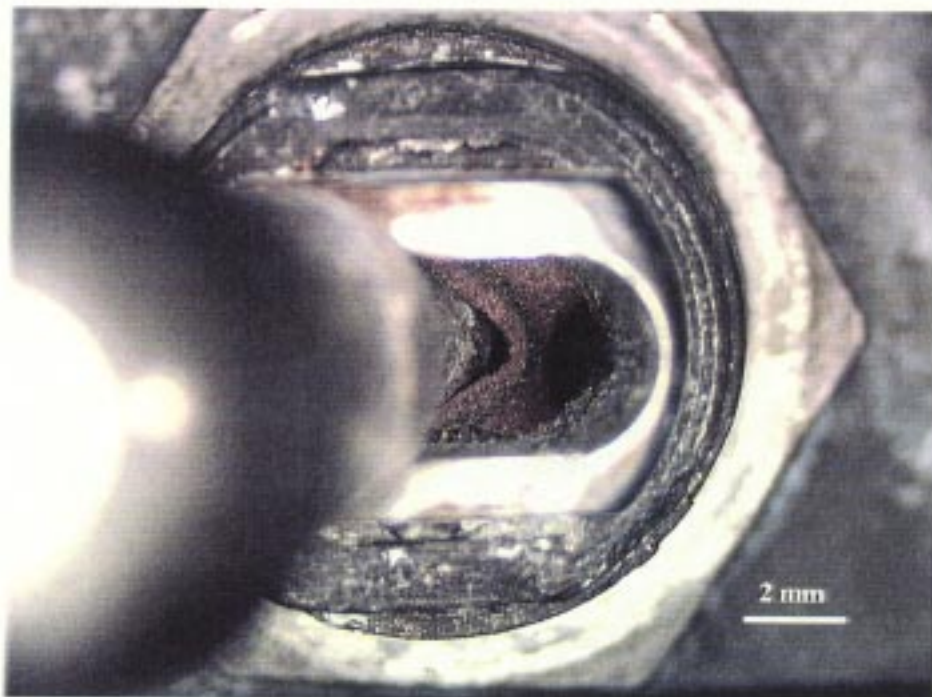


Figure 15. The environmental seal sleeve was displaced from the knob towards the "on" position.

000024

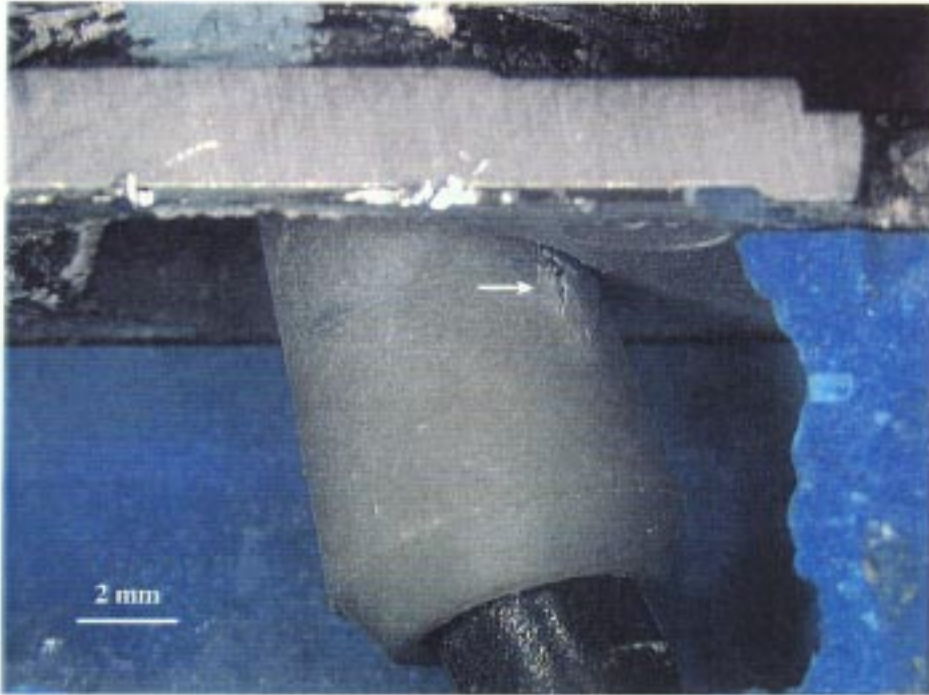


Figure 16. Scavenge pump switch plunger guide exhibiting surface cracks from the mold runner (arrow).

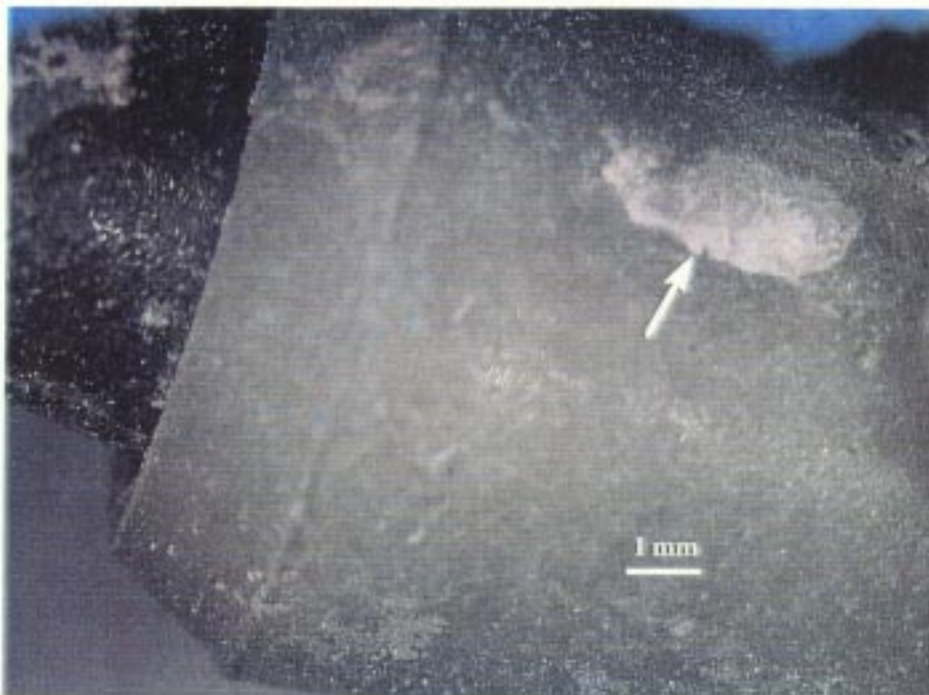


Figure 17. Right jettison switch plunger guide exhibiting typical mold runner marks (arrow).

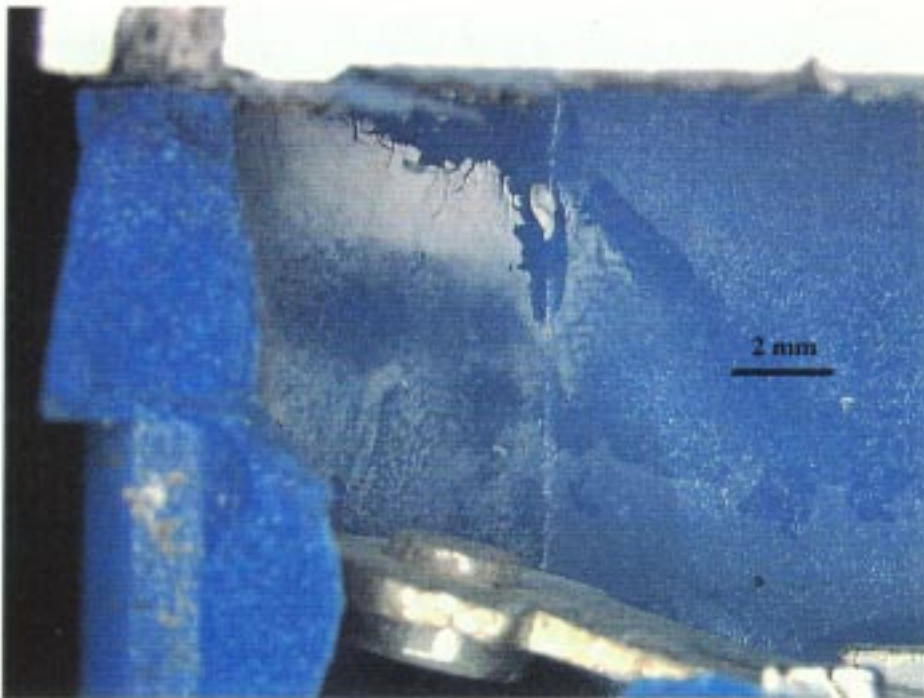


Figure 18. Evidence of internal salt water-like deposits on the scavenger pump switch case near the contact.

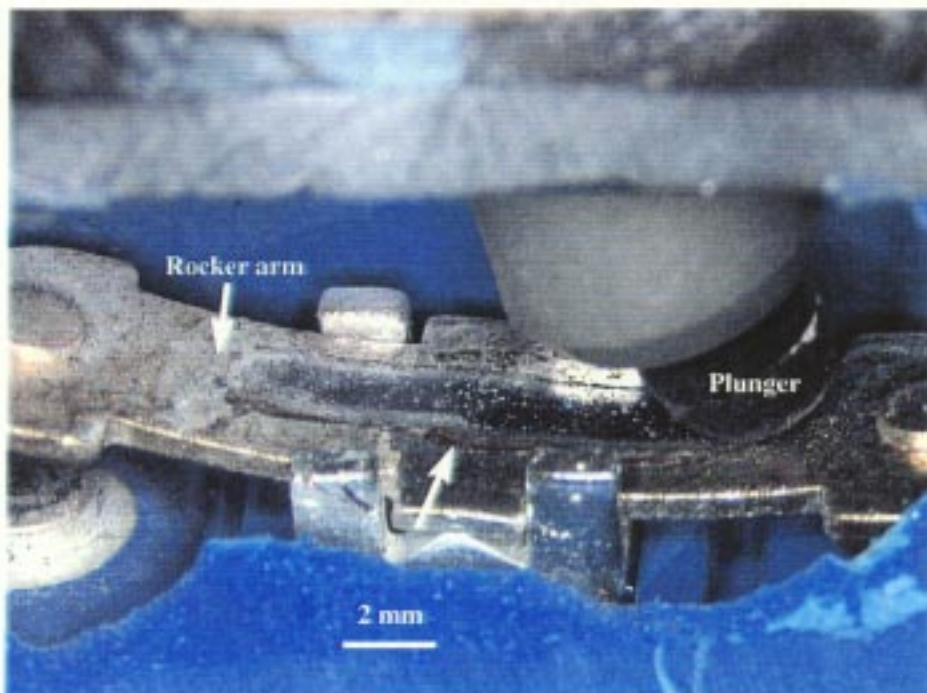


Figure 19. Internal view of the scavenger pump switch mechanism. The arrow indicates the lubricant material on the rocker arm which was chemically analyzed.

000026

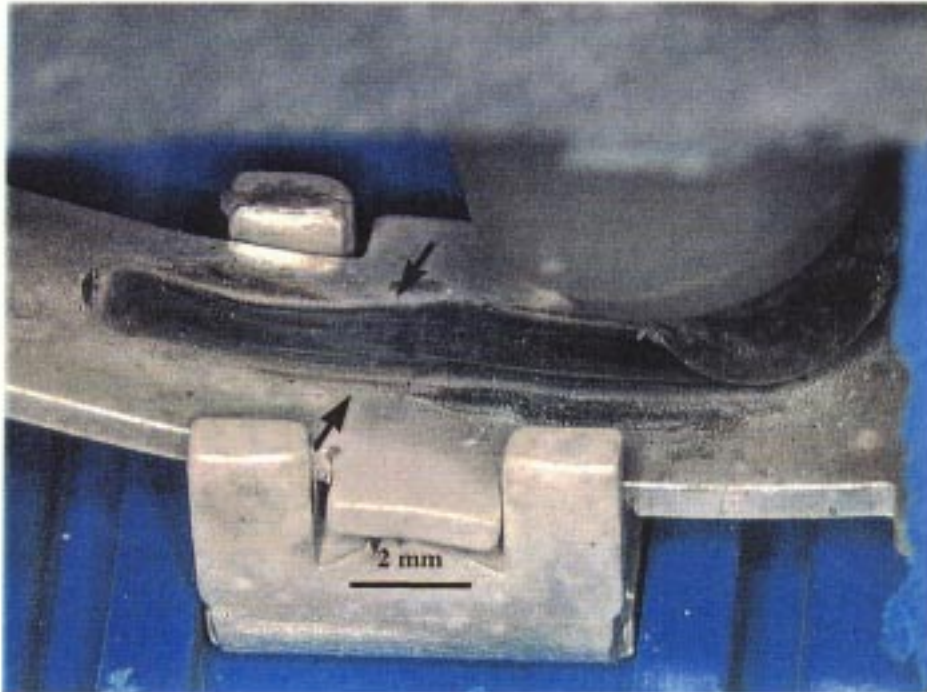


Figure 20. Internal view of the switch mechanism of the left jettison switch. The track is apparent as indicated between the arrows.

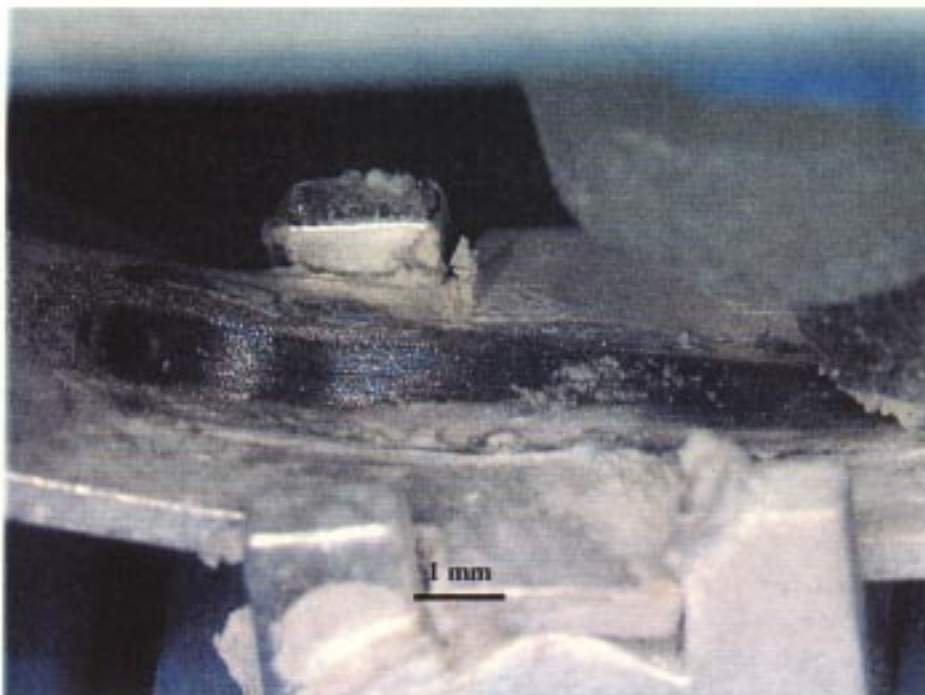


Figure 21. Internal view of the switch mechanism of the right jettison switch.

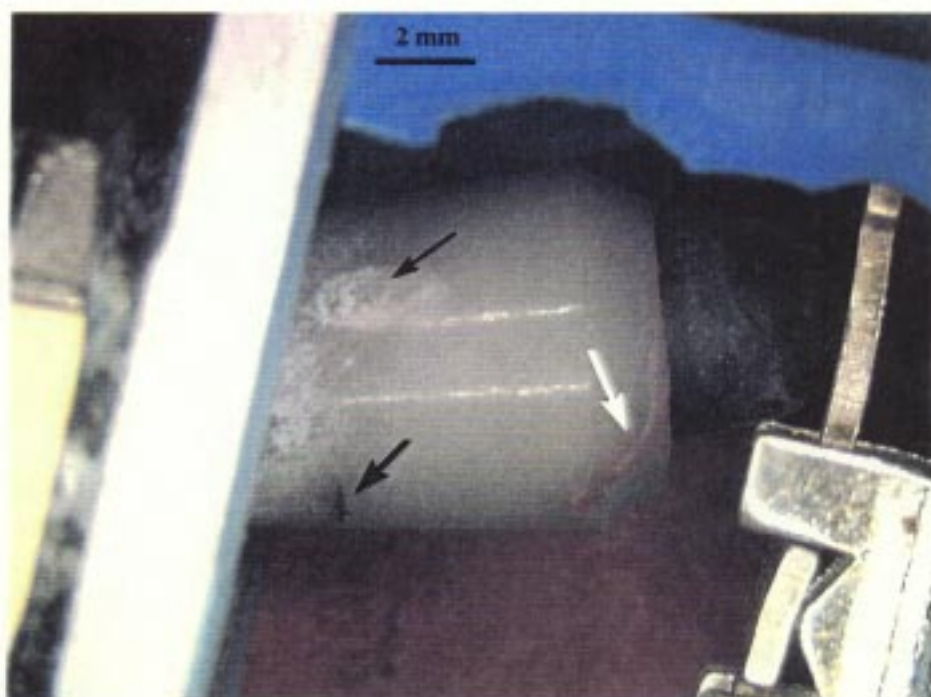


Figure 22. Internal view of the plunger and guide, red lubricant, (at white arrow, chemically analyzed) and rocker arm of switch S11. The mold runner mark on the plunger is apparent at the black arrow. The larger black arrow indicates the typical black marks on the plunger resulting from actuation impact with the plunger stop.

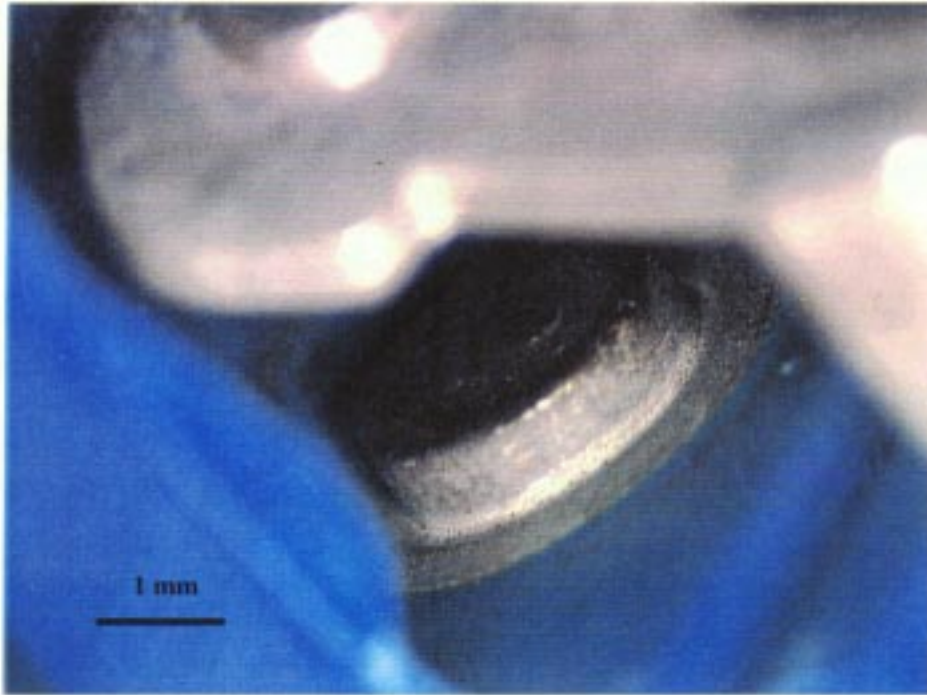


Figure 23. Normally open contact surface from the left jettison switch exhibiting typical wear.

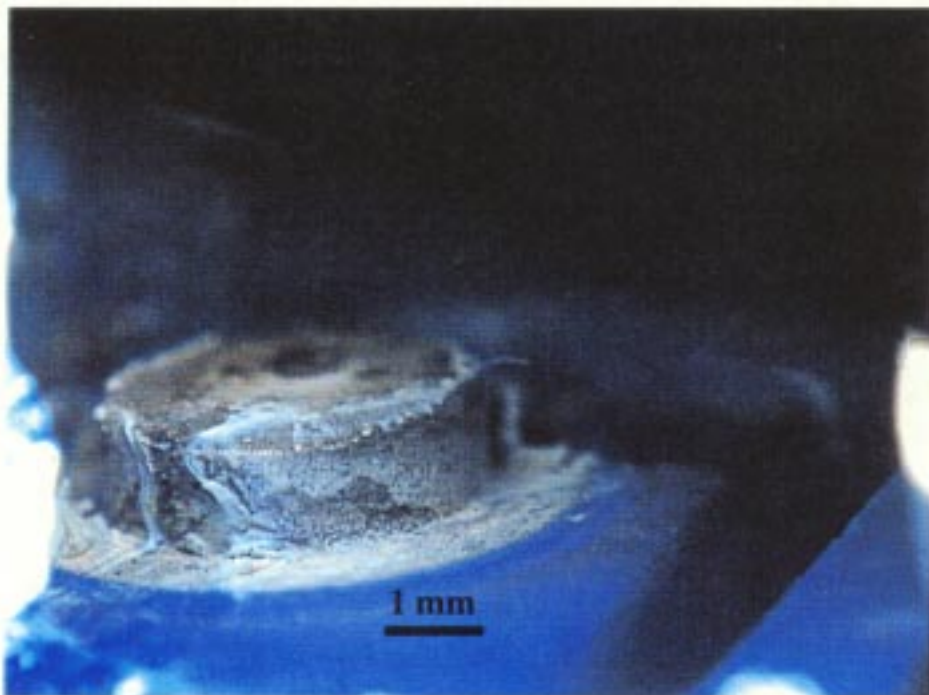


Figure 24. Normally open stationary contact surface of the right jettison switch exhibiting salt water-like residues.

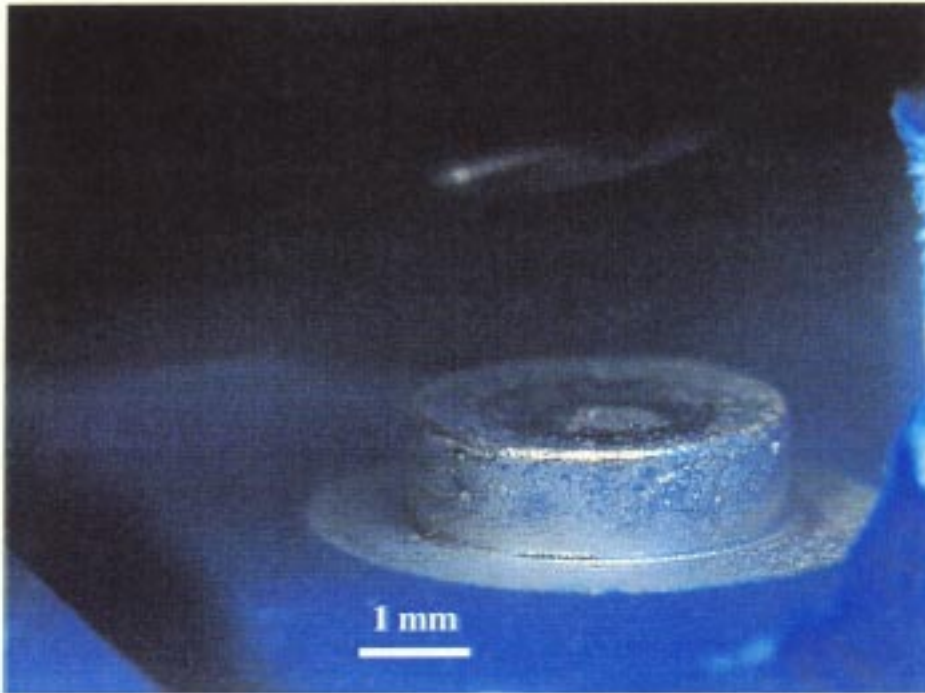


Figure 25. Normally closed stationary contact surface of the right jettison switch which exhibited little or no salt water-like residues.

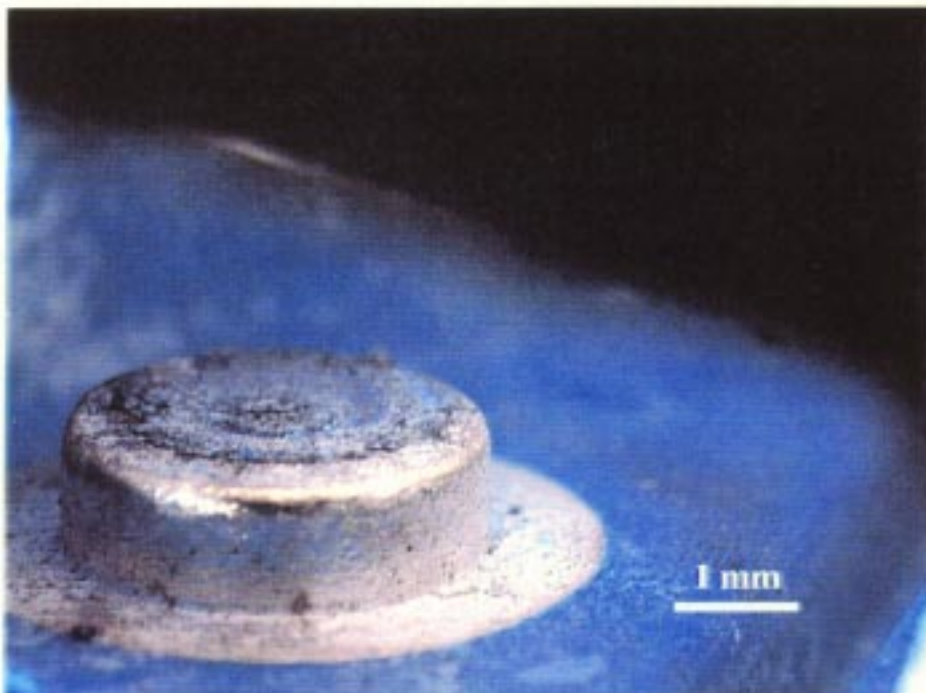


Figure 26. Normally open stationary contact surface of the scavenge pump exhibiting some salt water-like residues.

000030

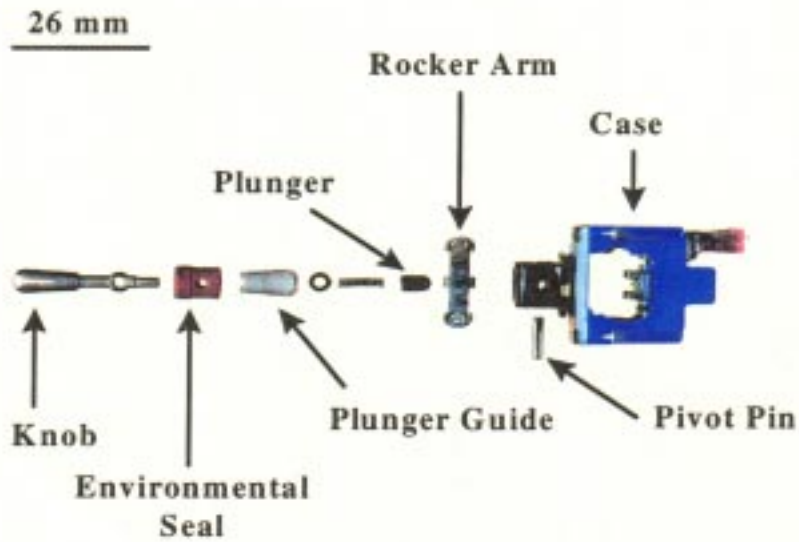


Figure 27. Exploded view of switch S-11 following disassembly.

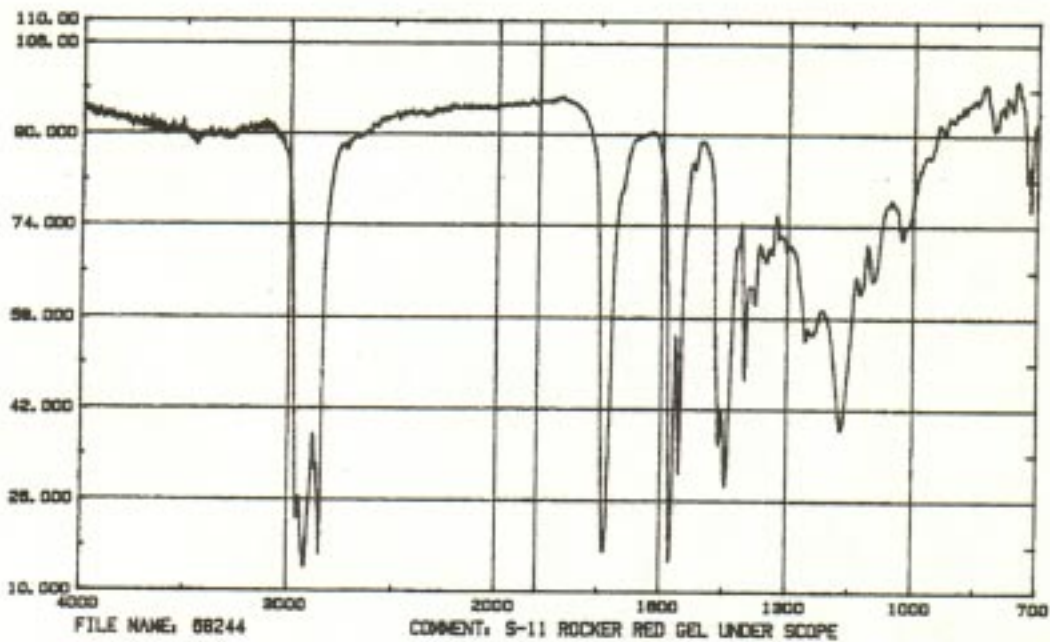


Figure 28. FTIR spectrum of the red lubricant in S-11 switch which was similar to the reference spectrum of ester-based lithium stearate.

000031

Table 1

Insulation and Contact Resistance Measurements

<u>Switch ID</u>	<u>Terminal/Case</u>	<u>Insulation Resistance (ohms)</u>	<u>Contact Resistance (mOhms)</u>
Left Jettison	normally open	4E10	17.3
	normally closed	2E12	20
	case to top	7E9	
	case to center	7E9	
	case to bottom	1E10	
Right Jettison	normally open	6E8	825
	normally closed	4E11	2.7
	case to top	3E9	
	case to center	3E9	
	case to bottom	3E9	
Scavenge	normally open	2E9	22.2KΩ
	normally closed	4E12	3.8

Table 2

Actuation Forces

Left Jettison	1.2 lb
Right Jettison	1.0 lb
Scavenge	3.2-3.5 lb -pull out of "off" position
	0.67 lb "on" to "off" position

Scavenge Pump Relay
(Failure Analysis)

28 August 1997

Evaluation Report
(4349LABR/NTSB)

Report No. WL/MLS 97-078

AUTHOR

Dale Hart
(University of Dayton Research Institute)
Materials Integrity Branch (WL/MLSA)
2179 Twelfth Street Suite 1
Wright-Patterson Air Force Base, Ohio 45433-7718

REQUESTER

Mr. Robert Swaim
National Transportation Safety Board
490 L'Enfant Plaza, East, S.W.
Washington DC 20594

DISTRIBUTION STATEMENT DISTRIBUTION STATEMENT F: Further dissemination only as directed by National Transportation Safety Board/NTSB; 28 August 1997 or DoD higher authority.

000033

TABLE OF CONTENTS

	Page
LIST OF FIGURES	iv
PURPOSE	1
FACTUAL DATA	1
SUMMARY OF FINDINGS.	2

LIST OF FIGURES

Figure		Page
1	Scavenge pump relay, as received.	5
2	Scavenge pump relay. Arrows show the brown and white residues on the case of the relay.	5
3	Radiograph of relay. Arrow indicates the coil that is tilted off its axis.	6
4	Radiograph of relay. Arrow shows the N.C. contacts.	6
5	Radiograph of relay. Arrow shows the N.O. contacts.	7
6	Electrical connector. Arrow shows the white residue on the mating surface.	7
7	Electrical connector pins of the relay. Arrows indicate a brown and white residue on the mating surface.	8
8	Residues on and surrounding the glass to metal seal of N.O. contact A1.	8
9	Corrosion products on glass to metal seal of N.O. contact A1.	9
10	Corrosion products on base of relay near A1.	9
11	The glass to metal seal area of N.O. contact A1 after the residue was brushed away.	10
12	Base of the relay surrounding the glass to metal seal of N.O. contact A1.	11
13	Base of the feedthrough pin and glass to metal seal of N.O. contact A1.	12

000035

Figure		Page
14	Mating surface of stationary contact A1. Arrow shows the residue covering the contact area.	13
15	Mating surface of moving contact A2. Arrow shows the contact area.	14

Scavenge Pump Relay

PURPOSE

Determine the condition of the scavenge pump relay following its recovery.

FACTUAL DATA

The relay, as received, is shown in Figure 1. The case of the relay was deformed on the top and sides. The case had a white film covering it. There was also a reddish brown corrosion in various locations on the case of the relay (Figure 2). Radiographs of the relay indicated the coil was tilting at approximately a 10 degree angle (Figure 3). The radiographs also revealed the normally open (N.O.) and normally closed (N.C.) contacts were all open (Figures 4 and 5).

Electrical measurements were made between the terminals of the coil. Measurements were also made between the N.O. and N.C. contacts to their common and the N.O. and N.C. contacts to the case of the relay. The measurements were made with a HP E2378A multimeter. The resistance of the coil was 109 ohms. The resistance measurement of the N.O. and N.C. contacts to common indicated they were all electrically open (greater than 20 M ohms). The resistance measurement of the N.O. and N.C. contacts to the case of the relay indicated they were also electrically open except N.O. contact A1. It had a resistance to the case of the relay of approximately 800 K ohms.

The socket of the relay was removed so the inner surfaces, pins, and glass to metal seals underneath the red environmental seal could be examined. White and reddish brown residues were present on the environmental seal, inner surfaces of the relay, and socket. These residues were also present on the mating male and female contacts of the socket and relay (Figures 6 and 7). The glass to metal seals were examined, no cracks were observed. The base of the pins for N.O. contact A1 and N.C. contacts B3, C3, and D3 had a reddish brown corrosion.

The solder seal at the base of the relay was carefully thinned with a file until it fractured. The case was removed. The N.O. and N.C. contacts were in the same position as previously shown by the radiographs. The coil and mechanics of the relay were separated from the base of the relay. The internal base of the relay was relatively bright and shiny

000037

except for the area surrounding N.O. contact A1. The area surrounding its glass to metal seal had a white residue (Figure 8). Analysis in the SEM by energy dispersive spectroscopy (EDS) suggests the area is composed primarily of the elements sodium, chlorine, and tin. Minor amounts of iron, nickel, copper, and zinc are also present (Figure 9). The glass to metal seal of A1 had a red, yellow, white, and green residue surrounding approximately one-third of the seal (Figure 8). Analysis of the area in the SEM found it to consist of the elements sodium, chlorine, tin, iron, nickel, copper, and zinc (Figure 10).

Electrical measurements were made again between the N.O. contact A1 and the case of the relay. The resistance was as before. The residue was removed and the electrical resistance measurement was repeated. The resistance increased and A1 to the case of the relay could now be considered as electrically open (greater than 20 M ohms). The area between the pin of A1 and the case of the relay was examined in the SEM for evidence an electrical short could have existed before the area had become corroded. The evidence would consist of melting of the pin or case material; no evidence of melting was found (Figures 11, 12, and 13).

The mating surfaces of the stationary and moving N.O. and N.C contacts were examined in the SEM, see Figures 14 and 15 for examples of A1 and A2. The mating surfaces of the contacts were generally free of residue except for the surface of stationary contact A1. Analysis in the SEM by EDS suggests the residue is composed primarily of the elements sodium, chlorine, and silver. The mating surfaces of the contacts did not exhibit arc erosion or excessive wear. The mating surfaces of the contacts did not exhibit signs of witness marks which could be distinguished from their normal making or breaking action.

SUMMARY OF FINDINGS

A summary of the significant findings is offered as a result of the examination of the scavenge pump relay.

External

The relay has impact damage as indicated by the deformed case and the tilted actuator coil inside the relay.

The N.C closed contacts are in the open position.

000038

The case of the relay as well as the mating surfaces of the electrical connector exhibit signs of being in a corrosive environment (white and reddish brown residues) .

The N.O contact (A1) had a resistance of 800 K ohms to the case of the relay.

Internal

The base of the relay was bright and shiny except for the area surrounding N.O. contact A1.

Analysis of the white residue suggests it is primarily a compound of tin(chloride) .

A multicolored residue lying on the glass to metal seal of A1 suggests it consists of compounds of iron, copper, and tin(chloride) .

The resistance of the N.O contact A1 increased once the residue on the glass to metal seal was removed.

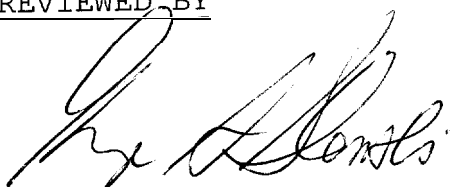
Evidence that an electrical short could have been present before the formation of the multicolored residue was not found.

The mating surfaces of the N.O. and N.C. contacts did not exhibit signs of witness marks.

The mating surfaces of the N.O. contacts did not exhibit arc erosion or excessive wear.

000039

REVIEWED BY



GEORGE SLENSKI, Team Lead
Electronic Failure Analysis
Materials Integrity Branch
Systems Support Division
Materials Directorate

PUBLICATION REVIEW: This report has been reviewed and approved.



RONALD H. WILLIAMS, Branch Chief
Materials Integrity Branch
Systems Support Division
Materials Directorate



Figure 1. Scavenge pump relay, as received.

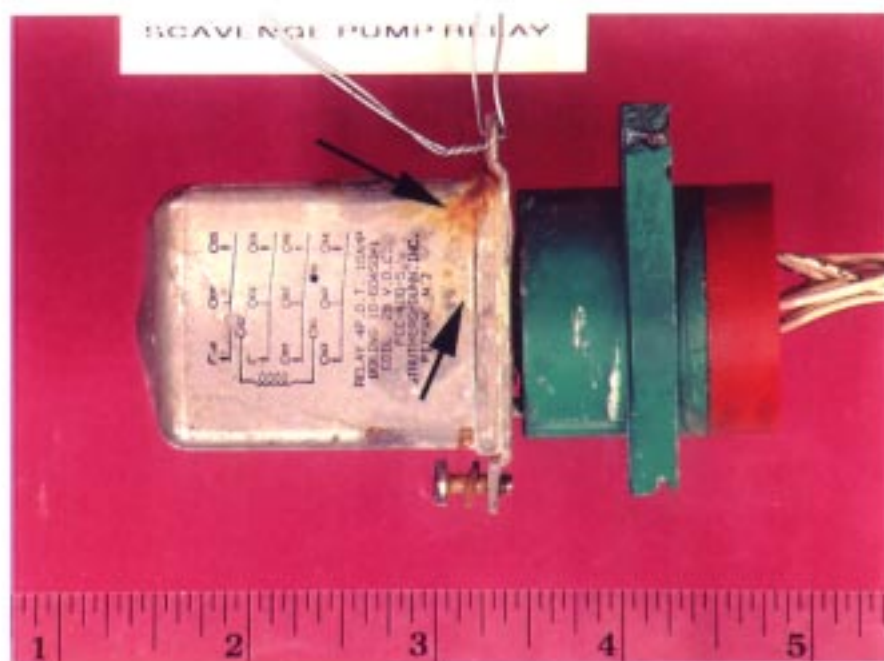


Figure 2. Scavenge pump relay. Arrows show the reddish brown and white residues on the case of the relay.

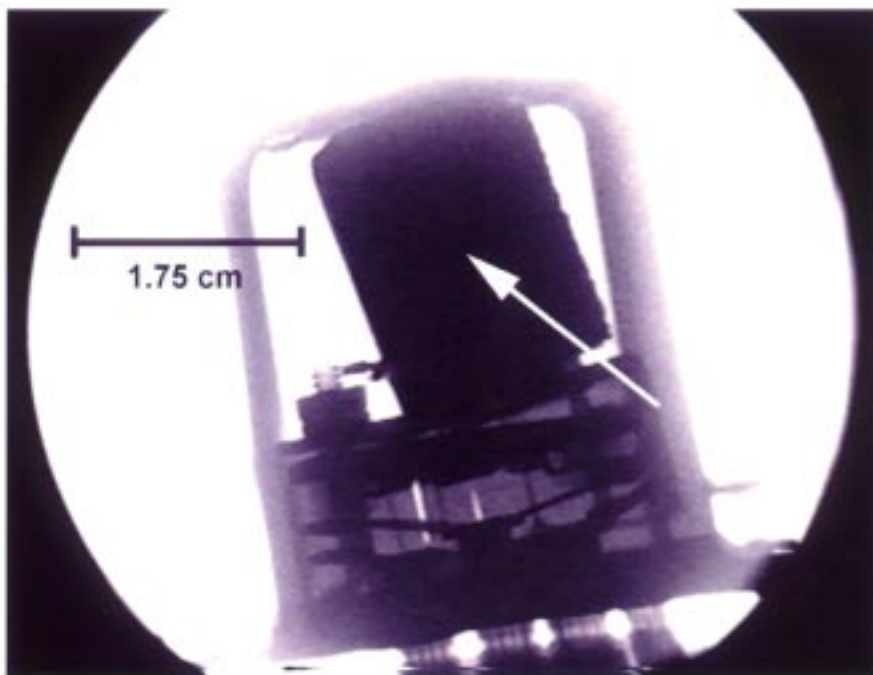


Figure 3. Radiograph of relay. Arrow indicates the coil that is tilted off its axis.

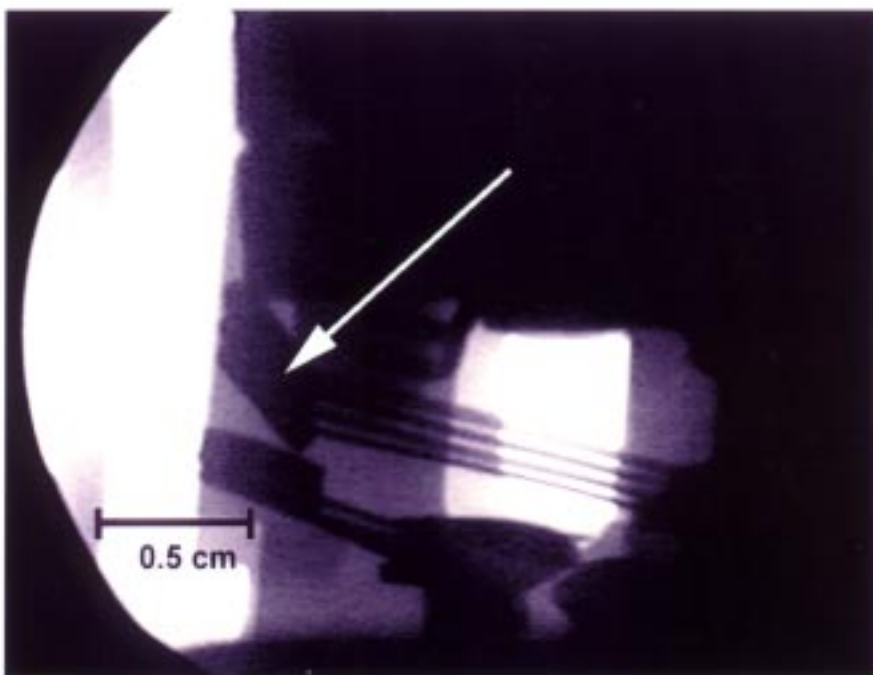


Figure 4. Radiograph of relay. Arrow showing the N.C. contacts are open.

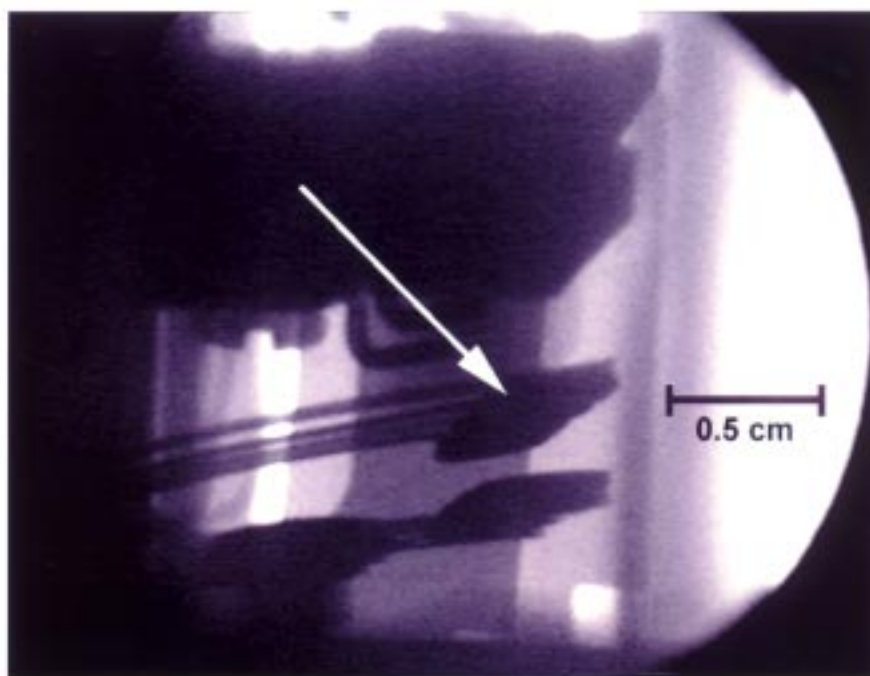


Figure 5. Radiograph of relay. Arrow showing the N.O. contacts are open.

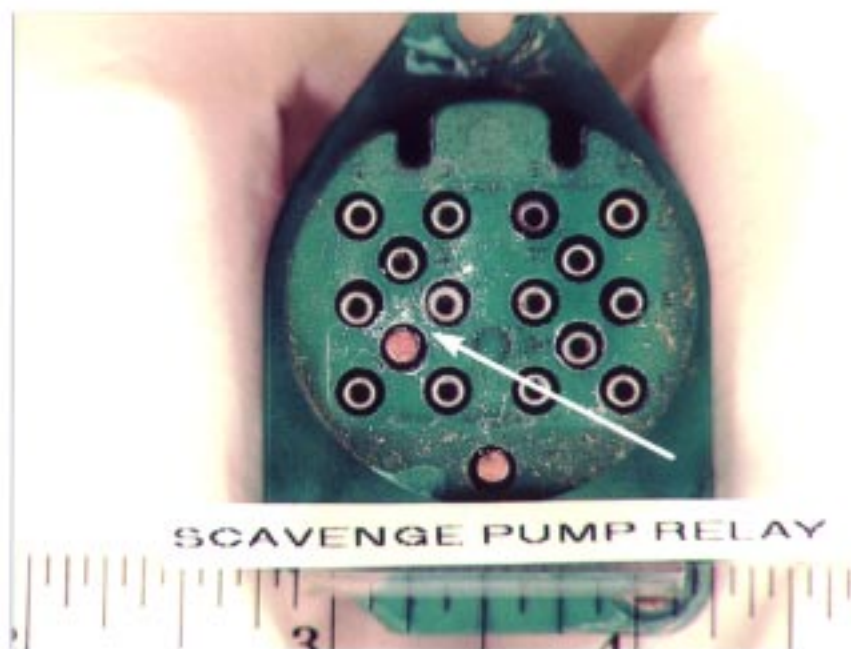


Figure 6. Electrical connector. Arrow shows the white residue on the mating surface.

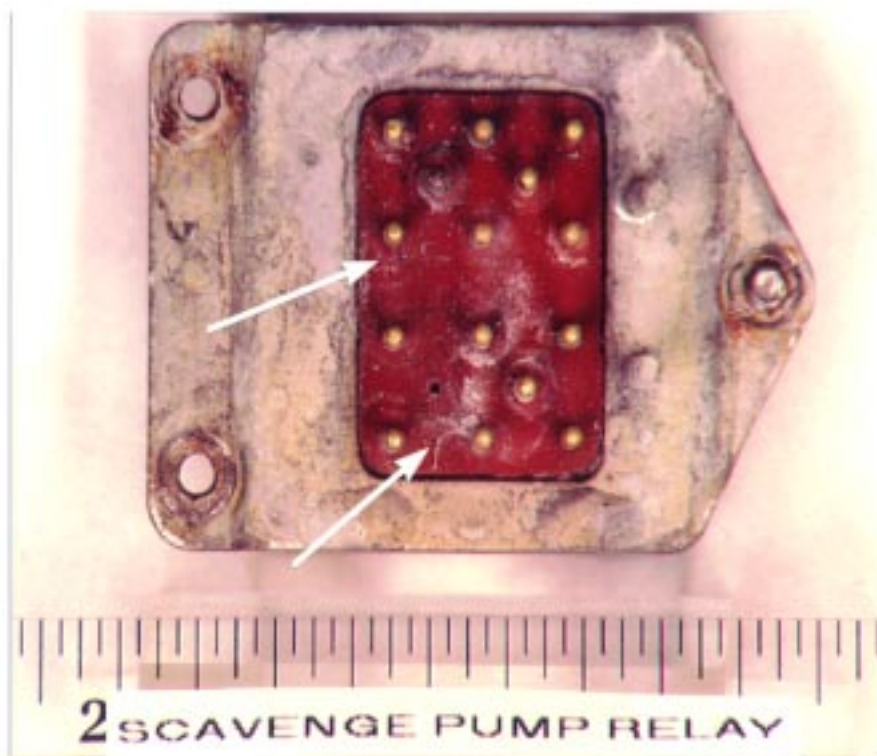


Figure 7. Electrical connector pins of the relay. Arrows indicate a brown and white residue on the mating surface.

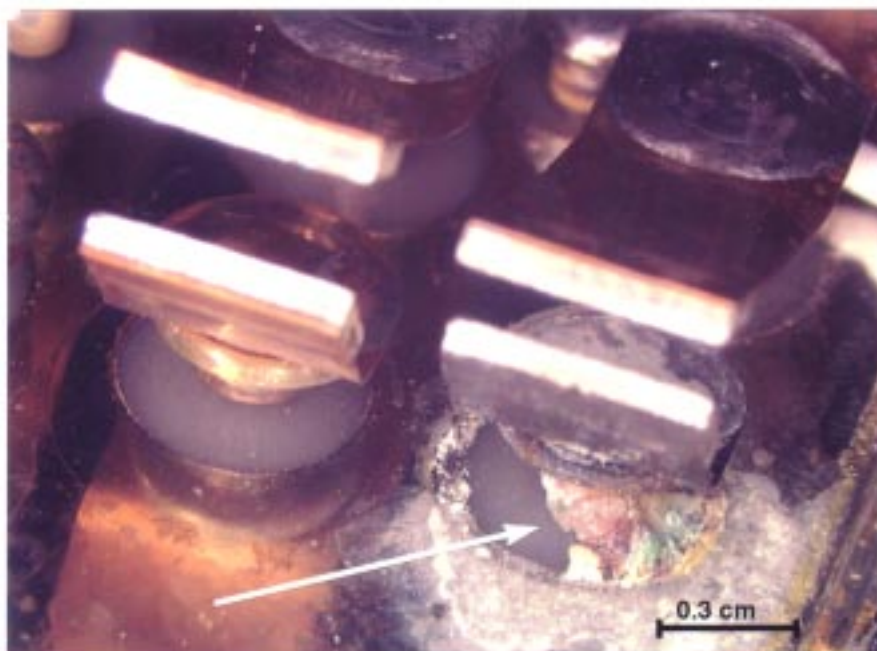


Figure 8. Residues on and surrounding the glass to metal seal of N.O. contact A1.

Series II Wright Patterson AFB THU 10-JUL-97 07:49
 Cursor: 0.000keV = 0 ROI (0) 0.000: 0.000

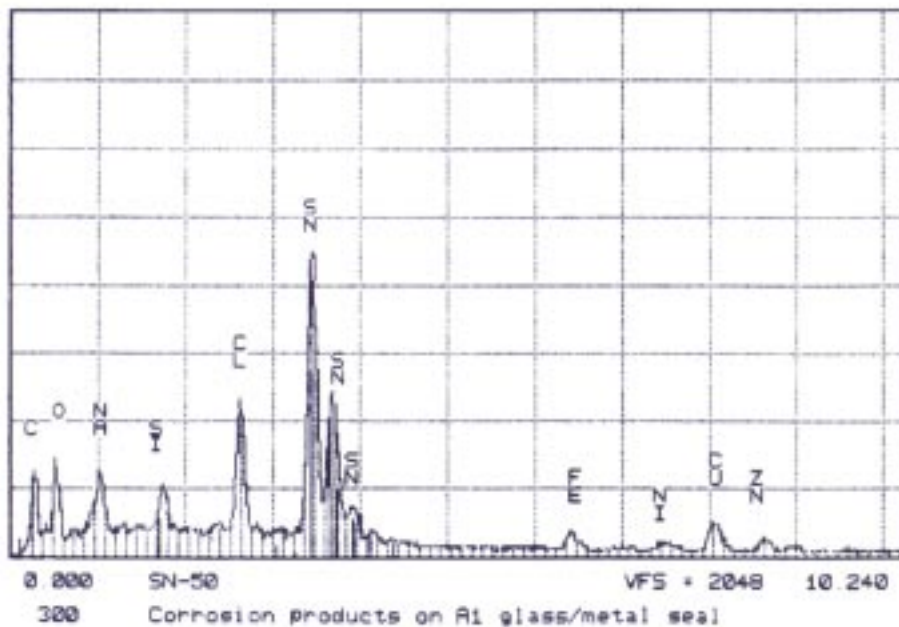


Figure 9. Corrosion products on glass to metal seal of N.O. contact A1.

Series II Wright Patterson AFB THU 10-JUL-97 08:45
 Cursor: 0.000keV = 0 ROI (0) 0.000: 0.000

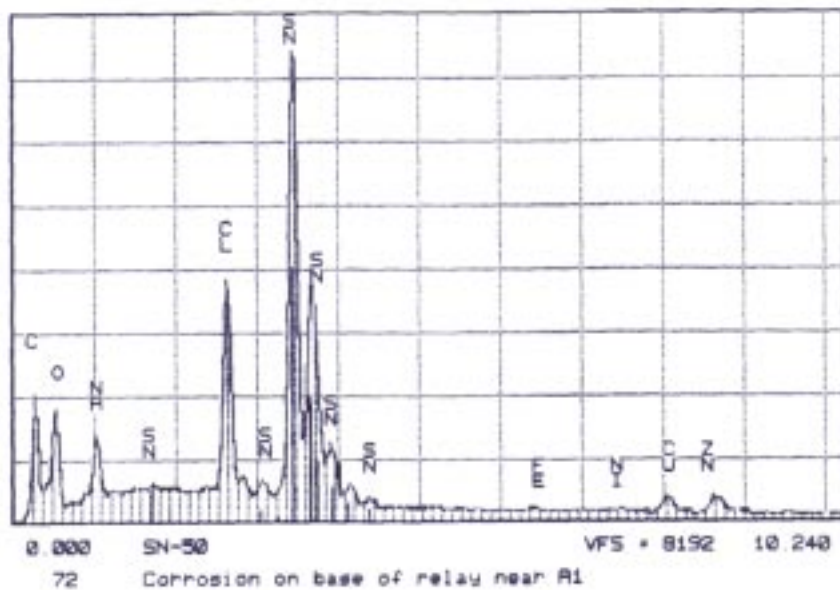


Figure 10. Corrosion products on base of relay near A1.

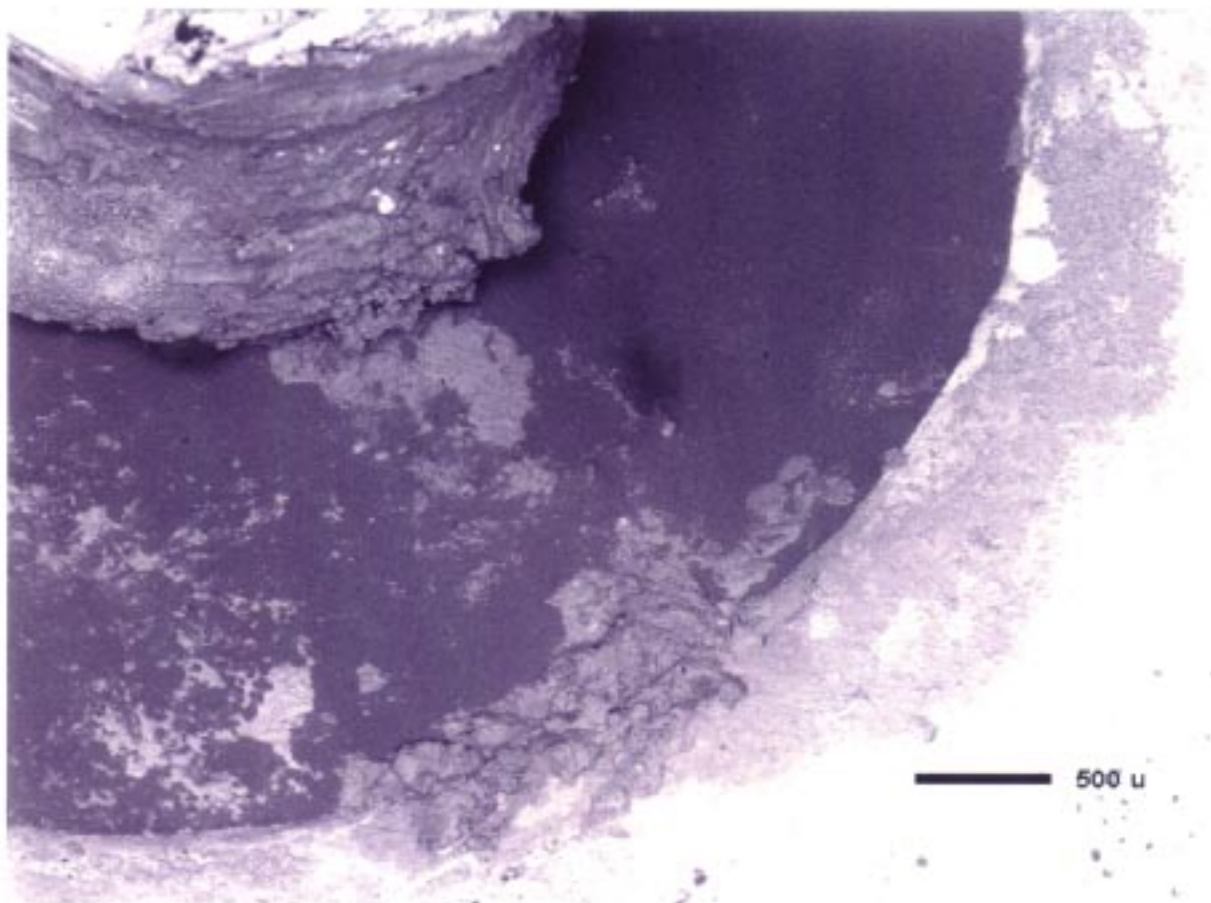


Figure 11. The glass to metal seal area of N.O. contact A1 after the residue was brushed away.

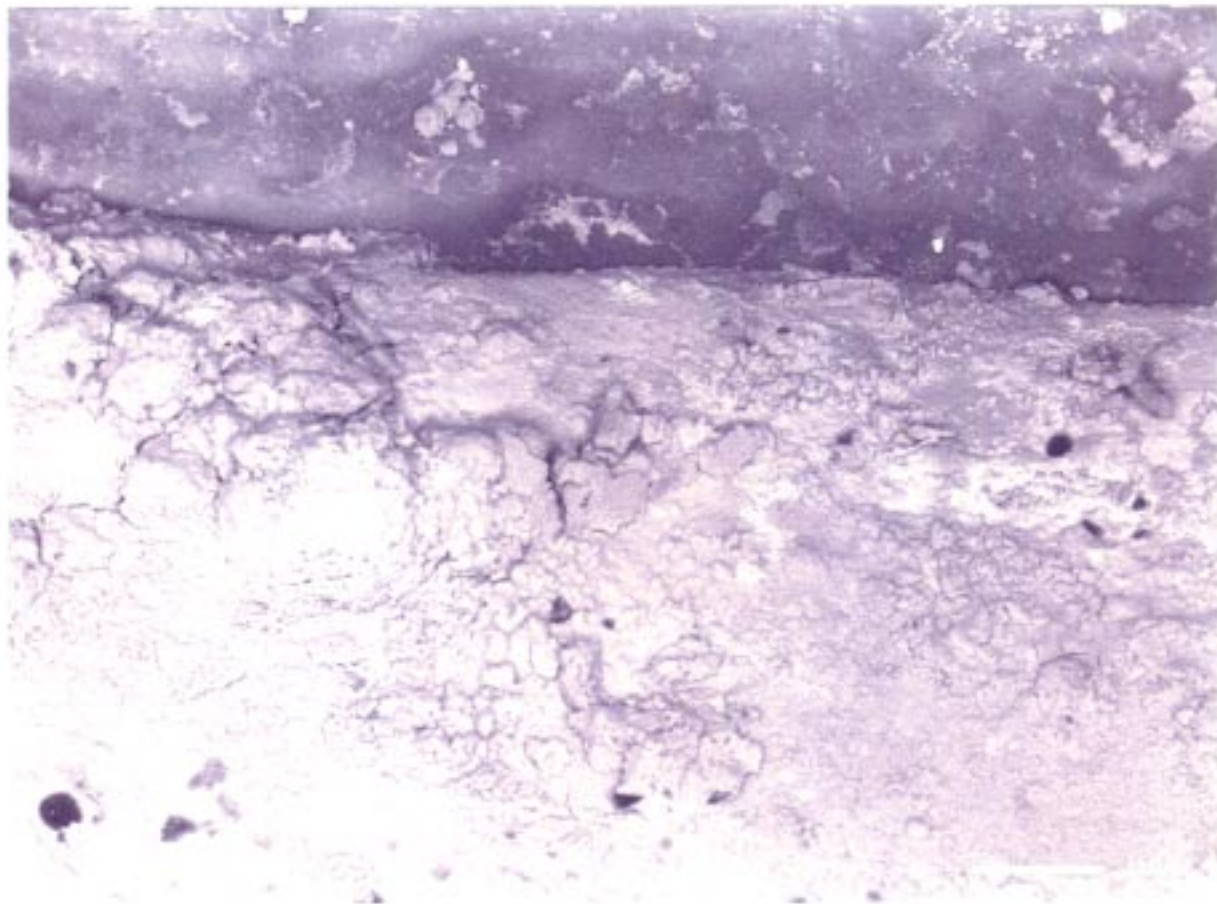


Figure 12. Base of the relay surrounding the glass to metal seal of N.O. contact A1.

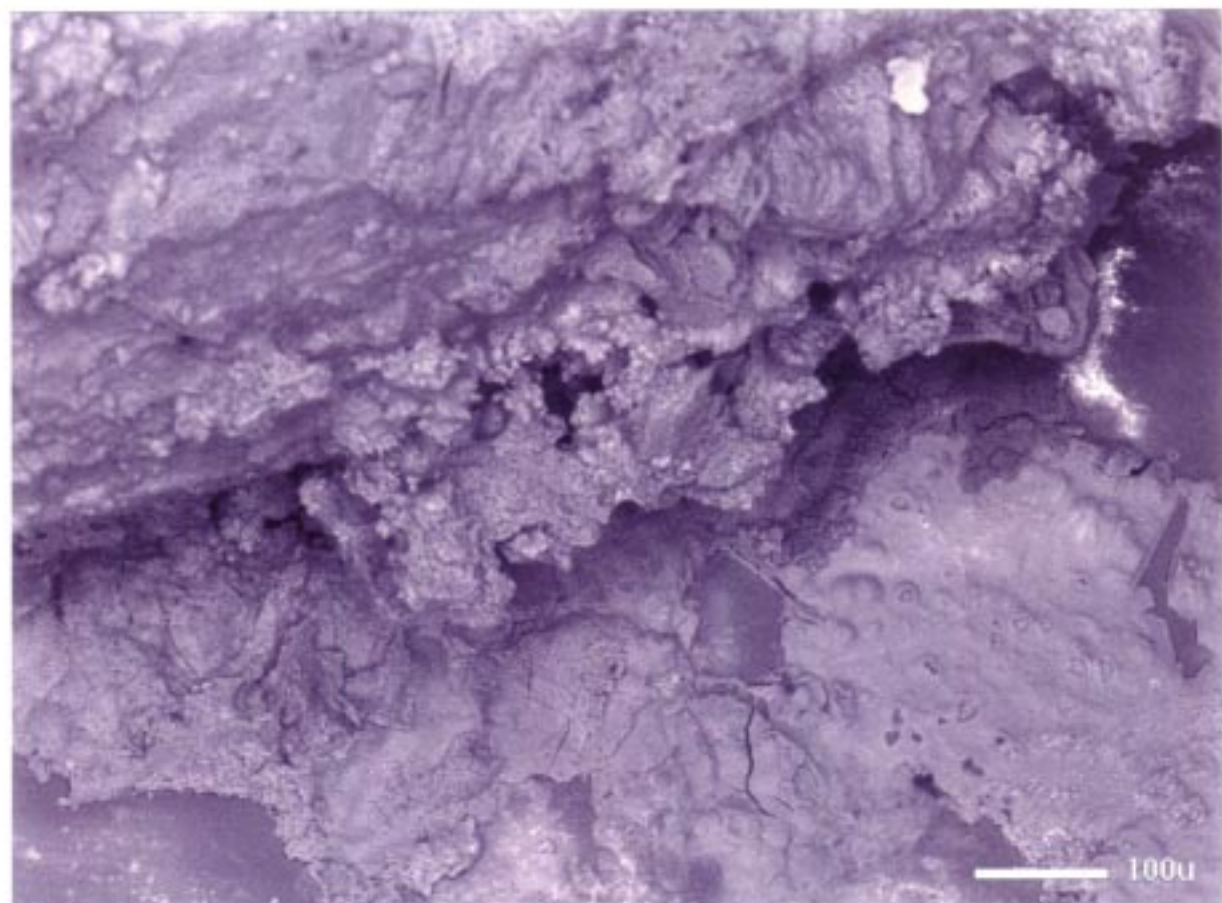


Figure 13. Base of the feedthrough pin and glass to metal seal of N.O. contact A1.

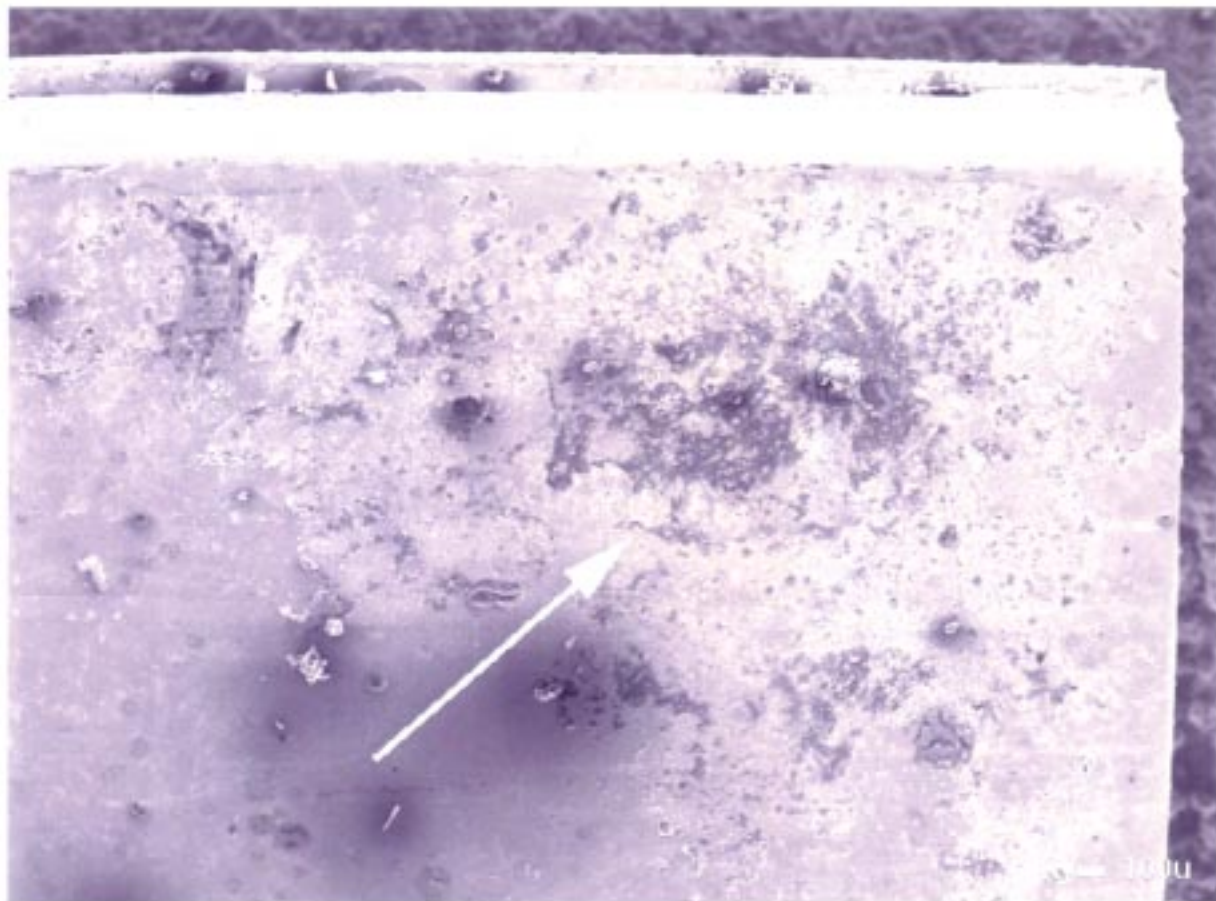


Figure 14. Mating surface of stationary contact A1. Arrow shows the residue covering the contact area.



Figure 15. Mating surface of moving contact A2. Arrow shows the contact area.

TWA 800 R296 Scavenge Pump Relay and
Reserve Transfer Valve Circuit Breakers
(Failure Analysis)

1 October 1997

Evaluation Report
(4349LABR/NTSB)

Report No. WL/MLS 97-086

AUTHOR

Dale Hart
(University of Dayton Research Institute)
Materials Integrity Branch (WL/MLSA)
2179 12TH Street Room 17
Wright-Patterson Air Force Base, Ohio 45433-7718

REQUESTER

Mr. Robert Swaim
National Transportation Safety Board
490 L'Enfant Plaza, East, S.W.
Washington DC 20594

DISTRIBUTION STATEMENT F: Further dissemination only as directed by National Transportation Safety Board (NTSB); 1 October 1997 or DoD higher authority.

000051

TABLE OF CONTENTS

	Page
LIST OF FIGURES	iii
PURPOSE	1
FACTUAL DATA	1
APPENDIX 1	16

LIST OF FIGURES

Figure		Page
1	As received condition of the SPR circuit breaker. The upper arrow highlights the corroded terminal hardware. The lower arrow highlights the missing actuator stem and mounting bushing.	6
2	As received condition of the SPR circuit breaker. The upper arrow highlights the corroded terminal hardware. The lower arrow highlights the cracked housing.	6
3	Various mechanical components of the SPR circuit breaker are corroded. The moving contacts are lying against the stationary contacts-	7
4	The moving contacts of the SPR circuit breaker have a tarnished appearance. White arrows highlight the mechanical wear from the making and breaking of the contacts. Black arrow highlights the fibrous residue.	7
5	The moving line contact of the SPR circuit breaker has a tarnished appearance. Black arrow highlights the mechanical wear from the making and breaking of the contacts. White arrow highlights the fibrous residue.	8
6	The moving load contact of the SPR circuit breaker has a tarnished appearance. The arrow highlights the mechanical wear from making and break of the contact.	8
7	The stationary line terminal and contact of the SPR circuit breaker have a tarnished appearance.	9
8	The stationary load terminal and contact of the SPR circuit breaker have a tarnished appearance.	9
9	The stationary line contact of the SPR circuit breaker has a tarnished appearance. Arrow highlights the mechanical wear from the making and breaking of the contacts.	10

000053

Figure		Page
10	The stationary load contact of the SPR circuit breaker has a tarnished appearance. Arrow highlights the mechanical wear from the making and breaking of the contacts.	10
11	Energy Dispersive Spectrometry (EDS) spectrum of the fibrous material on the moving line contact of the SPR circuit breaker.	11
12	EDS spectrum of a area described as being tarnished on the stationary line contact of the SPR circuit breaker.	11
13	As received condition of the RTV circuit breaker. Upper arrow highlights the corroded terminal hardware. Lower arrow highlights the missing actuator stem and mounting bushing.	12
14	As received condition of the RTV circuit breaker. Upper arrow highlights the corroded terminal hardware. Lower arrow highlights the cracked housing.	12
15	The various mechanical components of the RTV circuit breaker are corroded. The moving contacts are lying against the stationary contacts .	13
16	The moving contacts of the RTV circuit breaker have a tarnished appearance. White arrows highlight the mechanical wear from the making and breaking of the contacts. Black arrow highlights the fibrous residue.	13
17	The stationary line terminal and contact of the RTV circuit breaker have a tarnished appearance.	14
18	The stationary load terminal and contact of the RTV circuit breaker have a tarnished appearance.	14
19	EDS spectrum of the moving load contact surface of the RTV circuit breaker.	15
20	EDS spectrum of the stationary line contact surface of the RTV circuit breaker.	15

000054

**TWA 800 R296 Scavenge Pump Relay and Reserve Transfer Valve
Circuit Breakers**

PURPOSE

Determine the condition of the two submitted circuit breakers following their recovery.

FACTUAL DATA

R296 Scavenge Pump Relay Circuit Breaker (B #15)

The R296 Scavenge Pump Relay (SPR) circuit breaker, as received, is shown in Figures 1 and 2. The circuit breaker was manufactured by the KLIXON division of Texas Instruments (TI). The following information was molded and printed on the sides of the circuit breaker:

KLIXON
METALS & CONTROLS INC.
CORPORATE DIVISION OF
TEXAS INSTRUMENTS
INCORPORATED
MADE IN USA

1273

The following was printed on a fiberglass panel riveted to the body of the circuit breaker.

2TC6-1
MFD-0174A

Appendix 1 gives a breakdown of the mechanical and electrical components comprising a TI circuit breaker of this design.

A visual examination of the circuit breaker revealed the actuator stem and mounting bushing of the circuit breaker were missing. The plastic housing of the breaker was cracked in several locations. The load and line terminal hardware were still intact, however, they were corroded.

The Klixon side of the breaker was thinned by sanding through the wall of the plastic case. A knife was then used to carefully remove the remaining plastic to expose the interior of the breaker (Figure 3). An examination of the inside of the breaker revealed corrosion and a fibrous material. The thermal and compensator elements were observed to be corroded. The

000055

position of the bell crank on the compensator suggests the breaker is still in the set position. The spring between the bell crank and actuator stem assembly was no longer attached to the stem assembly. The moving line/load contacts were lying loosely against the stationary line/load contacts.

The moving contacts were removed for examination (Figure 4) . The surface of the contacts has a tarnished appearance. A fibrous material was present on the surface of the line contact. No arc erosion of the mating surfaces of the contacts was noted. No obvious witness marks were observed on the surfaces of the contacts . Some evidence of mechanical wear (smearing of the contact material) was evident on the surfaces of the contacts (Figures 5 and 6).

The stationary line/load contacts were also removed for examination (Figures 7 and 8) . The appearance of their surfaces was similar to that of the moving contacts. They have a tarnished appearance. No arc erosion of the mating surfaces of the contacts was noted. No obvious witness marks were observed on the surfaces of the contacts. Some evidence of mechanical wear (smearing) was evident on the surfaces of the contacts (Figures 9 and 10).

Analysis of relatively clean areas on the surface of the contacts in the scanning electron microscope (SEM) with energy dispersive spectroscopy (EDS) suggests the contacts are primarily silver . Analysis of areas on the contacts with the fibrous material suggests it is composed primarily of the elements carbon, oxygen, aluminum and silicon. Minor amounts of sodium, magnesium, chlorine and calcium are also present. The spectrum (Figure 11) of the fibrous material on the moving line contact is offered as an example. Analysis of an area of the contact described as having a tarnished appearance suggests it was composed primarily of the elements carbon, oxygen, sodium, magnesium, aluminum, silicon, chlorine, calcium, manganese, and iron. The spectrum (Figure 12) is offered as an example of a tarnished area on the stationary line contact. The silver in both spectrums is primarily from the contact material.

Reserve Transfer Valves 1 and 4 Circuit Breaker (B #16)

The Reserve Transfer Valve (RTV) circuit breaker, as received, is shown in Figures 13 and 14. This circuit breaker was also manufactured by the KLIXON division of Texas Instruments . The following information was molded and printed on the sides of the circuit breaker:

000056

KLIXON
METALS & CONTROLS INC.
CORPORATE DIVISION OF
TEXAS INSTRUMENTS
INCORPORATED
MADE IN USA

1070

The following was printed on a fiberglass panel riveted to the body of the circuit breaker.

2TC6-7½
BACC18Z7R
MFD-0370A

A visual examination of this breaker revealed damage similar to that seen in the scavenge pump breaker. The actuator stem and mounting bushing of the breaker were missing and the housing of the breaker was cracked. The load and line terminal hardware were still intact, however, they were corroded. Inside the circuit breaker corrosion and a fibrous material were observed. The thermal and compensator elements were also observed to be corroded. The position of the bell crank on the compensator suggests the breaker was still in the set position. The spring between the bell crank and actuator stem assembly was no longer attached to the stem assembly. The moving line/load contacts were lying loosely against the stationary line/load contacts (Figure 15).

The moving and stationary line/load contacts were removed for examination (Figures 16, 17, and 18). These contacts have a similar appearance to the ones examined from the scavenge pump circuit breaker. The surfaces of the contacts have a tarnished appearance. A fibrous material is covering the surface of the line contact. No arc erosion of the mating surfaces of the contacts was noted. No witness marks were observed on the surfaces of the contacts. Some evidence of mechanical wear (smearing) was evident on the surfaces of the contacts.

Analysis of the surfaces of the contacts by EDS produced spectrums similar to those of the scavenge pump circuit breaker. The spectrums of Figures 19 and 20 are from the moving load and stationary line contact surfaces. The silver in both spectrums is primarily from the contact material.

SUMMARY OF FINDINGS

A summary of the significant findings is offered as a result of the examination of the scavenge pump and reserve transfer

000057

valve circuit breakers.

External

The circuit breakers have impact damage as indicated by the missing actuator stems, mounting bushings, and cracked housings. The mounting hardware for the load and line terminals was corroded.

The mounting hardware for the load and line terminals were intact .

Internal

A fibrous material was present on many of the mechanical and electrical components of the circuit breaker.

The thermal and compensator elements of the circuit breakers were corroded.

The position of the beak of the bell crank on the compensators suggests they are still in the set position.

The moving load/line contacts were lying loosely against the stationary line/load contacts.

The mating surfaces of the line/load contacts did not exhibit signs of arc erosion.

The mating surfaces of the line/load contacts had some evidence of mechanical wear.

The mating surfaces of the line/load contacts did not exhibit signs of witness marks.

000058

REVIEWED BY

Edward L. White

EDWARD L. WHITE, Actg Team Lead
Electronic Failure Analysis
Materials Integrity Branch
Systems Support Division
Materials Directorate

PUBLICATION REVIEW: This report has been reviewed and approved.



GEORGE A. SLENSKI, Acting Branch Chief
Materials Integrity Branch
Systems Support Division
Materials Directorate

000059

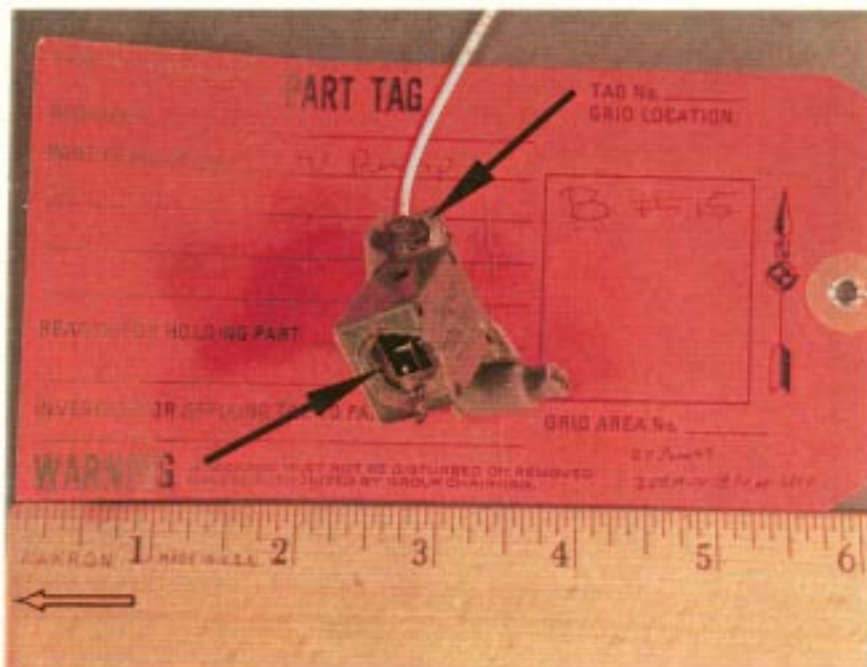


Figure 1. As received condition of the SPR circuit breaker. The upper arrow highlights the corroded terminal hardware. The lower arrow highlights the missing actuator stem and mounting bushing.

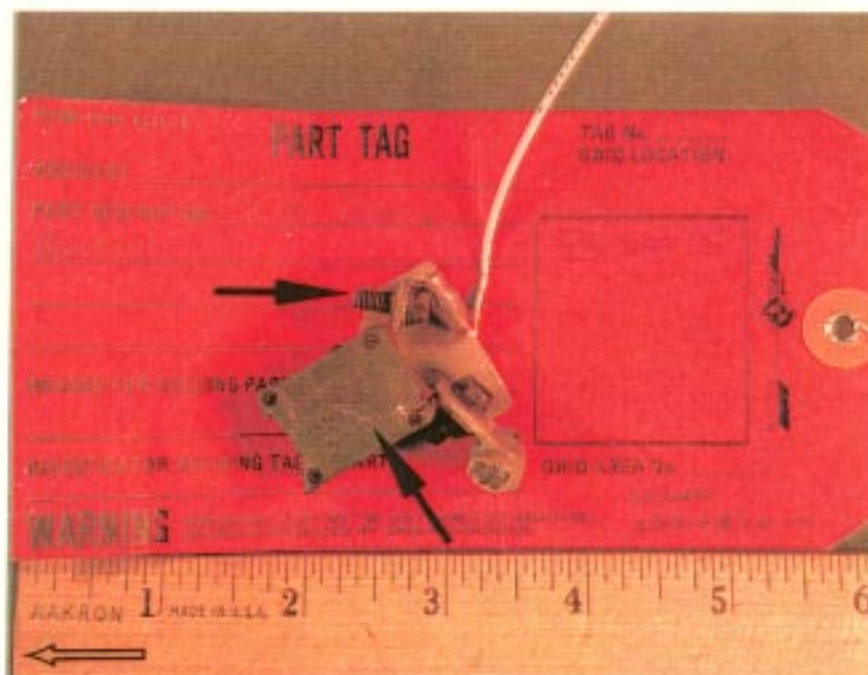


Figure 2. As received condition of the SPR circuit breaker. The upper arrow highlights the corroded terminal hardware. The lower arrow highlights the cracked housing.

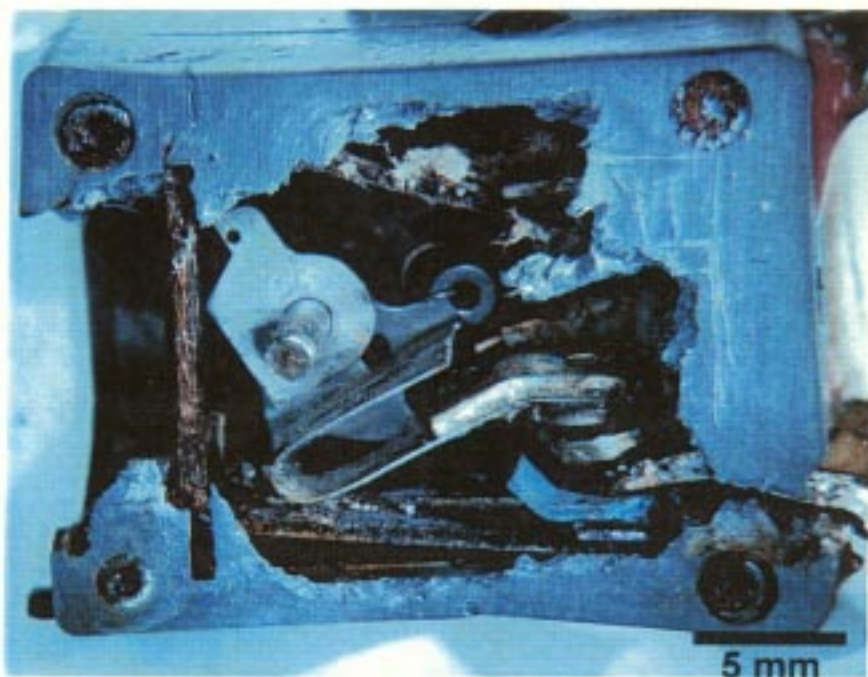


Figure 3. Various mechanical components of the SPR circuit breaker are corroded. The moving contacts are lying against the stationary contacts.

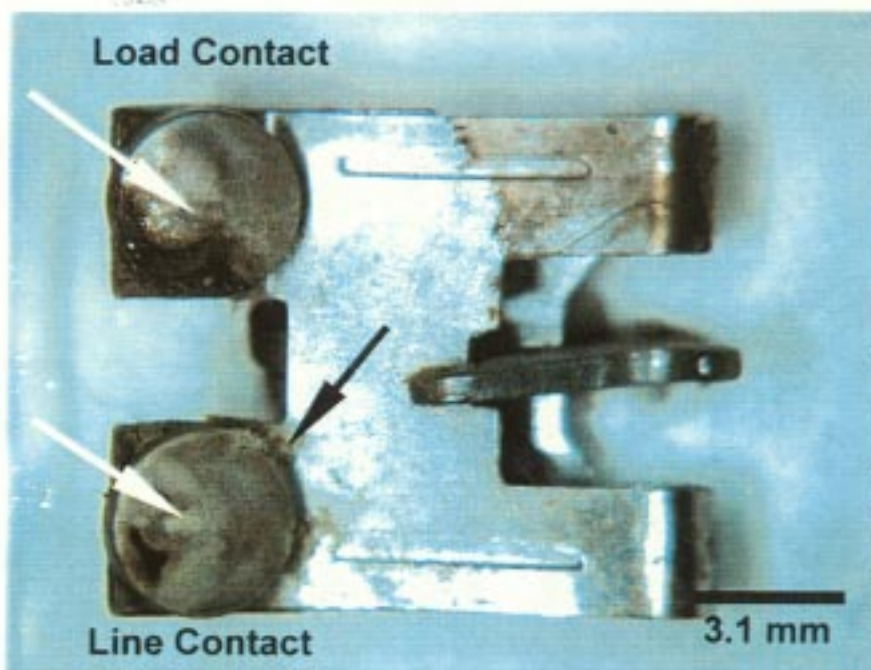


Figure 4. The moving contacts of the SPR circuit breaker have a tarnished appearance. White arrows highlight the mechanical wear from the making and breaking of the contacts. Black arrow highlights the fibrous residue.

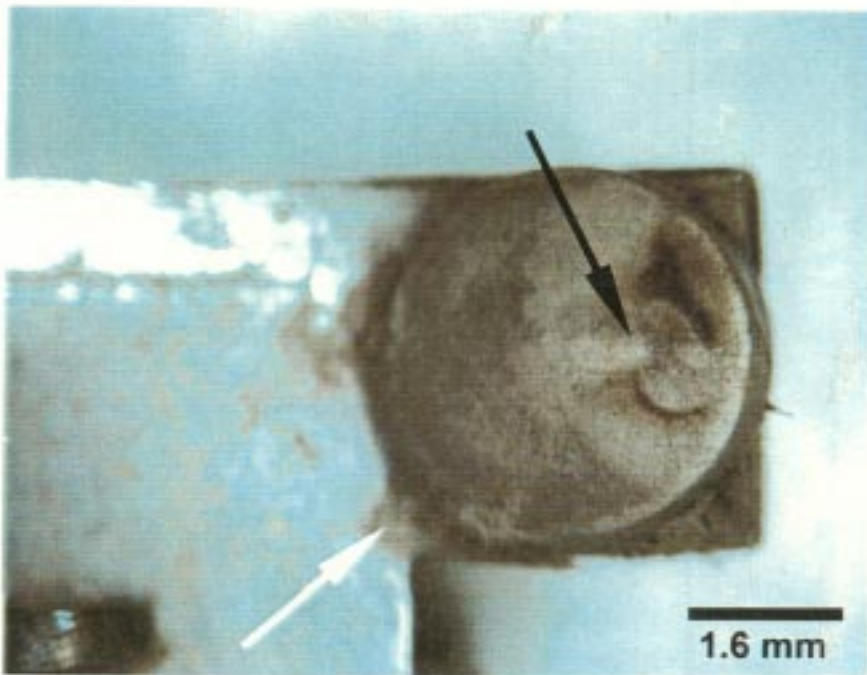


Figure 5. The moving line contact of the SPR circuit breaker has a tarnished appearance. Black arrow highlights the mechanical wear from the making and breaking of the contacts. The white arrow highlights the fibrous residue.

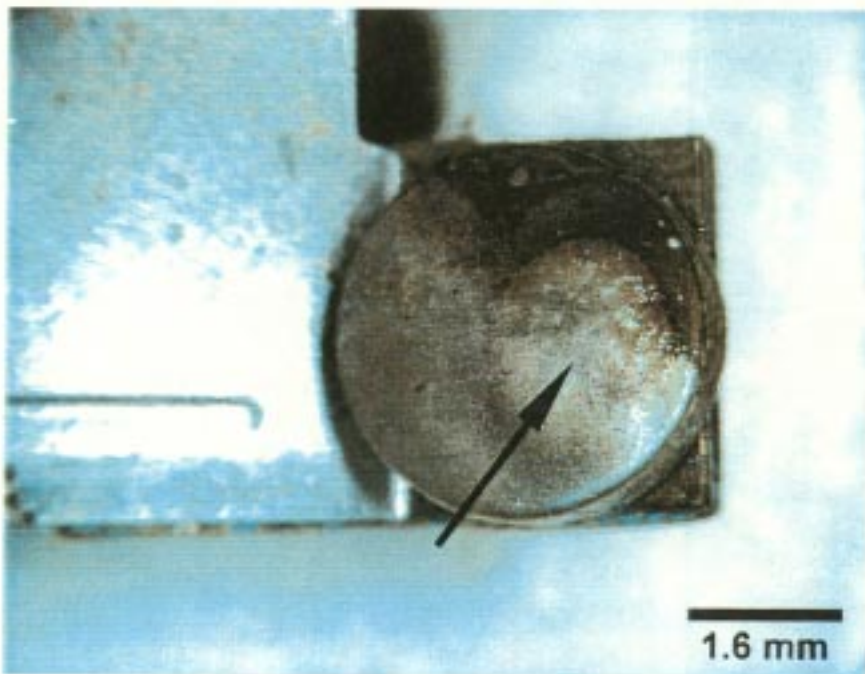


Figure 6. The moving load contact of the SPR circuit breaker has a tarnished appearance. The arrow highlights the mechanical wear from making and break of the contact.



Figure 7. The stationary line terminal and contact of the SPR circuit breaker have a tarnished appearance.

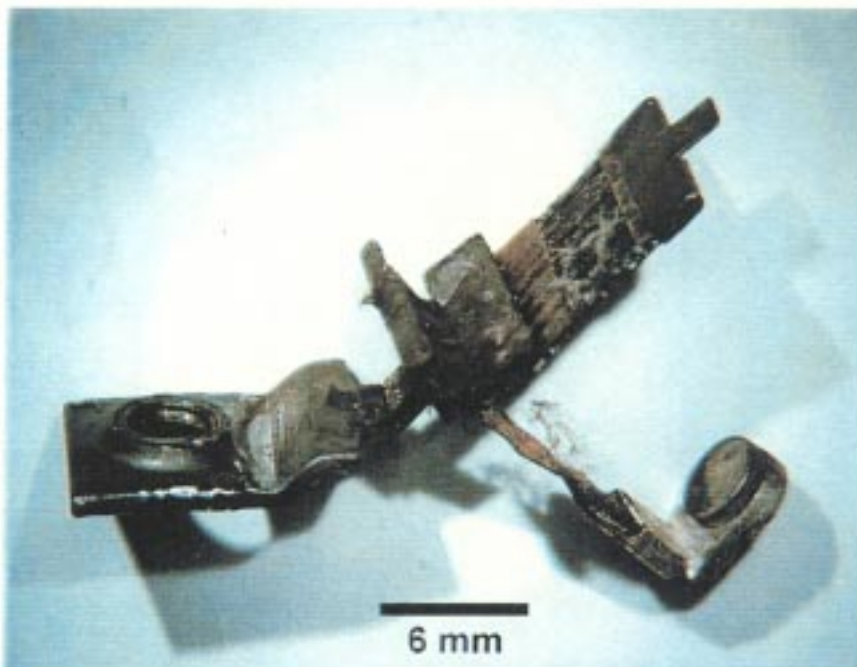


Figure 8. The stationary load terminal and contact of the SPR circuit breaker have a tarnished appearance.

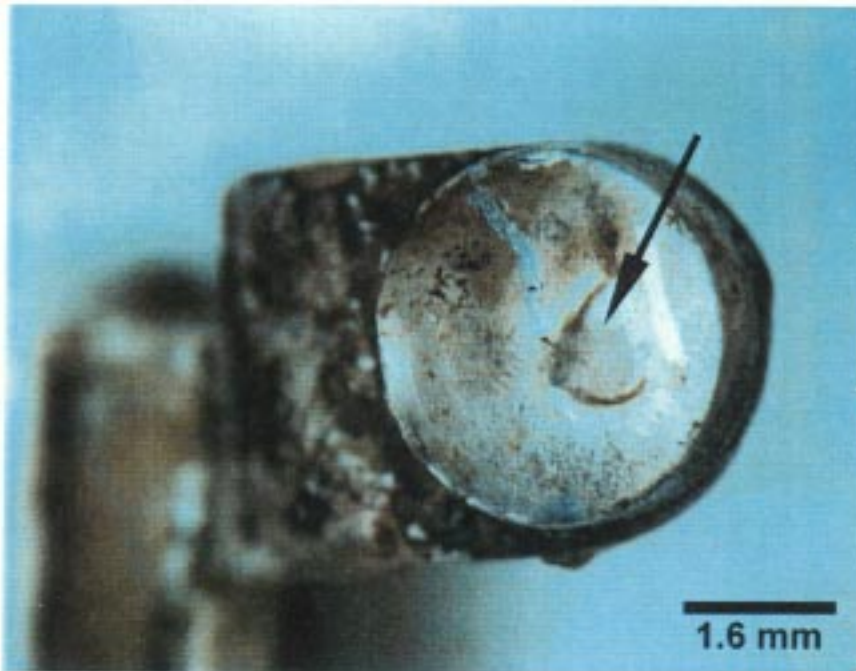


Figure 9. The stationary line contact of the SPR circuit breaker has a tarnished appearance. Arrow highlights the mechanical wear from the making and breaking of the contacts.

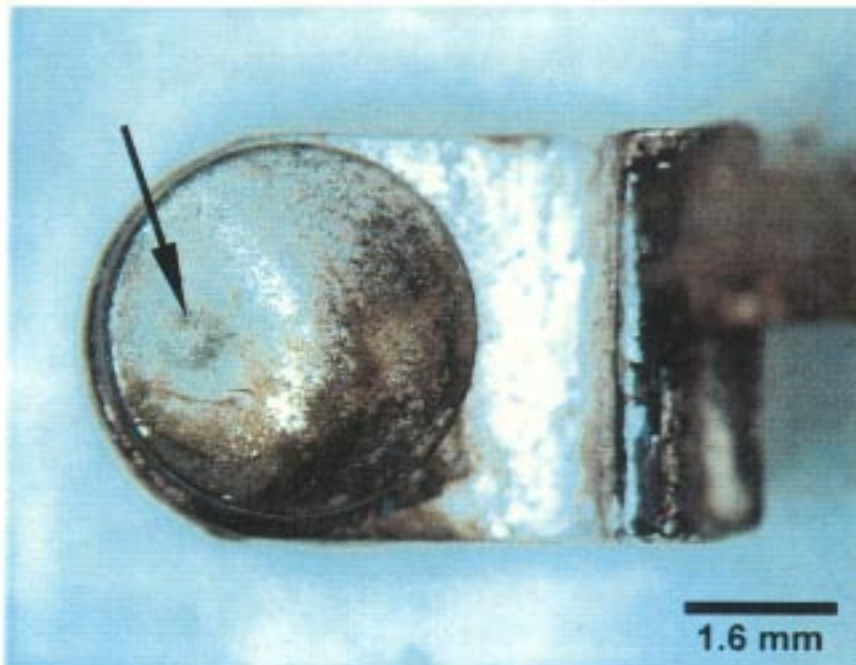


Figure 10. The stationary load contact of the SPR circuit breaker has a tarnished appearance. Arrow highlights the mechanical wear from the making and breaking of the contacts.

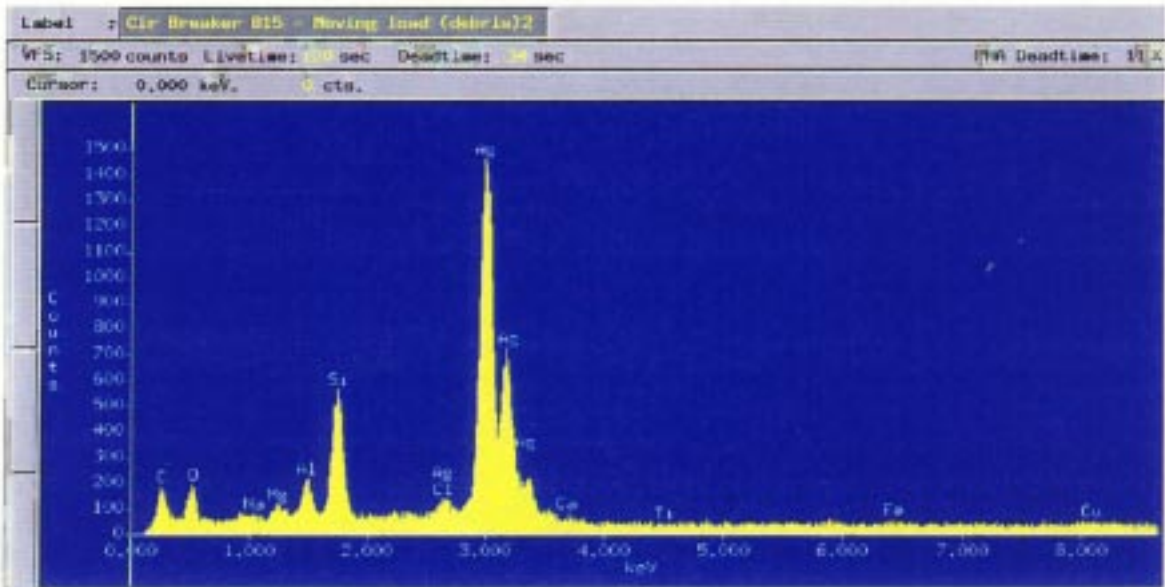


Figure 11. Energy Dispersive Spectrometry (EDS) spectrum of the fibrous material on the moving line contact of the SPR circuit breaker. The silver in both spectrums is primarily from the contact material.

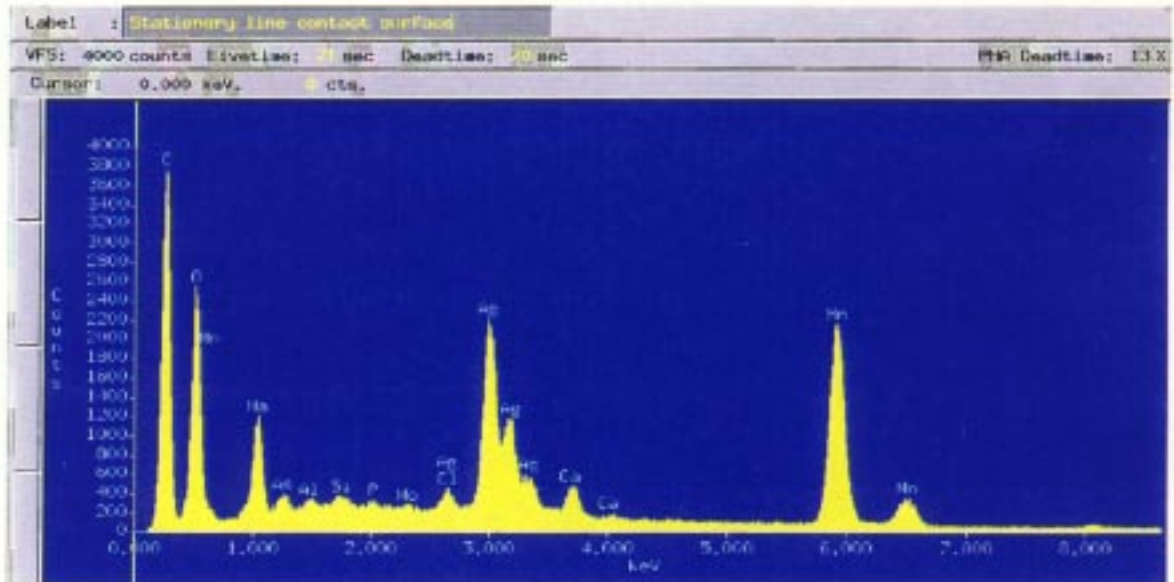


Figure 12. EDS spectrum of a area described as being tarnished on the stationary line contact of the SPR circuit breaker. The silver in both spectrums is primarily from the contact material.

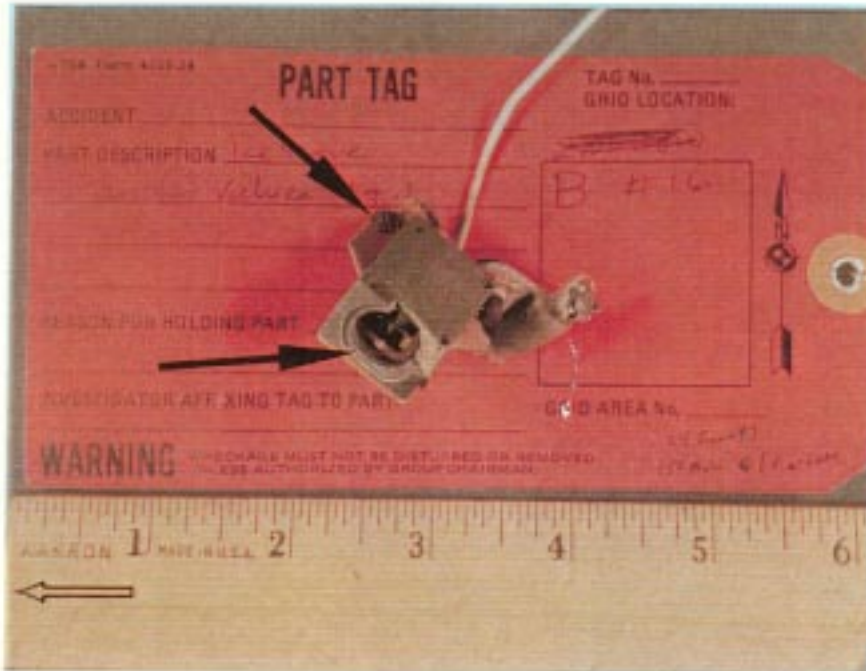


Figure 13. As received condition of the RTV circuit breaker. Upper arrow highlights the corroded terminal hardware. Lower arrow highlights the missing actuator stem and mounting bushing.

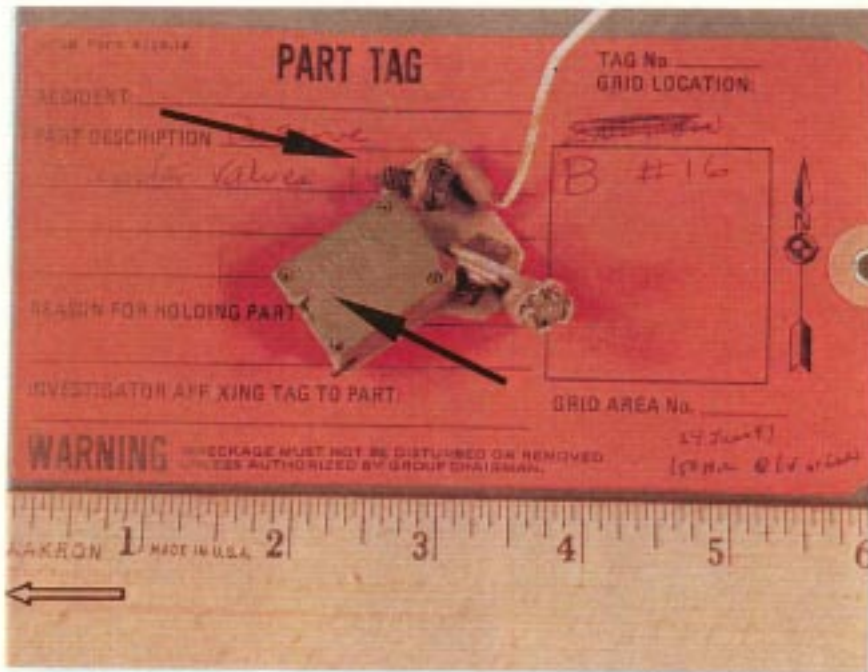


Figure 14. As received condition of the RTV circuit breaker. Upper arrow highlights the corroded terminal hardware. Lower arrow highlights the cracked housing.

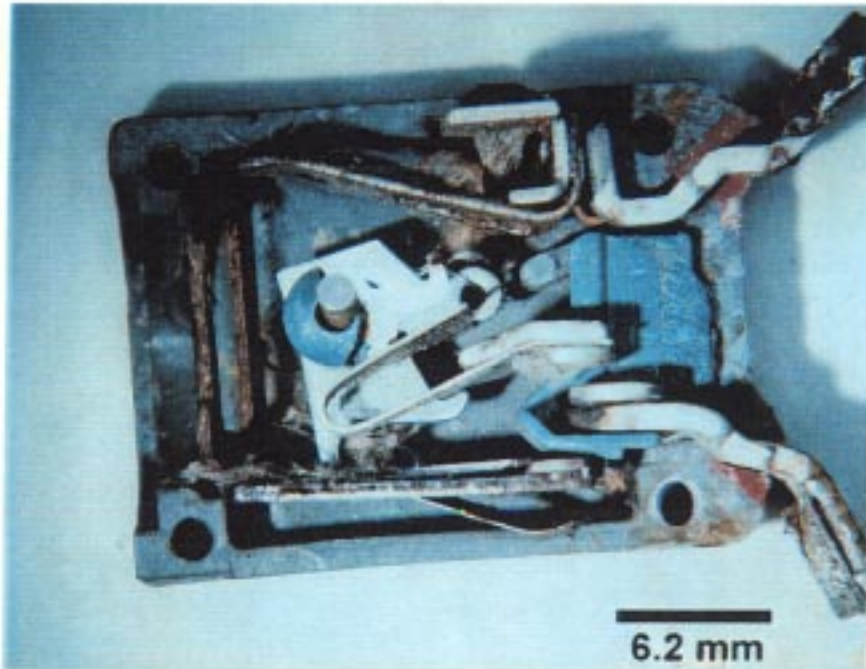


Figure 15. The various mechanical components of the RTV circuit breaker are corroded. The moving contacts are lying against the stationary contacts.

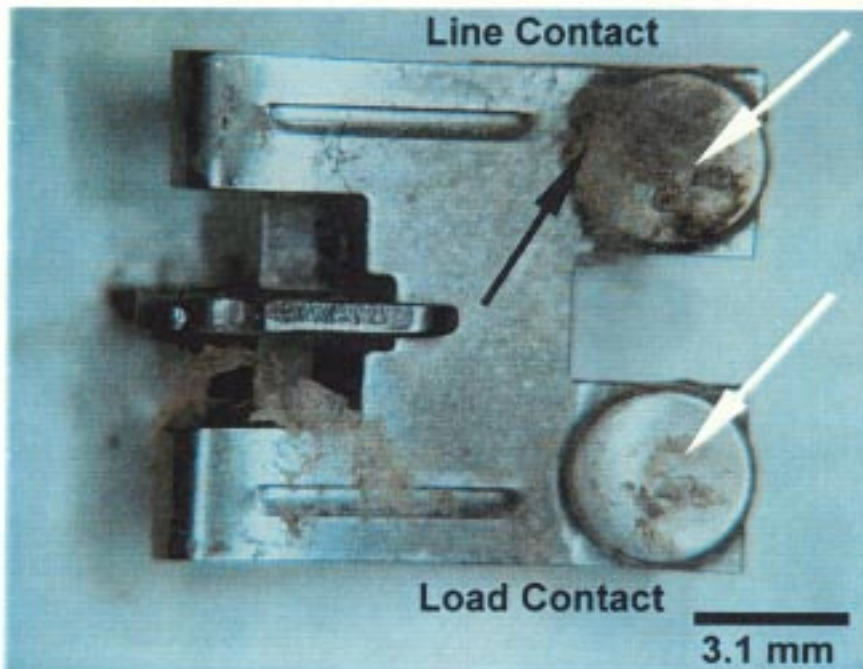


Figure 16. The moving contacts of the RTV circuit breaker have a tarnished appearance. White arrows highlight the mechanical wear from the making and breaking of the contacts. Black arrow highlights the fibrous residue.



Figure 17. The stationary line terminal and contact of the RTV circuit breaker have a tarnished appearance.



Figure 18. The stationary load terminal and contact of the RTV circuit breaker have a tarnished appearance.

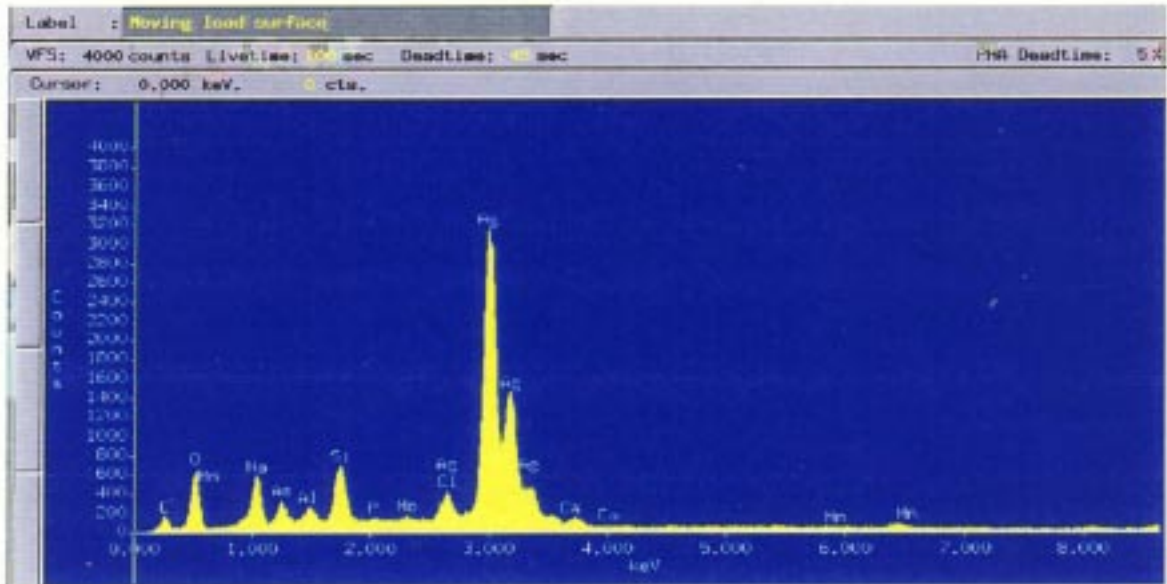


Figure 19. EDS spectrum of the moving load contact surface of the RTV circuit breaker. The silver in both spectrums is primarily from the contact material.

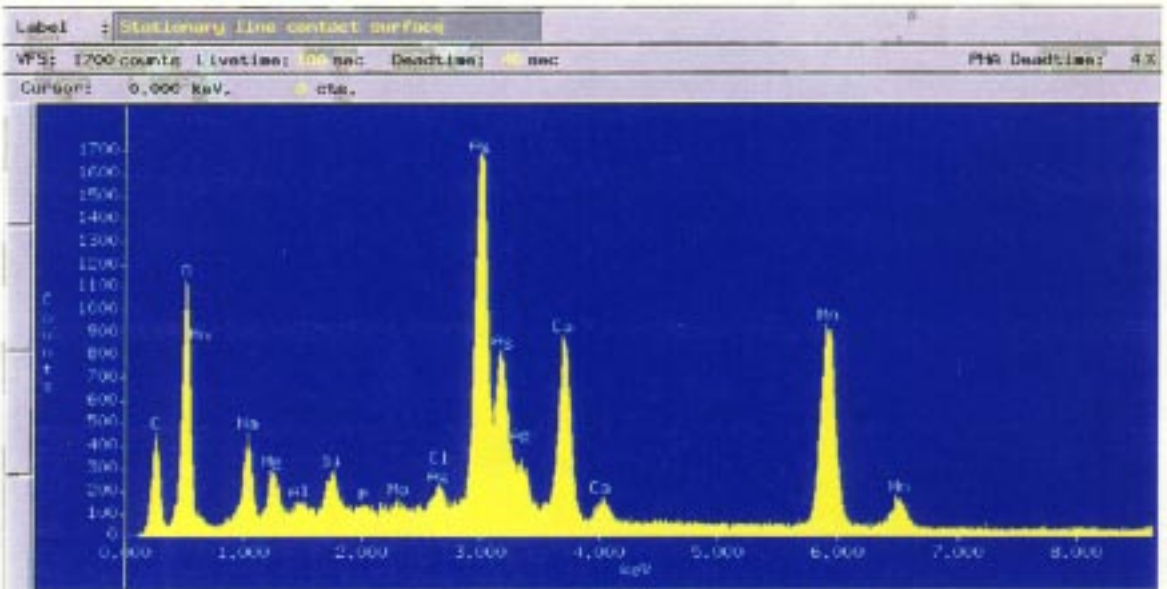
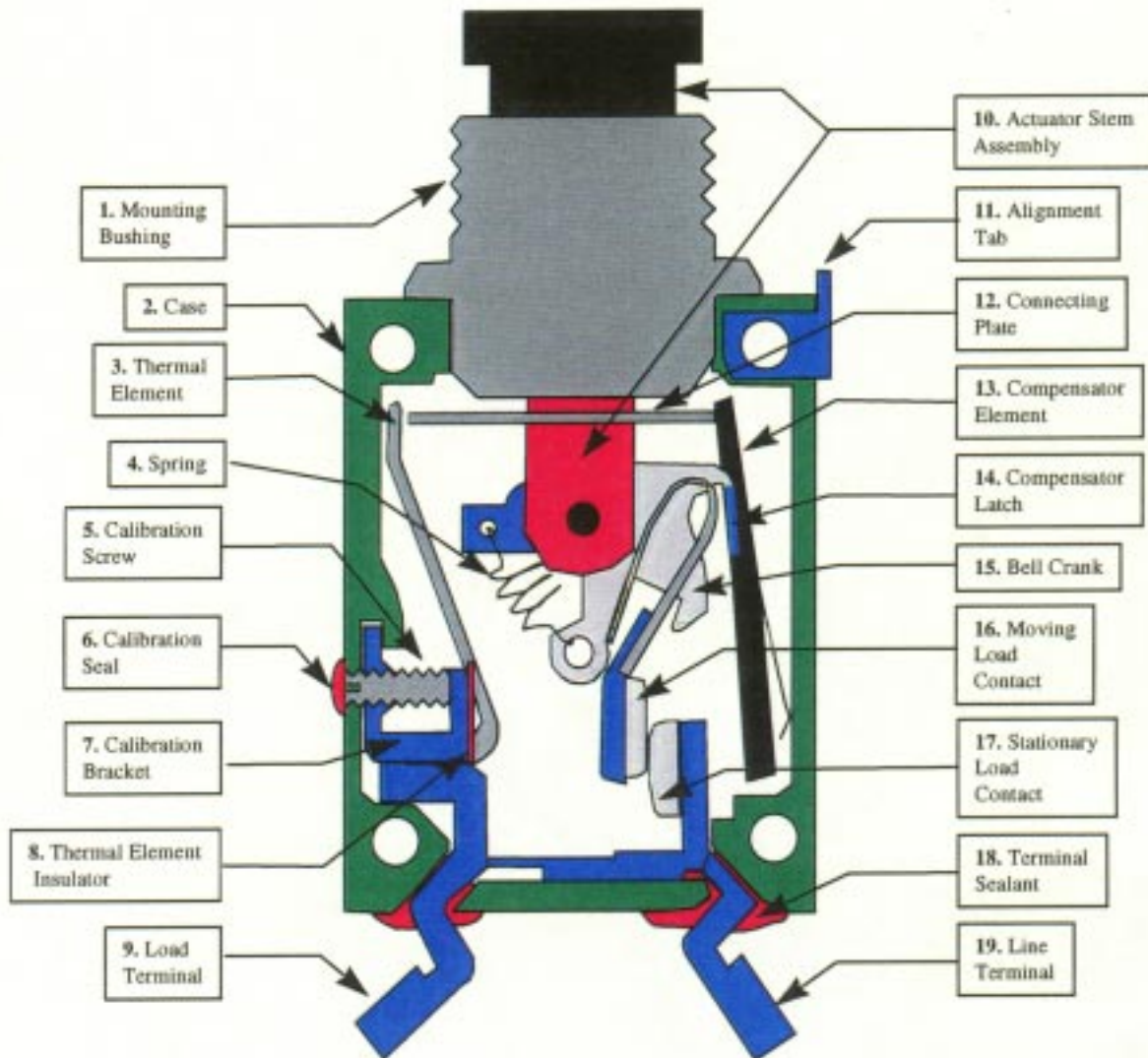


Figure 20. EDS spectrum of the stationary line contact surface of the RTV circuit breaker. The silver in both spectrums is primarily from the contact material.

Appendix 1

Circuit Breaker Parts Descriptions



Analysis of A Submitted Wire
(Failure Analysis)

21 October 1997

Evaluation Report
(43491NRD/NTSB)

Report No. WL/MLS 97-091

AUTHOR

George A. Slenski
Materials Integrity Branch (WL/MLSA)
2179 Twelfth Street Suite 1
Wright-Patterson Air Force Base, Ohio 45433-7718

REQUESTER

Mr. Robert Swaim
National Transportation Safety Board
490 L'Enfant Plaza, East, S.W.
Washington DC 20594

DISTRIBUTION STATEMENT F: Further dissemination only as directed by (National Transportation Safety Board) (21 October 1997) or DoD higher authority.

000072

ACKNOWLEDGMENTS

As is usual for this type of investigation the efforts of others are critical to its success. The author would like to thank Mr. John Ziegenhagen of the University of Dayton Research Institute for expert photography.

TABLE OF CONTENTS

	Page
LISTOFFIGURES.	iv
PURPOSE.	1
FACTUAL DATA	1
SUMMARY OF FINDINGS. - -	4

LIST OF FIGURES

Figure		Page
1	Wire sample submitted for analysis. The insulation exhibited blackened areas (black arrows) and mechanical damage (white arrows).	1
2	Multiple images of the largest blackened and thermally damaged area on the submitted wire.	2
3	Blackened and thermally damaged area on wiring. Note raised area (arrow) .	3
4	Typical mechanically damaged insulation area. Note the damage reveals the multiple layered insulation construction.	4

Analysis of A Submitted Wire

PURPOSE

Examine submitted wire for evidence of electrical arc damage.

FACTUAL DATA

A 73 cm length of primary wire was submitted by the National Transportation Safety Board (NTSB) for analysis (Figure 1).

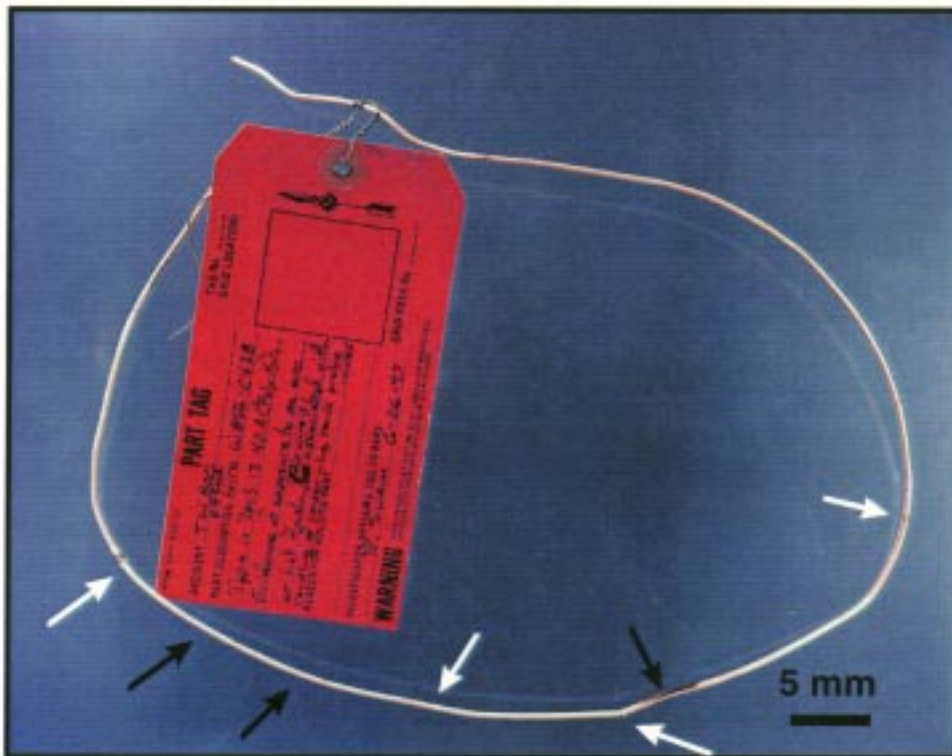


Figure 1. Wire sample submitted for analysis. The insulation exhibited blackened areas (black arrows) and mechanical damage (white arrows).

The wire was removed from TWA 800 wreckage on 26 June 1997 and was reported to be a BMS 1342A (Poly-X) type wire that was associated with the routing of center wing tank probe wires. There were three blackened areas (black arrows, Figure 1) and at least four mechanically damaged areas (white arrows, Figure 1) on the wire insulation. The blackened areas were typically associated with thermal damage. Multiple orientation images of the largest blackened area are shown in Figure 2.

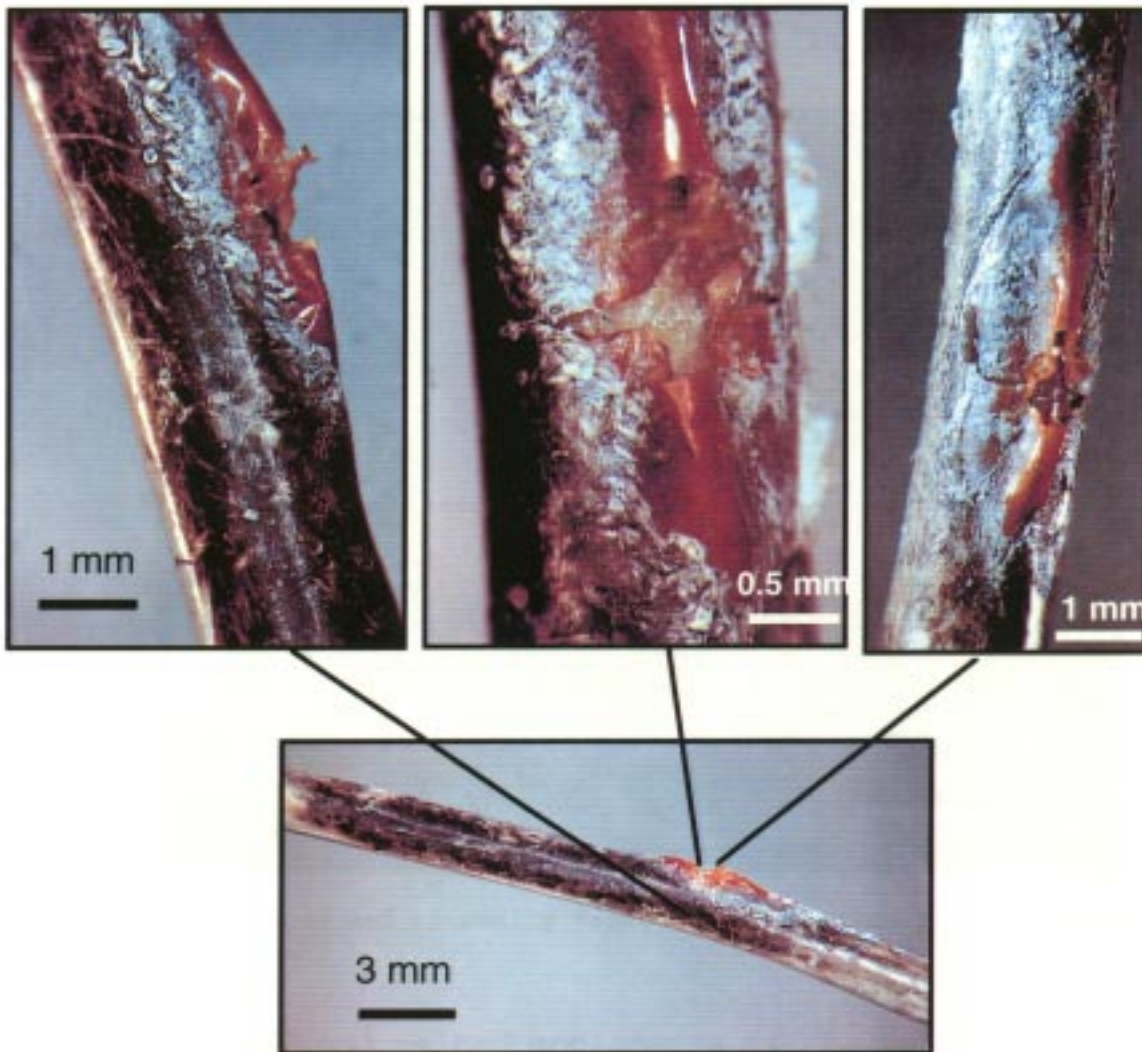


Figure 2. Multiple images of the largest blackened and thermally damaged area on the submitted wire.

Note the black residue on the insulation surface and mechanical damage to the multi-layered insulation. The amber tape was not carbonized and only exhibited mechanical damage. The black residue was easily removed mechanically from the insulation surface. Another blackened and raised area is shown in Figure 3.

000077

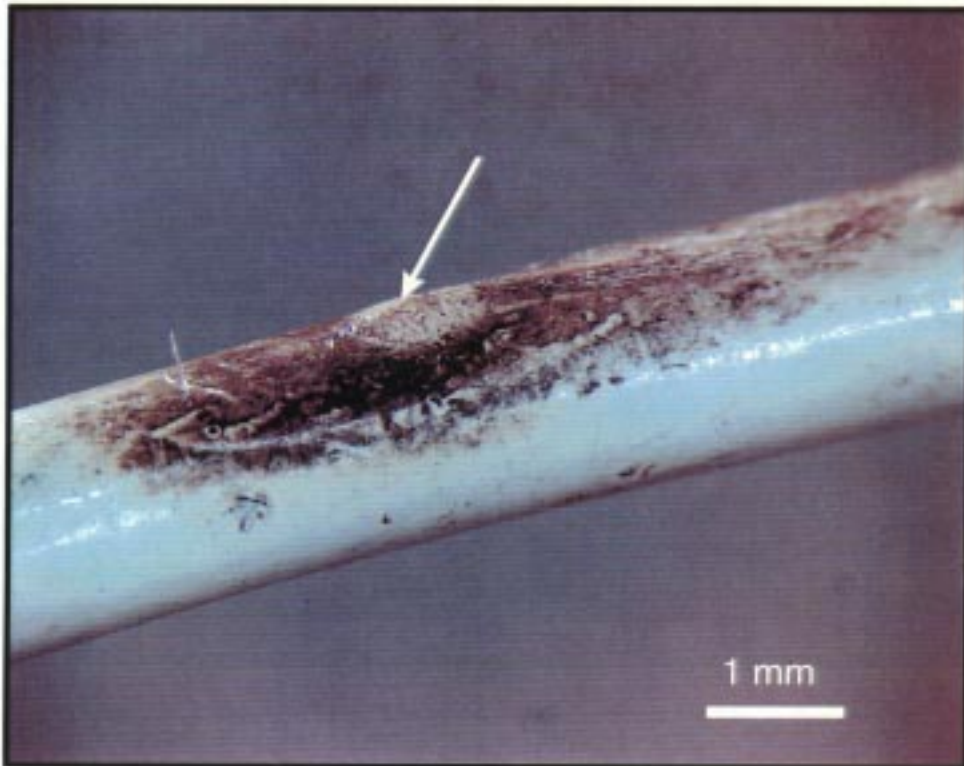


Figure 3. Blackened and thermally damaged area on wiring. Note raised area (arrow).

Note the crazed and melted appearance of the raised area. In all cases, the thermal damage progressed from the outside towards the conductor. A typical example of a mechanically damaged insulation area is shown in Figure 4.

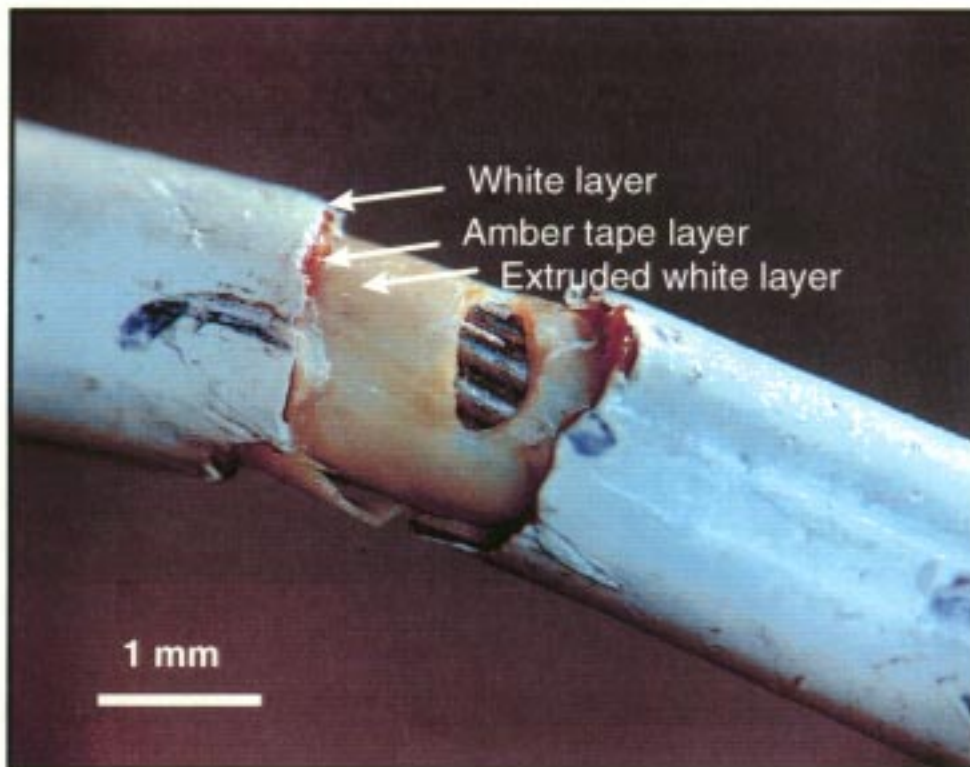


Figure 4. Typical mechanically damaged insulation area. Note the damage reveals the multiple layered insulation construction.

The insulation was flexible and bending of the insulation outside damaged areas did not produce cracks.

SUMMARY OF FINDINGS

There was no evidence of carbonization of the insulation or melting of exposed conductors which are typically associated with arc damage.

The thermal insulation damage progressed from the outside toward the conductor. This implies the insulation was exposed to an external thermal source.

The black residue could be removed mechanically.

Mechanical damage was isolated and there was no evidence of insulation embrittlement.

000079

PREPARED BY



GEORGE A. SLENSKI
Structural Failure Analysis
Materials Integrity Branch
System Support Division
Materials Directorate

REVIEWED BY

Edward L. White

EDWARD L. WHITE, Acting Team Lead
Structural Failure Analysis
Materials Integrity Branch
Systems Support Division
Materials Directorate

PUBLICATION REVIEW: This report has been reviewed and approved.



GEORGE A. SLENSKI, Acting Branch Chief
Materials Integrity Branch
Systems Support Division
Materials Directorate

000080

Electrostatic Charge Generation from
Turbine Fuels
(Material Evaluation)

29 October 1997

Evaluation Report
(43491HRD/NTSB)
(3048IHRD/1000)
(GOVP9702/9703)

Report No. WL/MLS 97-097

AUTHORS

Steven C. Gerken
and

Michael J. Manders
Materials Integrity Branch (WL/MLSA)

Dexter Kalt
Univ of Dayton Rsrch Institute

Cynthia Obringer
Fuels Branch (wL/POSF)

Marlin D. Vangsness
Univ of Dayton Rsrch Institute

REQUESTER

Mr. Robert L. Swaim
National Transportation Safety Board
490 L'Enfant Plaza East, S.W.
Washington, DC 20594

DISTRIBUTION STATEMENT F: Further dissemination only as directed
by National Transportation Safety Board (NTSB); 29 October 1997
or DoD higher authority.

000081

ACKNOWLEDGMENTS

This effort would not have been possible without the dedicated efforts of others. The authors would like to thank Mr. Tim Gootee Fuels and Lubrication Division, Wright Laboratory, for assistance with material procurement and setup and execution of tests.

TABLE OF CONTENTS

	Page
LIST OF FIGURES	iii
LIST OF TABLES	iv
PURPOSE	1
BACKGROUND	1
FACTUAL DATA	2
DISCUSSION(S)	10
SUMMARY OF FINDINGS	18
APPENDIX	44

LIST OF FIGURES

Figure		Page
1	Test facility.	23
2	Cushioned loop clamps.	24
3	Wiggins coupling.	24
4	Target plate current versus target plate angle (screen/no screen) (April 11).	25
5	Target plate current versus fuel temperature (April 10).	25
6	Target plate current versus target plate angle (screen/no screen, fuel CU) (April 11) .	26
7	Target plate current versus target plate angle (orifice to target plate distance) (April 9, 10, and 11) .	26
8	Minimum ignition energy curves and system test data points.	27

LIST OF TABLES

Table		Page
1	JFK Fuel Analysis	28
2	Wright Laboratory Fuel Analysis	29
3	Dry Electrical Measurements (Phase I)	30
4	Breakdown Voltage Measurements (Phase I)	37
5	Dry Electrical Measurements (Phase II)	38
6	Breakdown Voltage Measurements (Phase II)	40

000085

Electrostatic Charge Generation from Turbine Fuels

PURPOSE

Assess the electrostatic charging characteristics of electrically isolated or partially isolated conductors when subjected to turbine fuel impingement. Specific attention is given to aircraft fuel system components that might be the recipient of fuel impingement due to a leak in the pressurized fuel system. Also determine the electrical properties of the conductors (e.g. , resistance and capacitance) used in (1) the assessment of electrical isolation, and (2) the calculation of discharge energy that might be achieved through the charging process. Other goals were to ascertain whether significant electrostatic energies could be obtained through fuel misting or from fuel on fuel impingement.

BACKGROUND

Early in 1997 The National Transportation Safety Board (NTSB) contacted Wright Laboratory (WL) concerning the possibility of performing fuel tests in support of the ongoing TWA-800 accident investigation. The tests were to assess the charging characteristics of electrically isolated or partially isolated conductors when subjected to turbine fuel impingement. Conductors such as unbended loop clamps and couplings were to be used in the tests. The WL fuel laboratory, WL/POSF, had an existing fuel rig capable of handling the fuel impingement and test conditions to be investigated. The WL ESD control laboratory, WL/MLSA, supplied the electrostatic equipment necessary to perform the required measurements. This report summarizes a series of tests at WL between 1 March 1997 and 30 May 1997. A description of the individual tests run can be found in the Appendix and will be referred to throughout this report by their number. NTSB funded the tests under two contracts with WL.

The Phase I program (tests 1 through 26) was a one-week program to analyze electrostatic charging capabilities of fuel spraying on actual aircraft hardware. The facility was altered so that the NTSB investigation team could witness the tests by remote video. The fuel used for the Phase I testing was Jet-A from JFK. At the conclusion of Phase I the maximum charge generated was approximately 650 volts on a Teflon® cushioned loop clamp. The results of Phase I warranted further investigation and a Phase II program was developed.

000086

The Phase II study (tests 27 through 69) was a continuation of the Phase I study to further investigate electrostatic charging from fuel impingement on electrically isolated conductors . The Phase II study further investigated five scenarios : (1) the breakdown voltage of actual aircraft hardware under non fuel wetted conditions; (2) the potential of charge build up in a fuel mist; (3) the potential for charge build up due to fuel sprayed onto the surface of a fuel; (4) a parametric study of fuel impinging upon an aluminum target plate; and (5) further aircraft hardware studies as deemed necessary. The Phase II study was performed at WL over several weeks. The Safety Board party was present during the week of 7 April 1997 to witness parts 2, 3, and part of part 4. WL performed the remainder of the tests with Dr. Joe Leonard from Naval Research Laboratory representing the NTSB.

FACTUAL DATA

DEFINITION(S)

Triboelectrification/Tribocharging: The generation of electrostatic charges when two materials make contact or are rubbed together, then separated.

FUELS

For use in Phase I, fuel was shipped to WL from JFK. The USAF Aerospace Fuels Laboratory at Wright-Patterson Air Force Base, Ohio analyzed the fuel. The results of the analysis can be found in Table 1.

For Phase II testing, a Jet-A fuel that was on hand at WL was used. This fuel was known as 96POSF3305. The fuel was analyzed and the results of the analysis can be found in Table 2. For Phase II testing, several fuels were blended at WL by adding additives to base fuel 96POSF3305. The additives used were corrosion inhibitor, BHT antioxidant, metal deactivator (MDA) , DiEGME icing inhibitor, and conductivity additive Stadis-450. These additives were added to Jet-A to form JP-8. The amount of additive added was the amount required by specification in JP-8 unless otherwise noted. Betz thermal stability additive, currently under study to increase fuel thermal stability, was also added at 260 ppm. JP-8 with the Betz additive will be referred to as JP-8+100 in this report. Stadis-450 was added in various quantities to control the conductivity level. For several tests Jet-A fuel was clay treated to remove particulate, this will be annotated under the test conditions where appropriate.

ORIFICES

Throughout Phase I and Phase II tests, six different orifices were used to initiate a fuel leak. All of the orifices were manufactured from stainless steel caps. All but one of the orifices were manufactured using EDM. The diameter of the hole or the shape of the hole will be used to refer to the orifices if it was not round. The tests were run at three different pressures, 15, 25 and 42 psig. The orifices were calibrated at each pressure by collecting the spray in a bucket for a set time and measuring the volume. All calibrations were done with the test fuel at room temperature. A characterization of each of the orifices follows.

0.04 Inch Orifice: A single holed orifice with a 0.04 inch diameter was run at three pressures. Two calibrations were done at each pressure. The results were:

Pressure psig	Time minutes	Volume ml	Flow Rate ml/min
15	2	730	365
15	2	720	360
25	2	1000	500
25	2	1000	500
42	2	1310	655
42	2	1305	652.5

0.056 Inch Orifice: This orifice was only used at 42 psig. The orifice was calibrated at 42 psig for two minutes. The collected volume was 3740 ml, for a flow rate of 1870 ml/min.

0.07 Inch Orifice: This orifice was only used at 42 psig. The flow rate was calibrated to be 2,700 ml/min at 42 psig.

Five Hole Orifice: This orifice was made with five 0.030 inch diameter holes. There was one hole in the middle with four holes equally spaced around it. The orifice was calibrated at 25 psig for two minutes. The collected volume was 3900 ml, for a flow rate of 1,950 ml/min.

Slotted Orifice: A 0.063 inch by 0.016 inch slot was manufactured. The flow through the slot was very laminar so a fine mesh screen was added to the orifice to break up the fuel exiting the orifice. Two calibrations were run at 25 psig for 30 seconds. The collected volumes were 2100 ml and 1950 ml for a flow rate of 4200 and 3900 ml/min. All tests, including the calibrations, were run with the fine mesh screen inserted.

000088

Cracked Orifice: A cracked orifice was manufactured by first freezing the orifice in liquid nitrogen and then cracking it using a wedge. The crack was very irregular, resulting in an unstable flow and thus was unable to be calibrated. The flow rate of the crack was much higher than that of any of the other orifices .

TEST FACILITY

The tests were conducted at the WL fuels laboratory in a test chamber that could easily be modified to handle the required tests . A diagram of the test facility, as altered for the tests, can be found in Figure 1. The fuel was pumped from a recirculation tank through 60 feet of line before being delivered to the test chamber. The excess fuel was recirculated back to the recirculation tank. A centrifugal pump with a 60 psig/50 g.p.m. capacity was used. The fuel in the recirculation tank could be heated to 120°F. The 60 feet of line was installed downstream of the pump to give the fuel time to relax before reaching the test chamber. The test chamber was an enclosed metal cabinet that was nitrogen purged during the tests to eliminate the potential for fuel ignition. During Phase I testing, a Lexan viewing window was constructed to seal the entire front opening of the test chamber. This window was not used during Phase II testing. Instead, the front metal doors of the test chamber were closed to seal the chamber. For Phase II testing, a small Lexan viewing window was constructed on top of the test chamber. The fuel temperatures reported for Phase I were measured by a thermocouple located in the recirculation tank. For Phase II a thermocouple was placed in the fuel feed line downstream from the orifice.

EQUIPMENT LIST

Hewlett Packard Model HP4192A Impedance Analyzer: Provided capacitance measurements of isolated conductors.

Ion Systems Model 200 Charged Plate Monitor: Provided voltage measurement of isolated conductors.

Monroe Model 268A Charged Plate Monitor: Provided voltage measurement of isolated conductors.

Keithley Model 614 Electrometers: provided current and charge measurements.

3M Model 961 Ionized Air Blower: Used to neutralize charges on insulative surfaces such as the Lexan viewing window.

000089

ETS Model 512 Humidity Controller/Sensor: Provided percentage relative humidity measurements inside the enclosed test chamber.

Prostat Model PFM-711A Field Meter: Provided electric field strength measurements of various items. Used primarily to measure the electric field strength on the Lexan viewing window.

ACL Model 400 Field Meters: Provided electric field strength measurements during the fuel mist cloud testing and during the fuel spray on a pool of fuel tests.

Beckman Industrial Model L-10A Megohmmeter: Provided resistance measurements using variable test voltages.

ASTM F 150 Five Pound Electrodes: Used to measure the volumetric resistance of various o-rings. The o-ring to be tested was placed on a flat conductive surface with the ASTM F 150 electrode placed on top of it.

Hewlett Packard Model HP7132A Chart Recorder: Provided strip chart recordings of various signals measured by the test instrumentation.

Spool, 28 AWG Kynar Wiring: Provided electrical connection between the test items and the test instrumentation.

Fluke Model 77 Multimeter: Provided digital voltage readout of the output signal from the ACL 400 field meter.

Hewlett Packard Model E2378A Multimeter: Provided digital voltage readout of the output signal from the ACL 400 field meter.

Prostat Model PHT770 Hygro-Thermometer: Provided room temperature and percentage relative humidity measurements.

Lecroy Model 93141 Oscilloscope: Provided data acquisition and storage of various signals measured by the test instrumentation.

ISOLATED CONDUCTORS

Cushioned Loop Clamps: Loop clamps are used to support aluminum tubing and parallel aluminum tubing from primary fuel/vent lines in fuel tanks on aircraft. Per specification, the clamps were constructed of aluminum alloy or low carbon steel and cushioned with various materials. The cushion makes direct contact with the clamped tube or fuel/vent line. The cushion material of the clamps used for this study included,

000090

Polytetrafluoroethylene, PTFE (Teflon®), fluorosilicon, and nitrile. The type of cushion material will be noted for each test involving a loop clamp. A picture of the loop clamps can be found in Figure 2.

Wiggins Coupling: A fitting used to join adjacent sections of fuel tubes or vent lines on aircraft. The fitting allows for limited movement of connected lines through internal o-rings. The o-rings can be made of various materials including, nitrile, fluorosilicon, fluorocarbon, Viton, and Teflon®. The Wiggins couplings used in the testing were provided by NTSB and will be referred to by the "T" designation that was inscribed by NTSB. The "T" designators were located at the end of each fuel tube joined by a Wiggins coupling. A picture of a Wiggins coupling can be found in Figure 3.

Target Plate: An 8 by 12 inch aluminum target plate was used for the Phase II parametric study. The target plate was coated on one side with Boeing MBS 10-20 epoxy chromate primer. A smaller 4 x 3.5 inch uncoated aluminum target plate was also used in a few of the tests.

Fuel Collection Tank: A 32 x 14 x 10 inch fuel tank was used to collect the fuel being sprayed. The tank was coated on the bottom and up to 6 inches on the sides with the same Boeing MBS 10-20 epoxy chromate primer as the target plate. A siphon drain was used to control the fuel level within the tank.

PHASE I TESTS

The tests conducted in Phase I have been summarized in the Appendix, tests 1 through 26. The Appendix also gives a brief description of the tests conducted, date performed, test conditions, summary of results, and relative comments about the test. A summary of the dry electrical measurements and breakdown voltage measurements can be found in Tables 3 and 4, respectively.

Dry electrical measurements were made on Wiggins couplings, loop clamps, and o-rings supplied by NTSB. A one-inch Wiggins coupling and three, one-inch o-rings numbered 7 through 9 were supplied by WL/PO. The results of these measurements can be found in Table 3. A megohmmeter set at the specified test voltage was used for all resistance measurements unless otherwise noted. The anodized surfaces of the components were filed down to the underlying metal at the measurement connection points, before connection with the megoheter or impedance analyzer. O-ring volume resistance measurements were made by placing the o-ring on an isolated conductive plate with an ASTM F 150 electrode on top of it. The female to male shell resistance was

000091

checked for electrical continuity between those components. The male and female resistance to fuel tube measurements were a measure of the electrical isolation between the conductive shell components of a Wiggins coupling and its associated fuel tubes. The fuel tube to fuel tube resistance measurement gives an indication of the electrical isolation across a Wiggins coupling without a tube to tube bond wire installed. An impedance analyzer was used to measure the capacitance of the test items. The quality (Q), dissipation (D), and conductance (G) parameters were included with these measurements for supplemental information. Also noted was whether or not a safety wire was installed on the Wiggins coupling.

Fuel impingement tests were conducted in the test chamber using the Teflon® loop clamp, fluorosilicon loop clamp, Wiggins coupling T11/T12 Wiggins coupling T7/T8, and a WL/PO Wiggins coupling. The results of these tests can be found in the Appendix. Tests 3 through 5, 13 through 21, 23, and 24 were conducted with the Teflon® loop clamp. The fluorosilicon loop clamp was tested in test 10. Tests 7 and 8 were for Wiggins T11/T12, tests 9 and 11 for Wiggins T7/T8, and test 26 for the WL/PO Wiggins coupling. Test 26 was conducted after installing the highest resistance fluorocarbon o-rings readily available. To perform the fuel impingement tests, the test item was placed on a support stand beneath the orifice. The associated fuel tube(s) for the test item was bonded to the chassis of the grounded test cabinet. The chassis grounds for the test equipment used during these tests were also grounded at this same location. A bond wire was attached to the test item and routed through a small hole in the Lexan viewing window and attached to a charged plate monitor. Before the start of each spray test, any charge accumulated on the test item was removed by the "zero" button on the charged plate monitor. The surface of the Lexan viewing window was also ionized to reduce any electric fields originating from it. Jet-A fuel from JFK was sprayed from the orifice onto one of the isolated test items mentioned above. The spray test continued until it was determined that little or no additional gain in voltage potential would be achieved on the test item as a result of continued fuel impingement. Test variables, such as fuel temperature, orifice type, orifice to test item distance, and fuel flow rate were changed in the different tests. This was done in an attempt to achieve maximum voltage on the test item. For each test item, at least one resistance and capacitance measurement was made before and after the item was wetted with fuel. These measurements were made with the test item in place inside the test chamber and connected to the charged plate monitor. Streaming current measurements were also made during some of the fuel impingement tests. Streaming currents were measured by attaching the input cable from the electrometer to the electrically isolated section of tubing in

000092

the fuel supply lines. This section of tubing was located downstream of the fuel orifice inside the test chamber. This stainless steel section of three-quarter inch tubing measured 6 inches in length- Nylon ferrules were used to provide the electrical isolation.

Breakdown voltages of the Teflon® and fluorosilicon loop clamps, along with the T7/T8 Wiggins coupling, were measured. Results for these measurements can be found in Table 4. The test was conducted by applying voltage to the test article with the fuel tube grounded. The voltage on the test article was increased until a spark occurred. The breakdown voltage on the Teflon® loop clamp was measured for several gap distances between the clamp and fuel tube. Breakdown voltages for the Wiggins coupling could not be measured, due to insufficient electrical isolation between the coupling and the fuel tube.

PHASE II TESTS

The tests conducted in Phase II have been summarized in the Appendix, tests 27 through 69. The Phase II summary is in the same format that was used for Phase I. Dry electrical measurements and breakdown voltage measurements were also taken in Phase II. These results can be found in Tables 5 and 6, respectively.

The first test of Phase II (test 27) involved resistance measurements of the fuel collection tank described earlier in this report. An ASTM F 150 five-pound electrode was placed in the fuel collection tank. A megohmmeter was used to measure the resistance from the electrode, through the thin layer of epoxy chromate primer, to ground. The test voltage used on the first measurement was 100 volts. The high resistance reading of the first measurement (Appendix, test 27) prompted a second resistance measurement using the next higher available megohmmeter test voltage of 200 volts. These measurements were taken in preparation for two tests. The first test measured the electric field strength of a fuel mist cloud. The second test measured the electric field strength on the surface of a pool of fuel while fuel was sprayed upon it. These two types of tests were conducted concurrently with the use of two field meters. One field meter was mounted in the upper area of the test chamber to measure the electric field strength from a charged fuel mist that might be present during the test. The direction of measurement for this meter was horizontal across the width of the chamber. A second field meter was mounted with a vertical direction of measurement above the surface of fuel in the fuel collection tank. This meter measured the electric field strength originating from the surface of the fuel while fuel was sprayed onto its surface. The output of each field meter was connected

000093

to separate digital multimeters located external to the test chamber. The magnitude of voltage measured by the field meters, while fuel was sprayed during the test, was observed and recorded from the digital multimeters displays. The results of these tests, along with the specific test conditions, can be found in the Appendix, tests 28 through 31.

Fuel impingement tests were conducted in the test chamber during Phase II using the target plate described earlier in this report. A summary of these tests can be found in tests 32 through 42, 44 through 47, 49 through 51, and 56 in the Appendix. The fuel impingement tests conducted in Phase II were performed similarly to those conducted in Phase I. However, there were several alterations made to the test chamber for Phase II. An electrically conductive bar was mounted through the width of the test chamber. The bar allowed for rotation of the target plate that was attached to it. The bar was rotated during some of the fuel impingement tests to change the angle of fuel impact. Before test 49, this bar was grounded through contact with the test chamber walls and by a ground wire bonded at one end of the bar. The target plate was attached to the bar, but it was electrically isolated from the bar with the use of Teflon® sheeting. Beginning with test 49, the bar was electrically isolated from the wall of the test chamber using insulative sleeves and the grounded bond wire was removed. The target plate was clamped directly to the bar without the Teflon® insulation to provide electrical continuity to the bar. The reasons for these changes can be found in the discussion section of this report. The fuel collection tank was electrically isolated from ground to allow for charge or current measurements when desired, otherwise the tank was grounded through a bond wire. During some of the fuel impingement tests, a conductive screen was inserted into the fuel spray before the fuel spray reached the target- The Appendix contains notation under the test condition portion as to whether or not the screen was used for a specific test. Wires were bonded to the target plate and the fuel collection tank and routed through small holes in the wall of the test chamber. These two wires were insulated from the wall of the test chamber with insulative sleeving. These wires could be individually grounded, attached to a charged plate monitor, or attached to an electrometer as required for the particular test to be conducted.

Tests were conducted to determine whether or not the fuel spray exiting the orifice was charged before making contact with the test item. A conductive container was electrically isolated and suspended beneath the fuel orifice through the use of insulative cable ties. The input wire on an electrometer was connected to the conductive container. The amount of charge collected in the container over a period of time was measured

000094

with the electrometer. Measurements of target plate current and fuel collection tank currents were also recorded. The results of these tests, along with the specific test conditions, can be found in the Appendix, tests 52 and 53.

Several tests were conducted by dripping fuel onto a target plate as opposed to the continuous stream type of sprays that were used in the other fuel impingement tests. Test 54 in the Appendix was performed using the same fuel supply tubing and orifice configuration from the fuel impingement spray testing. The orifice outlet cap was loosened just enough to allow fuel to drip onto the target. Tests 55, 58, 61, 62, 64, and 65 were performed using a glass burette container of jet fuel with a grounded aluminum orifice for the source of the fuel drip. To measure the resultant voltage for these tests, the target plate was connected to the charged plate monitor. Fuel with and without additives was used as noted for each test.

Fuel resistance measurements were performed using an apparatus consisting of a glass beaker and two metal electrodes. The electrodes measured 1 x 2 x 1/16 inches each. The electrodes were submerged in the fuel with the face of the electrodes parallel. The approximate electrode spacings used in these tests were 1, 2, and 3 inches. A megohmmeter was used to measure the resistance between the two electrodes using test voltages of 10, 50, 100, 500, and 1000 volts. The types of fuel used and the results of the tests can be found in the Appendix, tests 57, 59, and 60.

Further dry electrical and breakdown voltages measurements were conducted on a Wiggins coupling as part of Phase II. These measurements were made in a similar fashion as described in the Phase I portion of this report. Measurements were made with both Teflon® and Viton o-rings installed in Wiggins coupling T7/T8. The results of these tests, along with the specific test conditions, can be found in the Appendix, tests 43, 63 and 68. In an attempt to electrically isolate the Wiggins coupling from the internal fuel tube, various configurations were tried. The configurations included the reduction in clamping force (shell tightness), removal of the internal locking ring, removal of the internal split rings, and changes in the relative position of the fuel tubes with respect to the Wiggins coupling.

DISCUSSION(S)

When reviewing the results of the tests performed in the Appendix, it is important to note there is some inherent instability in the measurements performed based upon the nature of the tests conducted. Factors such as electrical noise, test instrumentation settling and display update time, stray electric

000095

fields, and other factors more specific to the type of test being performed all contribute to this instability. Efforts were made to record the most accurate results possible for all measurements. It is understood the same measurements recorded by different personnel may show small differences in values.

PHASE I TESTS

The objective of Phase I testing was to measure the amount of charge produced on an isolated conductor due to impingement of charged fuel on the conductor and triboelectrification from fuel passing over the conductor. The conductors chosen for Phase I testing were from actual aircraft hardware and included Wiggins couplings and cushioned loop clamps. Both dry and wet tests were performed. Dry tests focused on the resistance and capacitance values of the couplings and clamps and components thereof. Wet testing consisted of spraying jet fuels onto the chosen conductors and measuring the generated voltage and fuel streaming current. Jet-A fuel from JFK airport was used during Phase I as mentioned previously in this report. Several variables were monitored and controlled during the wet test portions of Phase I. Fuel type, temperature, conductivity and pressure were monitored and controlled. Orifice (nozzle) type and orifice distance from the target test item (e.g., Wiggins coupling or loop clamp) were recorded. The initial and final resistance and capacitance measurements of the target item were also recorded. Ambient humidity within the test chamber was also monitored to ensure an adequate nitrogen purge was achieved.

Dry testing provided very useful information in determining the test item most likely to charge during wet testing. A summary of the Phase I dry electrical measurements can be found in Table 3. The goal was to find the item with the highest electrical resistance, with respect to the fuel tube to which each was connected. The higher the resistance, the better isolated the item was from the fuel tube, thus allowing for more charge or voltage to accumulate. Additionally, a larger item capacitance would result in more energy ($E = 1/2CV^2$) storage within the test item before discharge, given the same voltage potential on each item. The electrical isolation properties of the Wiggins couplings were very poor. This was due in part to the relatively low resistance of the inner o-rings that provided freedom of movement of adjacent fuel tube sections that it coupled together. As shown in Table 3, when measured independently, these o-rings varied in resistance from thousands of ohms to $1E12$ ohms. The resistance of the o-ring dropped when installed in the Wiggins coupling due to increased surface area contact with the inner wall of the coupling. The o-rings were thought to provide electrical isolation between the outer Wiggins shell and the fuel tubes. It was discovered later that the

000096

internal conductive components of the Wiggins coupling were almost always in contact with the surfaces of the Wiggins shell and fuel tubes. All surfaces of the Wiggins coupling were anodized and testing showed this anodized layer broke down at approximately 250 volts. Hence, when potentials reached approximately 250 volts, the outer shell of the Wiggins coupling would short to the fuel tube. The loop clamp with the Teflon® cushion had the best electrical isolation with respect to its fuel tube. The resistances measured were consistently much greater than $1E12$ ohms. Measured capacitance was found to be much greater for the Wiggins couplings than the loop clamps. The Wiggins coupling capacitance measurements ranged from approximately 90 to 10,000 picofarads. The capacitance of the loop clamps ranged from approximately 33 to 722 pF. The large variation in capacitance can be attributed to the quality of the insulating material between the conductive elements of the clamp or coupling. Low resistance o-rings or cushioning materials are poor insulating materials. Because of this, the capacitance is said to be of poor quality or "leaky" .

Based upon the results obtained during Phase I dry testing, it was decided that the Teflon® cushioned loop clamp would be the first item of choice for wet testing. During wet testing conducted on 4 March 1997, the Lexan viewing window of the test chamber, and similar materials used to support the item under test, became highly charged. This charging process originated from the fuel spray impinging upon the inner surface of the Lexan and on the support stand. Using a field meter, voltages as high as 5000 volts were measured. The highest charge concentration was on the lower half of the Lexan window. Since this could influence the item under test, a conductive mesh screen was applied to the lower half of the Lexan window. Aluminum foil was also placed around the support stand to suppress its electric field. The highest voltage measured on these surfaces, after the modifications, was approximately 350 volts with most areas less than 200 volts. Initially, resistance and capacitance measurements were made before and after the Teflon® cushioned loop clamp was sprayed with fuel. Changes in these measurements were found to be insignificant after monitoring them in the early tests of Phase I. Because of this, only the initial measurements of resistance and capacitance were recorded for the remaining tests. The small change in capacitance from 74 to 86 picofarads, in the early tests, was due to the additional length of wiring required after adding the conductive mesh to the Lexan window. The addition of the conductive mesh required the wire connecting the test item to the test instrumentation be moved up above the conductive mesh, thus the additional length of wire. The Teflon® loop clamp test results can be found in the Appendix, tests 3 through 5, 13 through 21, 23, and 24. Many factors had an affect on the maximum voltage potential measured during these

000097

tests . Fuel flow rate, fuel pressure, fuel orifice to target distance, fuel temperature, and isolation resistance generally increased the magnitude of the resultant voltage. Changes in the orifice style and in the fuel conductivity also had an affect on the voltages measured. The highest voltage potential measured on the Teflon® cushioned loop clamp during Phase I testing was -650 volts . A second loop clamp was also wet tested during Phase I. The results for this flourosilicon loop clamp can be found in the Appendix, test 10. The low voltage potential measured on this loop clamp can be attributed to the decrease in electrical isolation resistance when compared to the Teflon® loop clamp. Wet testing of Wiggins couplings was also conducted during Phase I and the results can be found in the Appendix, tests 7, 8, 9, 11, and 26. The maximum voltage potential measured during these tests was -14 volts. The insufficient electrical isolation of the Wiggins couplings as mentioned previously was responsible for the low voltage measurements.

The resistance of many materials decreases with a corresponding increase in applied test voltage. In an effort to determine what affect this may have on jet fuels a test was conducted. A Teflon® loop clamp attached to the small section of fuel tubing was completely submerged in jet fuel. Resistance measurements were made with a megohmmeter at different test voltages. The results of these tests are shown in the Appendix, test 25. As can be seen from the test results, the resistance of jet fuel decreases significantly with an increase in test voltage.

At the completion of Phase I wet testing, breakdown voltage measurements were conducted on the Teflon® loop clamp, the flourosilicon based loop clamp, and the T7/T8 Wiggins coupling. A summary of the first phase of breakdown voltage measurements can be found in Table 4. These data give an indication of the relative voltage potential that might be required to cause a spark to occur between the test item and its associated fuel tube. It also allowed for a visual observation as to the location where the spark may occur. The spark gap distance was altered on the Teflon® loop clamp to demonstrate its relationship to breakdown voltage. Breakdown voltage measurements on the Wiggins coupling were not successful. The low isolation resistance of 2E9 ohms, measured with a test voltage of only 100 volts, loaded down the output of the high voltage power supply.

000098

PHASE II TESTS

The objective of Phase II testing was to expand upon the tests that were conducted during Phase I. Further work went into optimizing conditions that would result in obtaining higher voltage potentials on the test items during wet testing. Phase II testing also included additional dry electrical measurements, breakdown voltage measurements, electric field strength measurements of a fuel mist cloud, and measurements of the electric field strength from the surface of a pool of fuel while the same type of fuel was being sprayed upon it.

An attempt was made during Phase II testing to optimize conditions that would yield the maximum voltage potential possible on an isolated conductor. To simplify this task, an epoxy chromate coated aluminum target plate was used as the isolated test object. The epoxy chromate coating was similar to that found on inner tank walls and fuel lines in fuel tanks of commercial aircraft. Factors such as fuel flow rate, fuel pressure, fuel orifice to target distance, fuel spray to target impact angle, fuel temperature, orifice type, spray pattern, plate coatings, and fuel conductivity were investigated. During this portion of Phase II testing, electrical current measurements were also taken of the target plate and fuel catch tank. The current measurement represents the rate of charge transfer to the target plate or catch tank. The resultant voltage on an isolated conductor, if charged by a constant current source, is the product of the charging current and isolation resistance. An increase in the charging current, or the net resistance to ground, or both, causes a corresponding increase in voltage. The difficulty was in not being able to measure the net resistance to ground during the fuel spray testing. Finding a variable that increases the charging current will not necessarily increase the voltage if that variable causes a corresponding decrease in the overall resistance to ground. During some of the tests, a conductive screen was inserted into the fuel spray between the orifice and the target plate. This was done to alter the fuel spray pattern which resulted in an increase in the fuel spray breakup.

Resistance measurements were made on the thin layer of yellow epoxy chromate primer coating the interior of the fuel catch tank. This primer was also on the fuel tubes of the test items, and on one side of the 8 x 12 inch target plate. Using a test voltage of 100 volts, the resistance measurement was greater than $1E12$ ohms. The same measurement at a test voltage of 200 volts resulted in a resistance that was less than $5E4$ ohms. Therefore, at voltages less than 100 volts, the fuel catch tank would typically be classified as electrically insulative. However, at voltages greater than 200 volts, the fuel catch tank

000099

would typically be classified as conductive. Under these circumstances, little or no electrostatic voltage potentials would be expected if the fuel catch tank was grounded. The breakdown voltage of the epoxy chromate primer on the fuel catch tank occurred somewhere between 100 and 200 volts. This low breakdown voltage may have contributed to the low electric field strengths measured on the surface of the fuel in tests 27 through 31. The electric field strength measurements of the fuel mist cloud were also minimal during these tests. There were several possible reasons why this occurred. First, the spray patterns originating out of the fuel orifices may not have been sufficient to generate a charged mist cloud. Second, the exit vent required for the nitrogen purge may have removed any mist cloud from the upper area of the cabinet. Finally, the accumulation of sufficient charge in the mist cloud to reach a level detectable by the field meter, may take many minutes, or even hours, to occur. The duration of the tests conducted during the fuel misting tests only lasted a few minutes each.

A series of tests were conducted to determine the effect of several variables on the voltage generated from fuel impingement on the target plate. Specifically tests 32 through 42, 44 through 47, 49 through 51, and 56 (Appendix) were dedicated to variable analysis. Several variables appeared to increase the magnitude of voltage or current measured on the target plate. The insertion of the conductive screen in the fuel flow increased both the voltage and current. The impact of the insertion of the screen is shown in Figures 4 and 6. Coating the plate with epoxy chromate primer also produced higher charging currents. Charging currents were also highly influenced by fuel temperature and conductivity (Figures 5 and 6). As fuel temperature increased, charging currents increased significantly. Charging currents using fuels with conductivities of 31 and 94 picosiemens/meter (pS/m) were significantly higher than those observed using fuels with conductivities less than 10 pS/m. Note that fuels with a higher CU also provided a lower resistive path for charge to flow to ground through the fuel itself when a continuous stream exists. Other variables such as target to orifice distance and target plate angle had a less significant effect on charging current (Figure 7). Increases in charging current and voltage were observed for plate angles of 30, 45, and 60 degrees, as opposed to 0 degrees (plate perpendicular to the flow) and 90 degrees (parallel). The concept of "residence time" should be introduced here. Residence time is the amount of time a particle of fuel resides on the target plate. Residence time decreases with a corresponding increase in target plate angle when measured from the horizontal. Increased fuel residence time allows charged fuel particles a longer opportunity to neutralize before leaving the target plate. The target plate was grounded by the electrometer when measuring charging current.

000100

Additional attempts were made to increase charging current. A Teflon® sheet was used to electrically isolate the target plate from the rotating bar on which it was mounted. This Teflon® sheet may have become saturated with the spraying fuel creating a low resistive path between the target plate and bar. The bar was grounded through contact with the walls of the test chamber. The sheeting was removed and the target plate connected to the rotating bar. The bar was then electrically isolated from the test chamber walls with Teflon®. Electrical resistance measurements were made to confirm isolation of the target plate. JP-8 fuel was introduced to the test process at this time. Care was taken to maintain test parameters at conditions suitable for maximum charging based on prior Phase I and II tests. This included a fuel temperature of approximately 105-110°F, a target plate angle of 60°, a slotted orifice, a target to orifice distance of 24 inches, and fuel pressure of 25 psig. A charging current of 12.7 nA and -1132 volts was achieved on the target plate during this test sequence. During test 51, an instability in the test system caused the fuel spray pattern to fluctuate between two distinct patterns. This variation also caused the current on the target plate to fluctuate between two distinct values. This indicates that fuel spray pattern impacts the current achieved on the target plate.

Additional tests were conducted to determine whether or not the fuel spray exiting the orifice is charged before making contact with the test item. An electrically isolated, conductive container was used to collect the fuel exiting the orifice during the test. The amount of charge collected in the container over a period of time was measured with an electrometer. The results of these tests can be found in the Appendix, tests 52 and 53. JP8+100 fuel was used for these tests. The two tests were run with two different orifices. The five hole orifice was selected in the second test to obtain a more consistent fuel flow spray pattern. Test data showed that for the given conditions, the fuel was charged before contact with the test item. In the second test, target plate and fuel catch tank currents were measured in addition to the collection tank charge. This was done to examine the overall test system and to determine whether the sum of all charge currents (e.g., orifice, target plate, collection tank and misting) equaled zero or nearly zero. It was noteworthy that the average value of the calculated fuel collection currents was approximately equal to the sum of the target plate and fuel catch tank currents. If this was not the case, it would be expected there was a loss of charge in the test chamber, most likely through fuel misting. The misting fuel would not be collected in the fuel catch tank, therefore, causing a change in the expected tank current measurement. These data appeared to support the reason why little or no charge was

000101

measured during the misting tests. Although these limited test data were not conclusive, it suggests that very little misting may have actually taken place inside the test cabinet during wet testing.

The test team pursued preliminary work using dripping fuel (as opposed to a continuous stream) as the charging source (Appendix, test 54). As mentioned previously in this report, the fuel itself has been suspected to be a charge dissipation path to ground due to relatively low resistive properties. It was thought that interrupting the continuous stream of fuel would eliminate this charge dissipation path and allow for larger charge levels to remain on the target plate. It was also felt that the overall charge build-up process might take much longer due to the relatively small amount of charge transfer that may occur for each fuel drop. Using JP-8 (CU approximately 450) as the "dripping" fuel, voltages in excess of 400 volts were observed during the first test. Several factors may have limited the voltage level seen in this test. The fuel temperature during the test was approximately 70°F, much lower than the 110°F value found to produce maximum charging in previous tests. Charge decay may have occurred through a fuel film that had accumulated on the cabling used to measure voltage. The cabling exited the test chamber through the grounded chamber wall thus providing a potential ground path through the fuel film itself. Finally, the ambient relative humidity was high at the time the drip tests were conducted. This could impact the accuracy of voltage measurements made by the charged plate monitor that depends on electrical isolation of the 6x6 inch charge collection plate. Additional drip tests were conducted, but several changes were made from the original test. Fuel was dispersed from a glass burette with a grounded aluminum foil orifice and not from the original orifice used for the previous test. The drip rate was also increased to nearly a continuous flow to minimize test time. During much of the previous spray testing, Stadis 450 was added to the baseline fuel in an attempt to increase the charging capability of the fuel. Adding the Stadis 450 also increased the fuel conductivity, creating a fuel wetted, low resistive path. During this drip testing, an attempt was made to increase the charging capability without increasing the conductivity by adding various additives to the fuel. Fuel temperature also remained far below what had produced maximum charging in previous tests. Detailed information on these additional drip tests can be found in the Appendix, tests 55, 58, 61, 62, 64, and 65. In summary, clay filtered Jet-A fuel and Jet-A fuel with icing inhibitor, showed the greatest tendency to charge the target plate. Voltages in excess of 350 volts were recorded. The addition of Stadis 450, BHT, MDA, and corrosion inhibitor produced much smaller voltage levels. Water was also added during this series of drip tests. Its impact on resultant voltage levels on the

000102

target plate was minimal.

Drip testing, and the use of test fuels with and without additives, provided an opportunity to better assess the electrical resistance of each. Fuel electrical resistance measurements were made on the test fuels using the same test apparatus and voltages described earlier in this report. The Appendix, tests 57, 59, and 60 show the results of these tests. The results of the tests showed a significant decrease in resistance of both the baseline clay treated Jet-A fuel and the same fuel with the icing inhibitor added. As mentioned earlier, these fuels produced the most significant voltage levels during the drip tests. Note that all fuels showed some degree of sensitivity to increased voltage. As the voltage increased, the resistance decreased.

Breakdown voltage tests were also conducted during Phase II on the Wiggins coupling. The initial attempt to measure the breakdown voltage on a Wiggins coupling in Phase I was unsuccessful. A summary of the breakdown voltage test results can be found in Tables 4 and 6. The original o-rings in the Wiggins coupling were removed and replaced with a pair of higher resistance Viton o-rings. Several attempts were made without success to physically position the components of the Wiggins coupling to achieve electrical isolation. The internal conductive components of the Wiggins coupling were removed in an effort to determine the cause of this problem. Electrical isolation was obtained when the two split rings and locking ring were removed. After completely reassembling the coupling, and many attempts to physically position the components of the coupling to achieve isolation, a breakdown voltage measurement was taken. The breakdown voltage occurred at 1080 volts. It was nearly impossible to configure the T7/T8 Wiggins coupling in such a way to produce breakdown voltages that exceeded 1000 volts. This was due to continuous contact between anodized surfaces internal to the coupling and breakdown of that anodized layer at fairly low voltage levels (i.e., less than 1000 volts). This was not readily obvious during dry testing when test voltages of 100 volts or less were used to measure resistance between these surfaces. When all the internal components of the coupling were removed, except for the o-rings, a breakdown voltage of approximately 5700 volts was achieved.

SUMMARY OF FINDINGS

As mentioned in the opening paragraph of this report, the purpose of this work was to assess the charging characteristics of electrically isolated conductors when sub-jetted to fuel impingement. Specifically, conductors that are commonly found in aircraft fuel systems. Experiments were conducted on aircraft

000103

hardware (e.g., Wiggins couplings and cushioned loop clamps) as well as simulated hardware (e.g., epoxy chromate coated metal plate). The experiments were run to determine if the hardware could become electrostatically charged when turbine fuels were impinged upon them. Those properties, combined with the basic electrical properties (e.g., resistance and capacitance) of each test item, allowed for some estimation of the possible discharge energies that could be expected if substantial charging did occur. Figure 8 shows the potential energies achieved from the measured voltages (maximum) and capacitances of the various test items used in this study. This energy, expressed by the equation $E = \frac{1}{2} CV^2$ is the energy dissipated in a discharge where C is the capacitance between two conductors with a potential difference, V, in volts. This value can be compared against the estimated minimum ignition energy (MIE) for flammable fuel vapor-oxidant mixtures at specific temperatures and pressures. This report does not cover MIE for explosive vapor-oxidant mixtures, but recognizes that other work has been done in this area. AFWAL-TR-85-2057, "Aircraft Mishap Fire Pattern Investigations," August 1985, states that the MIE for many hydrocarbon combustibles is approximately 0.25 mJ. This value may increase substantially, however, with a decrease in pressure. The work outlined throughout this report focused on three important items that may aid in the estimation of discharge energy. First, the voltage potential that could be achieved on each conductor through fuel impingement was evaluated. Second, the capacitance of each item when dry and when subjected to fuel impingement was measured. Third, the electrical resistance to ground of each item under test and how well each item was electrically isolated from ground was assessed.

A large portion of the work accomplished during this study was dedicated to experimentally finding the maximum voltage potential that could be attained on each conductor through fuel impingement. During the course of testing, a multitude of fuel types, orifice styles, fuel temperatures and pressures, and spray distances were tried to achieve maximum voltage and charging current. Appendix provides a detailed summary of each of these tests. Testing revealed that fuel temperature, flow rate and conductivity, additive content, and spray pattern were the most significant variables in the charging process. As fuel temperature and flow rate increased, so did the maximum charging current on the test item. The fuel spray pattern also increased the measured current. The fuel spray pattern was influenced by the insertion of the break-up screen, the distance from the orifice to the target, the orifice style, and flow instabilities in the system. As the spray pattern became more dispersed, the charging current increased. Fuel conductivity significantly influenced the maximum current measured on the test item. As conductivity increased, the current increased. The highest

000104

currents were achieved using JP-8 fuels with a conductivity in excess of 400pS/m. The resistance of the higher CU fuel also decreased, providing a charge dissipation path for charge to flow to ground. This resulted in lower voltage potentials on the test item than those achieved with the lower CU fuel. A higher CU fuel may also allow for recombination of charge to occur while the fuel was still in contact with the target plate.

Of the items tested from actual aircraft, the Teflon® cushioned loop clamp was the most susceptible to charging and achieved the highest voltage potentials. The Wiggins couplings could not be significantly charged due to the low electrical resistance of their internal o-rings. The low breakdown voltage and likelihood of physical contact of all internal surfaces and components may also have contributed to the inability to significantly charge the couplings. The Teflon® cushioned loop clamp retained good electrical isolation throughout the experiment and a maximum voltage of approximately 650 volts was achieved. The capacitance of the clamp, without attached wiring or test instrumentation, throughout the test process was approximately 45 pF. A Teflon® loop clamp with these properties could produce a discharge energy of approximately 0.0095 mJ.

A series of tests were done using an epoxy chromate coated aluminum target plate. Testing produced a maximum voltage of approximately 1150 volts. Assuming the Teflon® cushioned loop clamp could also attain this voltage, a discharge energy of 0.030 mJ could be produced. Both values (0.0095 and 0.030 mJ) are well below the 0.25mJ MIE value discussed earlier.

Testing done to assess the impact of fuel misting, or fuel on fuel impingement on the charging process, was also conducted. Misting was analyzed by attempting to measure the electric field strength in the upper area of the test chamber. Little, if any, voltage was observed. This was most likely due to the lack of fuel mist produced by the orifices used in these tests. Very little voltage was produced during the flow of fuel onto a puddle of similar fuel. Maximum charging is typically observed when different materials contact and separate from one another. This may have contributed to the relatively low results. Fuel resistance may also have allowed charge to flow through the fluid to the walls of the collection tank and then to ground. This too would have minimized the voltage values observed-

Drip testing was conducted to eliminate any parallel resistance that might exist when fuel flows to, and exits from, the test item. It was thought the elimination of these paths would allow for greater amounts of charge to reside on the test item and, hence, increase the maximum voltage observed. It was understood that the time for a maximum voltage level to be

000105

reached might be substantial when a drip was used as the charging mechanism versus continuous flow. Preliminary drip testing produced voltages over 400 volts on a small, electrically isolated aluminum plate. Subsequent tests using various fuels, additives, and drip rates, produced lower values.

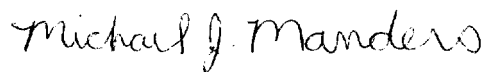
The breakdown voltage measurement results for the Teflon® cushioned loop clamp showed that increasing the spark gap required an increase in voltage potential across the gap to achieve the spark. Typically, the larger the spark gap, the more energy discharged in the spark. The cushioned loop clamps have two areas where breakdown could occur. Breakdown could occur between the clamp and fuel pipe, through the cushioning material itself or through air where voids in the cushioning material exist between the clamp and the fuel pipe. For the clamps tested, the discharge always occurred through air where voids in the cushioning material existed. No physical damage to the clamps was visible on inspected surfaces. Referencing the Phase I breakdown voltage data, the air gap was varied between 0.018 and 0.033 inches. The respective breakdown voltages varied between 2000 and 3550 volts. The capacitance of the clamp was relatively stable between 49 and 46 picofarads over the gaps mentioned. The corresponding discharge energies over this range of voltage, capacitance and gap spacing varied between approximately 0.1 and 0.29 mJ. Evidently the orientation of the clamp was extremely important in determining the discharge energy produced. During testing of the Wiggins couplings in Phase I and II, breakdown voltages of any significance were extremely difficult to achieve. The resistance of the outer coupling shell to the inner fuel tube was very low ($< 1E11$ ohms), preventing significant charge accumulation. This was due to the low resistance of the inner o-rings as well as contact between anodized surfaces inside the coupling.

000106

PREPARED BY



STEVEN C. GERKEN
AF Electrostatic Discharge
Technology
Materials Integrity Branch
Systems Support Division
Materials Directorate



MICHAEL J. MANDERS
AF Electrostatic Discharge
Technology
Materials Integrity Branch
Systems Support Division
Materials Directorate



CYNTHIA OBRINGER
Fuels Branch
Fuels & Lubrication Division
Aero Propulsion & Power Directorate

REVIEWED By



GEORGE A. SLENSKI
Structural Failure Analysis
Materials Integrity Branch
Systems Support Division
Materials Directorate

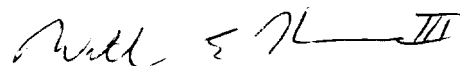


WILLIAM E. HARRISON, III
Chief, Fuels Branch
Fuels & Lubrication Division
Aero Propulsion & Power
Directorate

PUBLICATION REVIEW: This report has been reviewed and approved.



GEORGE A. SLENSKI, Actg Br Chf
Materials Integrity Branch
Systems Support Division
Materials Directorate



WILLIAM E. HARRISON, III
Chief, Fuels Branch
Fuels & Lubrication Division
Aero Propulsion & Power
Directorate

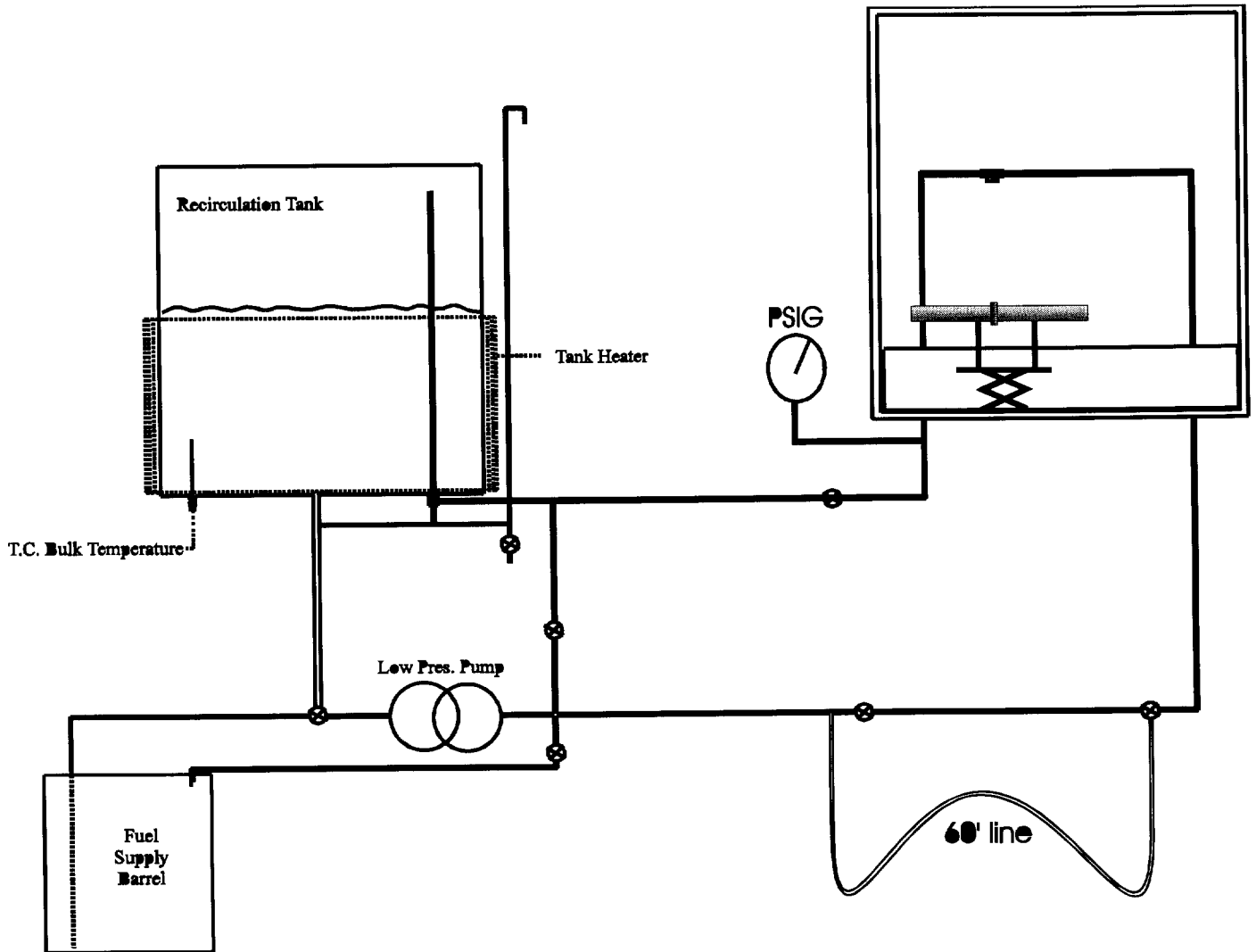


Figure 1. Test facility.

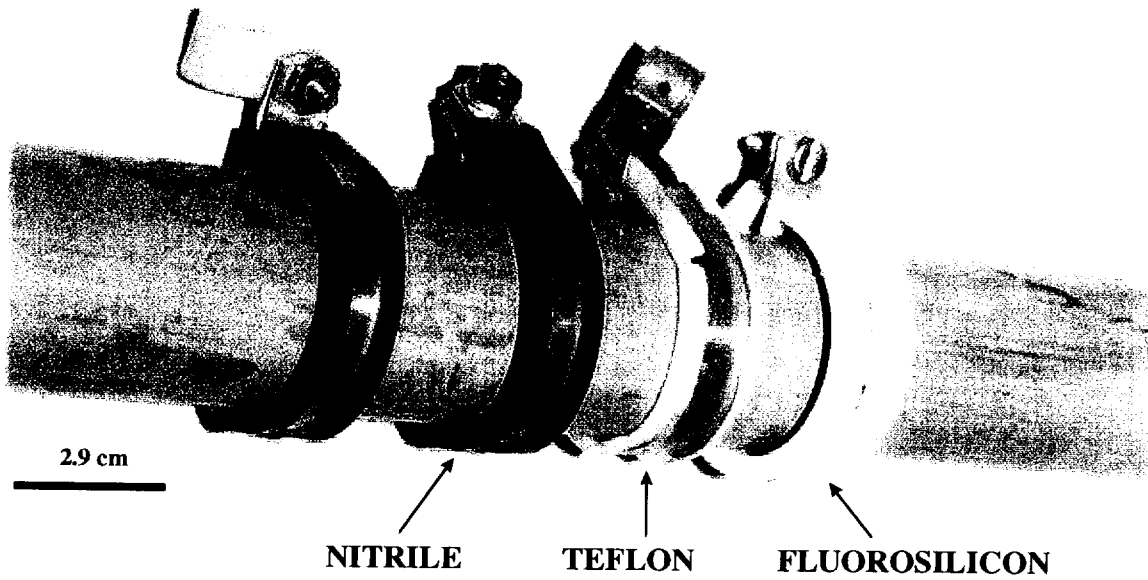


Figure 2. Cushioned loop clamps.

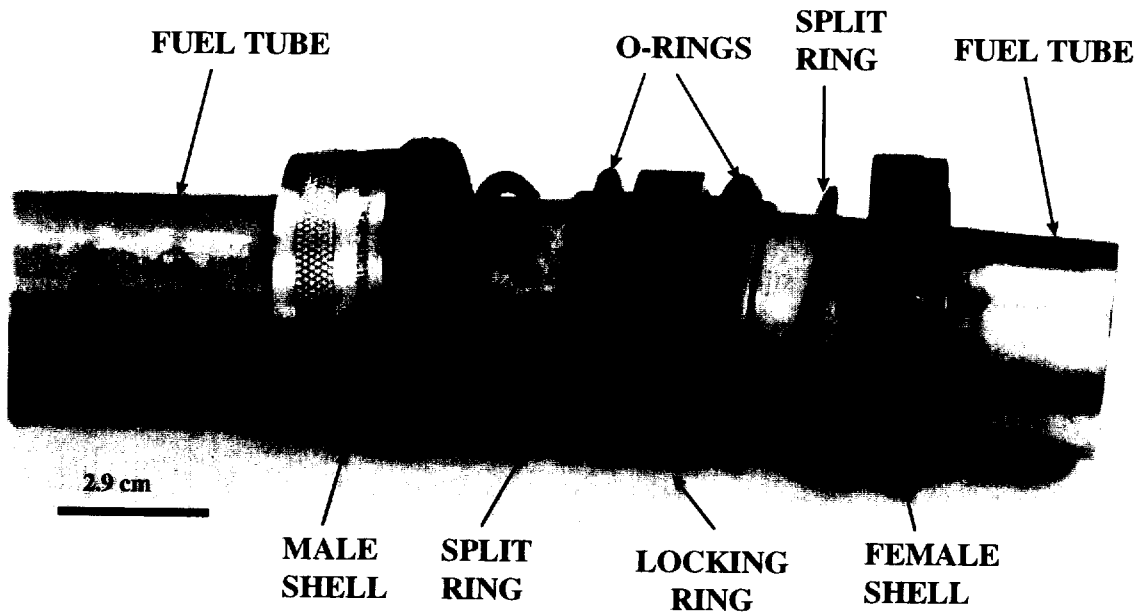


Figure 3. Wiggins coupling.

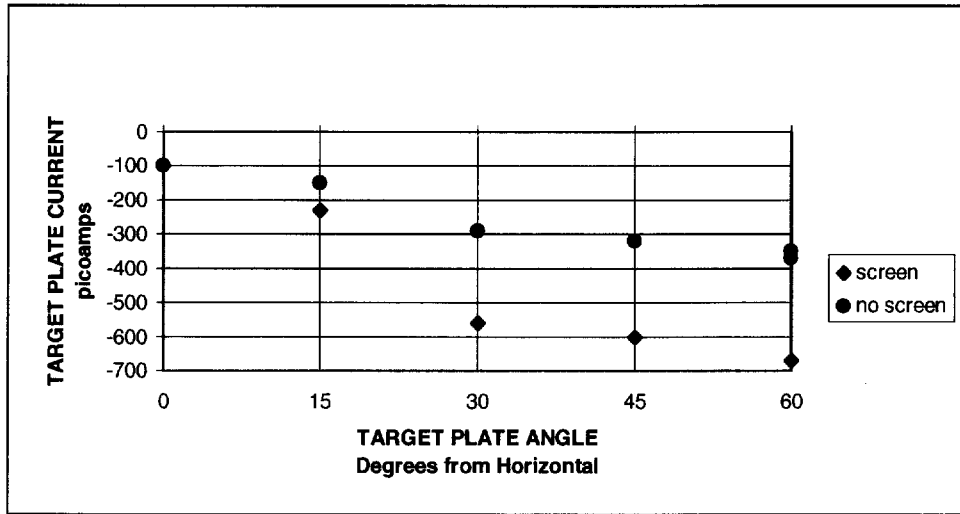


Figure 4. Target plate current versus target plate angle (screen/no screen) (April 11).

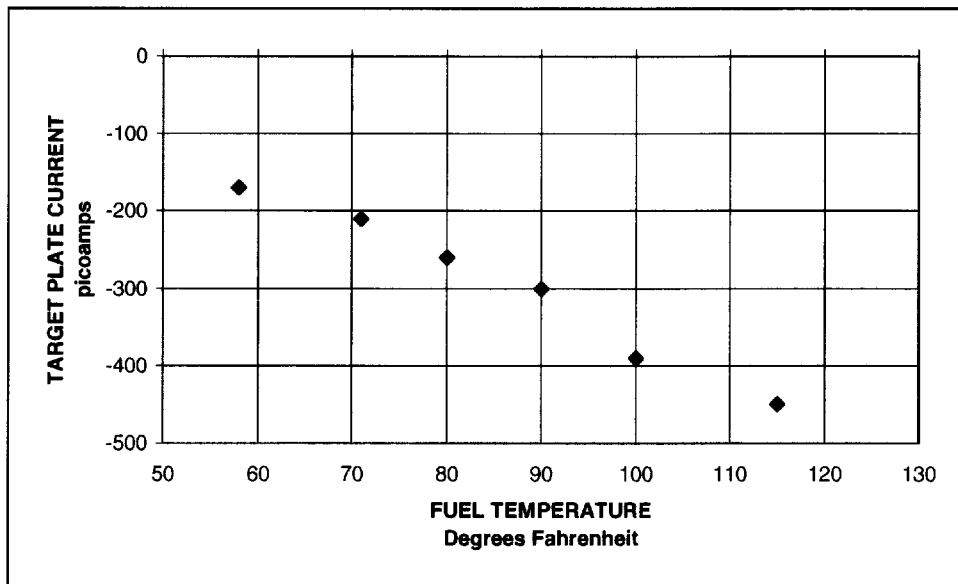


Figure 5. Target plate current versus fuel temperature (April 10).

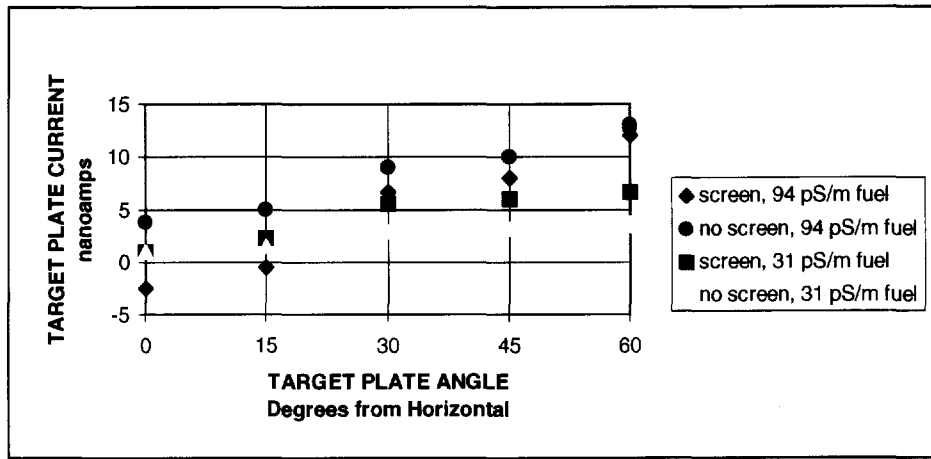


Figure 6. Target plate current versus target plate angle (screen/no screen, fuel CU) (April 11).

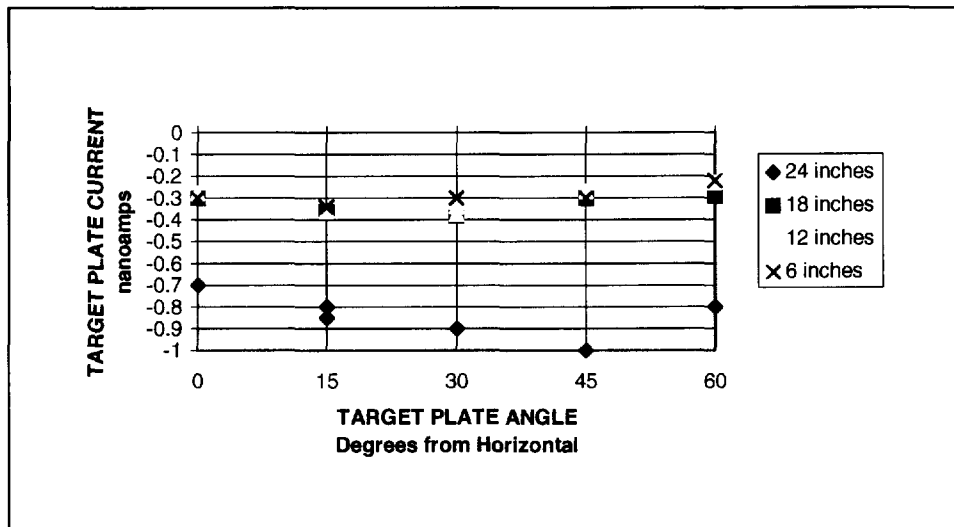


Figure 7. Target plate current versus target plate angle (orifice to target plate distance) (April 9, 10, and 11).

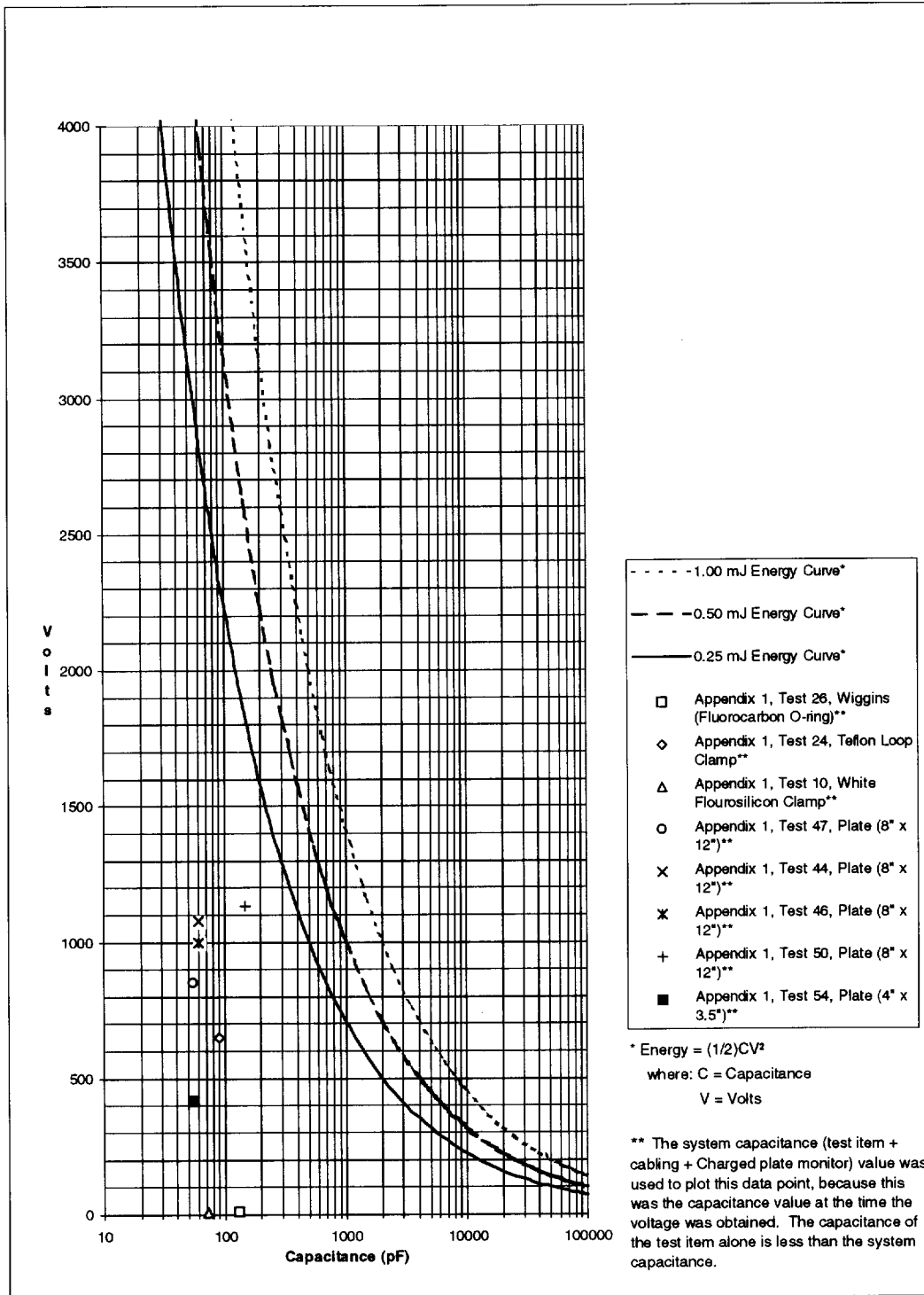


Figure 8. Minimum ignition energy curves and system test data points.

000112

Table 1

JFK Fuel Analysis

SPECIFICATION: ASTM D-1655 JET-A				
METHOD	TEST	SPEC LIMITS		LAB
		MIN	MAX	RESULTS
D3242	Total Acid Number, MG KOH/gm		0.1	0
D86	Distillation, °C			
	10% Recovered		205	181
	50% Recovered		Report	212
	90% Recovered		Report	254
	Final Boiling Point		300	280
	Residue, % Volume		1.5	1.2
	Loss, % Volume		1.5	0.9
D56	Flash Point, °C	38		49
D1298	Density at 15°,kg/cu meter	775	840	805
D130	Copper Corrosion		1	1b

000113

Table 2

Wright Laboratory Fuel Analysis

SPECIFICATION TEST	MIL-PER-83133D	ASTM D1655	
	JP-8	JET-A	96POSF3305
Specific Gravity @ 60°F	0.775 - 0.840	0.7753-0.8398	0.8076
Distillation, ASTM D86, °C (°F)			
Initial Boiling Point	Report	No Rqmt.	158 (316)
10% Recovered	205 (401) max	204 (400) max	172 (342)
20% Recovered	Report	No Rqmt.	185 (365)
50% Recovered	Report	Report	208 (406)
90% Recovered	Report	Report	248 (478)
End Point	300 (572) max	300 (572) max	268 (514)
Residue, vol %	1.5 max	1.5 max	0.2
Distillation Loss, vol%	1.5 max	1.5 max	0.8
Sulfur, total, wt %	0.30 max	0.3 max	0.0587
Doctor's Test	Negative	Negative	Sweet
Net Heat of Combustion, Btu/lb	18,400 min	18,400 min	18,552
Freezing Point, °F	-53°F max	-40°F max	-52
Aromatics, vol %	25 max	20 max	19.5
Olefins, vol %	5.0 max	No Rqmt.	BDL
Smoke Point	25 min	25 min	20
Copper Strip Corrosion	1 max	1 max	1a
Viscosity @ -4°F, cSt	8.0 max	8.0 max	5.01
Water Reaction	1b max	1b max	1
Delta P, mm Hg	25 max	25 max	2
Deposit Code	<3 max	<3 max	<1
Hydrogen content, mass %	13.4 min	No Rqmt.	14.25

000114

Table 3

DRY ELECTRICAL MEASUREMENTS (PHASE I)

Specimen	Volume Resistance (Ohms)		Female to Male Shell Resistance (Ohms)	Male Resistance To Fuel Tube With Both T Sections Bonded (Ohms)		Female Resistance To Fuel Tube With Both T Sections Bonded (Ohms)		T/T Resistance Fuel Tube to Tube (Ohms)	Average Female Capacitance @ 1 kHz, 1 VRMS W/Both T Sections Bonded (nF)		Average Male Capacitance @ 1 kHz, 1 VRMS W/Both T Sections Bonded (nF)		M/F Safety Wire
	10 Volt	250 Volt		Fluke 77	10 Volt 60 sec. Max wait	250 Volt	10 Volt 60 sec. Max wait		250 Volt	10 Volts 60 sec. Max wait	Cap.	Q D G (uS)	
Wiggins Coupling T9/T10 ¹	N/A	N/A	0.2	<50k		<50k		4.5x10 ⁹ ^{1A}	1.08	0 F2 0.3478 ^{1B}	1.08	0 F2 0.3487 ^{1B}	Y
Wiggins Coupling T1/T2 ²	N/A	N/A	1.0	<50k		<50k		2.6x10 ⁶ ^{2A}	-2.49 ^{2B}	0 F2 0.869	-0.145 mF ^{2B}	0 7.2 6.585	Y
Wiggins Coupling T5/T6 ³	N/A	N/A	0.3	1.0x10 ⁸		1.1x10 ⁸		5.0x10 ⁸ ^{3B}	2.887	4.3 0.2325 4.21	2.884	4.3 0.2318 4.20	Y
Wiggins Coupling T7/T8 ⁴	N/A	N/A	0.2	1.1x10 ⁷		1.1x10 ⁷			10.460	5.0 0.1988 13.06	10.460	5.0 0.1988 13.06	Y
Wiggins Coupling T11/T12 ⁵	N/A	N/A	0.0	7.0x10 ⁷		1.0x10 ⁸		5.0x10 ⁸	3.609	3.4 0.2953 6.76	3.829	5.8 0.1720 4.14	N
Wiggins Coupling T3/T4 ⁶									0.2627 T3 gnd. Only	5.6 0.1800 0.298	3.4		Y ^{6A}
Wiggins Coupling T3/T4 ⁷	N/A	N/A	Open Circuit	1.4x10 ⁷		9.0x10 ⁶		3.8x10 ⁸	.6158	9.2 0.1092 0.423	3.396	3.6 0.2775 5.92	Y ^{7A}
Clamp, Teflon DG26 ⁸	N/A	N/A	N/A	>1x10 ¹²	>1x10 ¹²	N/A	N/A	Single Tube N/A	N/A	N/A	0.0447	---	N
Clamp, Red/Black Coating ⁹			N/A	1.3x10 ⁷	<50k	N/A	N/A	Single Tube N/A	N/A	N/A	0.7215	11.6 0.0862 0.390 ^{9A}	N
Clamp, White Rubber WH29 ¹⁰	>1x10 ¹²	>1x10 ¹²	N/A	>1x10 ¹²	>1x10 ¹²	N/A	N/A	Single Tube N/A	N/A	N/A	0.0325	---	N

30

000115

WL/MLS 97-097

Table 3

DRY ELECTRICAL MEASUREMENTS (PHASE I)

Specimen	Volume Resistance (Ohms)		Female to Male Shell Resistance (Ohms) Fluke 77	Male Resistance To Fuel Tube With Both T Sections Bonded (Ohms)		Female Resistance To Fuel Tube With Both T Sections Bonded (Ohms)		T/T Resistance Fuel Tube to Tube (Ohms) 10 Volts 60 sec. Max wait	Average Female Capacitance @ 1 kHz, 1 VRMS W/Both T Sections Bonded (nF)		Average Male Capacitance @ 1 kHz, 1 VRMS W/Both T Sections Bonded (nF)		M/F Safety Wire Y/N
	10 Volt	250 Volt		10 Volt 60 sec. Max wait	250 Volt	10 Volt 60 sec. Max wait	250 Volt		Cap.	Q D G (uS)	Cap.	Q D G (uS)	
Clamp, Black DG32 ¹¹			N/A	6.0×10^5	<50k	N/A	N/A	Single Tube N/A	N/A	N/A	0.5765	2.9 0.3420 1.240	N
Wiggins Coupling, Fuels Lab, #1, (purple) ¹²			0.7	6.0×10^7		6.0×10^7		<50k	3.034nF	2.4 0.4115 7.85	3.040nF	2.4 0.4116 7.87	N
Wiggins Coupling T11/T12 ¹³			13.7	1.0×10^8		1.0×10^8		5.0×10^8	3.818	5.6 0.1788 4.29	3.823	5.6 0.1782 4.28	Y
Teflon Clamp, DG26 ¹⁴				$>>1 \times 10^{12}$	$>>1 \times 10^{12}$						0.0494	--- --- 0.001	N
Wiggins Coupling T11/T12 ¹⁵									3.580	5.7 0.1754 3.93	3.582	5.8 0.1714 3.83	Y
Wiggins Coupling T11/T12 ¹⁶			0.2	1.0×10^8		1.0×10^8		5.0×10^8	2.294	4.0 0.2477 3.57	2.300	4.0 0.2471 3.57	Y
Wiggins Coupling T Section ¹⁷						1×10^{11} 2.5×10^5 Short			0.2950 0.3431 -0.093				
Wiggins Coupling, Fuel Lab, #2 ¹⁸			4×10^{10}	1.2×10^9		3.5×10^{10}		1.6×10^9	0.1000	40.0 0.025 0.016	0.1199	26.6 0.037 0.027	N
Wiggins Coupling, Fuel Lab, #2 ¹⁹				1.5×10^{10}		1.3×10^{10}							N

Table 3

DRY ELECTRICAL MEASUREMENTS (PHASE I)

Specimen	Volume Resistance (Ohms)		Female to Male Shell Resistance (Ohms)	Male Resistance To Fuel Tube With Both T Sections Bonded (Ohms)		Female Resistance To Fuel Tube With Both T Sections Bonded (Ohms)		T/T Resistance Fuel Tube to Tube (Ohms)	Average Female Capacitance @ 1 kHz, 1 VRMS W/Both T Sections Bonded (nF)		Average Male Capacitance @ 1 kHz, 1 VRMS W/Both T Sections Bonded (nF)		M/F Safety Wire
	10 Volt	250 Volt		Fluke 77	10 Volt 60 sec. Max wait	250 Volt	10 Volt 60 sec. Max wait		250 Volt	10 Volts 60 sec. Max wait	Cap.	Q D G (uS)	
Wiggins Coupling, Fuel Lab, #2 ²⁰			8x10 ⁹ ^{20A}	1x10 ¹¹		1x10 ¹¹		>1x10 ¹¹	0.089 ^{20B}	0.0422 23.8 0.023	0.095 ^{20B}	26.5 0.0400 0.025	
O-ring #1 ²¹	6.5k												
O-ring #2 ²²	7.0x10 ⁷	2.4x10 ⁷											
O-ring #3 ²³	8.7k												
O-ring #4 ²⁴	28.5k												
O-ring #5 ²⁵	37.0k												
O-ring #6 ²⁶	1.0x10 ⁷	2.6x10 ⁶											
O-ring #7 ²⁷	9.5x10 ¹⁰	9.0x10 ¹⁰											
O-ring #8 ²⁸	>1x10 ¹²	>1x10 ¹²											

Table 3

DRY ELECTRICAL MEASUREMENTS (PHASE I)

Specimen	Volume Resistance (Ohms)		Female to Male Shell Resistance (Ohms)	Male Resistance To Fuel Tube With Both T Sections Bonded (Ohms)		Female Resistance To Fuel Tube With Both T Sections Bonded (Ohms)		T/T Resistance Fuel Tube to Tube (Ohms)	Average Female Capacitance @ 1 kHz, 1 VRMS W/Both T Sections Bonded (nF)		Average Male Capacitance @ 1 kHz, 1 VRMS W/Both T Sections Bonded (nF)		M/F Safety Wire
	10 Volt	250 Volt		Fluke 77	10 Volt 60 sec. Max wait	250 Volt	10 Volt 60 sec. Max wait		250 Volt	10 Volts 60 sec. Max wait	Cap.	Q D G (uS)	
O-ring #9 ²⁹	4.75x10 ⁷	<50k											

Table 3

DRY ELECTRICAL MEASUREMENTS (PHASE I)

- ¹ 5 MAR 97 (72.3°F, 28.8%RH); Punch through of anodized layer occurred 3 MAR 97 when trying to take a resistance measurement a 250 volts.
- 1A Current must pass through both O-rings & anodized layer.
- 1B Measurement recorded in mini Siemens.
- ² 5 MAR 97;
- 2A Resistance T2 to either Male or Female is <50k ohms. T1 to Female is 2×10^6 , T1 to male is 2×10^6 .
- 2B Negative capacitance due to little or no resistance from female coupling to fuel tube.
- ³ 5 MAR 97;
- 3B Safety wire disconnected during this measurement.
- 4 5 MAR 97; Safety wire was installed on this coupling.
- ⁵ 5 MAR 97;
- ⁶ 5 MAR 97: These measurements were taken before it was realized that T4 ground had fallen off or was not connected. See test #7 for the complete set of measurements for this coupling.
- 6A Safety wire movement seems to influence capacitance measurement.
- ⁷ 5 MAR 97; "Touching" contact produced Similar capacitance to that measured through drilled hole and clamp.
- 7A Safety wire movement seems to influence capacitance measurement.
- ⁸ 4 MAR 97 (71.5°F, %RH); There is only one capacitance measurement for the isolated clamp. Its value was recorded in the male capacitance column.
- ⁹ 5 MAR 97; (TA4C44D28AF) There is only one capacitance measurement for the isolated clamp. Its value was recorded in the male capacitance column.
- 9A Measurement recorded in mini Siemens.
- 3.0 5 MAR 97; There is only one capacitance measurement for the isolated clamp. Its value was recorded in the male capacitance column.

000119

Table 3

DRY ELECTRICAL MEASUREMENTS (PHASE I)

- 10A Volume resistance measurement of clamp taken without fuel tube using an ASTM F150 electrode and a base metal plate.
- 11 5 MAR 97;
- 12 5 MAR 97;
- 13 5 MAR 97;
- 14 5 MAR 97;
- 15 5 MAR 97; After addition of feed through wire (not in test stand). The feed through wire was connected to the safety wire on the coupling. Capacitance measurements were measured first. Inadvertently applied 250 volts to the coupling during the resistance test and broke down the anodized layer.
- 16 5 MAR 97; The female side of the coupling was readjusted in an attempt to remove the short circuit caused by inadvertently applying 250 volts with megohmmeter.
- 17 5 MAR 97; This test was done to check the variation of resistance and capacitance measurements while varying the O-ring pressure. The order from top to bottom are loose connection, initial contact, tightened. The short occurred with both the Beckman megohmmeter and Fluke ohmmeter.
- 18 6 MAR 97; 1 inch test coupling with the original O-rings that were in it. The resistance measurements were approximate values.
- 19 6 MAR 97; 1 inch test coupling with "new" O-rings installed.
- 20 7 MAR 97; 1 inch test coupling with the highest resistance O-rings that were readily available installed. Preparing for possible test.
- 20A Measured with Beckman Megohmmeter due to high resistance.
- 20B Measurement taken with contact pressure only, no clamping.
- 21 3 MAR 97; Measurement made with Fluke ohmmeter.
- 22 3 MAR 97; Measurements made with Beckman Megohmmeter.
- 23 3 MAR 97; Measurement made with Fluke ohmmeter.
- 24 3 MAR 97; Measurement made with Fluke ohmmeter.

Table 3

DRY ELECTRICAL MEASUREMENTS (PHASE I)

25	3 MAR 97; Measurement made with Fluke ohmmeter.
26	3 MAR 97; Measurements made with Beckman Megohmmeter.
27	3 MAR 97; Measurements made with Beckman Megohmmeter.
28	3 MAR 97; Measurements made with Beckman Megohmmeter.
29	3 MAR 97; Measurements made with Beckman Megohmmeter.

Table 4

BREAKDOWN VOLTAGE MEASUREMENTS (PHASE I)

Test Date: 26 MAR 97

Temp: 71.9°F

Hum: 24.8%RH

Test Equipment: Hewlett-Packard, HP4192A Impedance Analyzer

Beckman, L-10A Megohmmeter

Simco, PN25A Static Generator

Item Nomenclature	Capacitance @1kHz, 1VRMS (pF)	Resistance @100 Volts (Ohms)	Approximate Gap (Inches)	Breakdown Voltage #1 (Volts)	Breakdown Voltage #2 (Volts)	Breakdown Voltage #3 (Volts)
Teflon Clamp ¹	49	> 10 ¹²	0.018	2000	2240	2270
Teflon Clamp ²	48.6	> 10 ¹²	0.025	2430	2420	2420
Teflon Clamp ³	45.6	> 10 ¹²	0.033	2920	3110	3550
Silicon Based Clamp ⁴	43.9	> 10 ¹²	0.150	7400	6900	7000
Wiggins Coupling T7/T8 ⁵	530	2 x 10 ⁹	Not Measured	See Footnote ^{5A}	See Footnote ^{5A}	See Footnote ^{5A}

¹ Teflon thickness approximately 0.020 inches² Teflon clamp located over coated area of fuel tube³ Teflon thickness doubled under clamp near arc point to increase spacing (gap)⁴ Test conducted 2 April 97, 71.5°F, 13.8%RH⁵ Wiggins Coupling still containing the electrical tape modification from 5 March 97 fuel spray testing.^{5A} Little or no potential observed on outer shell (power supply voltage set to +20KV but output appears loaded down by a low resistance load)

Table 5

DRY ELECTRICAL MEASUREMENTS (PHASE II)

Specimen	Volume Resistance (Ohms)		Female to Male Shell Resistance (Ohms)	Male Resistance To Fuel Tube With Both T Sections Bonded (Ohms)		Female Resistance To Fuel Tube With Both T Sections Bonded (Ohms)		T/T Resistance Fuel Tube to Tube (Ohms)	Average Female Capacitance @ 1 kHz, 1 VRMS W/Both T Sections Bonded (nF)			Average Male Capacitance @ 1 kHz, 1 VRMS W/Both T Sections Bonded (nF)			M/F Safety Wire
	10 Volt	250 Volt		Fluke 77	10 Volt 60 sec. Max wait	250 Volt	10 Volt 60 sec. Max wait		250 Volt	10 Volts 60 sec. Max wait	Cap.	Q D G (uS)	Cap.	Q D G (uS)	
Wiggins Coupling T7/T8 ¹	>10 ¹² >10 ¹²		2.1 ^{1A}	7x10 ¹¹ ^{1A}		4.5x10 ¹¹ ^{1A}		2.5x10 ¹¹ ^{1B}						N	
Wiggins Coupling T7/T8 ²								3.5x10 ¹¹						N	
Wiggins Coupling T7/T8 ³								8x10 ¹¹						N	
Wiggins Coupling T7/T8 ⁴								5x10 ¹¹						N	
Wiggins Coupling T7/T8 ⁵			720						0.338		1.018			N	
Wiggins Coupling T7/T8 ⁶			<1						0.196		0.196			N	
Wiggins Coupling T7/T8 ⁷			<1						0.195		0.195			N	

38

000123

Table 5

DRY ELECTRICAL MEASUREMENTS (PHASE II)

-
- ¹ 7 MAY 97; Volume resistance measurements reported were O-ring tests prior to assembly into the coupling. The first measurement was dry and the second was made with the lubrication used for assembly of the coupling.
- ^{1A} The coupling was fairly loose, it was not tightened.
- ^{1B} This measurement was with the fuel tubes separated as far apart as possible.
- ² 7 MAY 97; This measurement was made with both fuel tubes angled out of the coupling.
- ³ 7 MAY 97; This measurement was made with the fuel tubes in as close as possible to each other.
- ⁴ 7 MAY 97; This measurement was made with the fuel tubes approximately mid range from each other (not all the way out and not all the way in together) .
- ⁵ 7 MAY 97; These measurements were made with a loose coupling, not tightened, and with the fuel tubes separated by their maximum position.
- ⁶ 7 MAY 97; These measurements were made with the coupling tightened and with the fuel tubes separated by their maximum position.
- ⁷ 7 MAY 97; These measurements were made with the fuel tubes together as close as they could be.

000124

WL/MIS 97-097

Table 6

BREAKDOWN VOLTAGE MEASUREMENTS (PHASE II)

Test Date: 7 MAY 97
 Temp: 74.4°F
 Hum: 21.6%RH

Test Equipment: Hewlett-Packard, HP4192A Impedance Analyzer
 Beckman, L-10A Megohmmeter
 Simco, PN25A Static Generator

Item Nomenclature	Capacitance @1kHz, 1VRMS (pF)	Resistance @10 Volts (Ohms)	Resistance @100 Volts (Ohms)	Resistance @1000 Volts (Ohms)	Breakdown Voltage (Volts)
Wiggins Coupling T7/T8 with Viton O-rings ⁱ	95	>> 10 ¹²	> 10 ¹²	≈ 10 ¹²	Footnote ^{1A}
Wiggins Coupling T7/T8 with Viton O-rings ⁱⁱ	---	2.7x10 ¹¹	1.8x10 ¹⁰	<< 5x10 ⁴	Footnote ^{2A}
Wiggins Coupling T7/T8 with Viton O-rings ⁱⁱⁱ	---	2x10 ¹¹	3x10 ⁹	<< 5x10 ⁴	Footnote ^{3A}
Wiggins Coupling T7/T8 with Viton O-rings ^{iv}	---	2x10 ¹⁰	8x10 ⁸	<< 5x10 ⁴	Footnote ^{4A}
Wiggins Coupling T7/T8 with Viton O-rings ^v	---	6x10 ¹¹	4x10 ¹¹	<< 5x10 ⁴	Footnote ^{5A}
Wiggins Coupling T7/T8 with Viton O-rings ^{vi}	---	5x10 ¹¹	4.5x10 ¹¹	6x10 ¹⁰	5700-5780
Wiggins Coupling T7/T8 with Viton O-rings ^{vii}	---	---	---	---	No Discharge
Wiggins Coupling T7/T8 with Viton O-rings ^{viii}	---	---	---	---	≈ 3500
Wiggins Coupling T7/T8 with Viton O-rings ^{ix}	---	---	---	---	3000-3400

40

000125

WL/MLS 97-097

Table 6

BREAKDOWN VOLTAGE MEASUREMENTS (PHASE II)

Item Nomenclature	Capacitance @1kHz, 1VRMS (pF)	Resistance @10 Volts (Ohms)	Resistance @100 Volts (Ohms)	Resistance @1000 Volts (Ohms)	Breakdown Voltage (Volts)
Wiggins Coupling T7/T8 with Viton O-rings ^x	---	---	---	---	≈ 3300
Wiggins Coupling T7/T8 with Viton O-rings ^{xi}	36-45	---	---	---	---
Wiggins Coupling T7/T8 with Viton O-rings ^{xii}	59-74	---	---	---	---
Wiggins Coupling T7/T8 with Viton O-rings ^{xiii}	56	---	---	---	≈ 1250
Wiggins Coupling T7/T8 with Viton O-rings ^{xiv}	76	---	---	---	≈ 1080
Wiggins Coupling T7/T8 with Teflon O-rings ^{xv}	36	---	---	---	>500 <1000

Table 6

BREAKDOWN VOLTAGE MEASUREMENTS (PHASE II)

ⁱ Removed the original pair of O-rings from T7/T8 Wiggins coupling and installed a pair of higher resistance Viton O-rings. The identifier T7 corresponds to the fuel tube on the female coupling/shell side, and T8 corresponds to the fuel tube on the male coupling/shell side. The test voltage was applied to T7 fuel tube and monitored with a charged plate monitor. A ground wire was connected to the female coupling/shell only.

1A The applied voltage reached approximately 1000 volts then decreased back towards 0 volts.

ⁱ Repeated test #1 resistance measurements to see if the resistance measurements have changed after power was applied in test #1. .

2A Breakdown Voltage not attempted with Simco power supply. Shorting and/or breakdown occurred during resistance measurement at 1000 volts.

ⁱⁱ Repositioned fuel tubes to try to electrically separate both tubes from the inner locking ring. The anodized layer is apparently breaking down between two metal surfaces in contact with each other.

3A Breakdown Voltage not attempted with Simco power supply. Shorting and/or breakdown occurred during resistance measurement at 1000 volts.

^v Applied less clamping force to the coupling in an attempt to electrically isolate the components.

4A Breakdown Voltage not attempted with Simco power supply. Shorting and/or breakdown occurred during resistance measurement at 1000 volts.

^v Removed red locking ring from the coupling in an attempt to electrically isolate the components.

5A Breakdown Voltage not attempted with Simco power supply. Shorting and/or breakdown occurred during resistance measurement at 1000 volts.

ⁱ Removed split rings in addition to the locking ring in an attempt to electrically isolate the components. Applied power to fuel tube T8 and monitored with charged plate monitor. Grounded male coupling/shell only.

^{vii} Locking ring and split rings still removed. Applied power slowly to fuel tube T8 and monitored female coupling/shell with charged plate monitor. Grounded fuel tube T7. Simco power supply set between 5000 and 6000 volts when breakdown occurred.

ⁱⁱⁱ Locking ring and split rings still removed. Applied power slowly to fuel tube T8 and monitored female coupling/shell with charged plate monitor. Grounded fuel tube T7. Simco power supply set between 5000 and 6000 volts when breakdown occurred.

42

000127

WL/MLS 97-097

Table 6

BREAKDOWN VOLTAGE MEASUREMENTS (PHASE II)

`* Locking ring and split rings still removed. Pulled fuel tubes out away from each other as far as they would go. Angled T7 fuel tube slightly to make a smaller gap to the coupling/shell. Applied power slowly to fuel tube T8 and monitored female coupling/shell with charged plate monitor. Grounded fuel tube T7. Simco power supply set at approximately 6000 volts when the breakdown occurred. CPM voltage only dropped about 400 volts during breakdown.

* Same setup conditions as test #9 except that power was applied to the female coupling/shell and the female tube T7 is grounded.

^{x1} Locking ring and split rings still removed. Measured capacitance from female coupling/shell to female fuel tube T7 with no other connections to test coupling/shell or fuel tubes. positioned fuel tube in various position to get a range of capacitances.

`ii Measured capacitance from female coupling/shell to female fuel tube T7 with no other connections except that fuel tube T8 was grounded. positioned fuel tube in various position to get a range of capacitances.

`iii Installed red locking retainer. The two split rings are still removed. Applied power to female coupling/shell and monitored with CPM. Grounded female tube T7. Capacitance measured from female coupling/shell to female fuel tube with nothing else connected.

`iv 8 May 97. Completely assembled coupling with split rings and red locking retainer. Applied power to female coupling/shell and monitored with CPM. Grounded female tube T7. Capacitance measured from female coupling/shell to female fuel tube with nothing else connected.

xv 8 May 97. Viton O-rings removed and replaced with Teflon O-rings. Completely assembled coupling with split rings and red retainer. T7 and T8 fuel tubes have exchanged positions (i.e. T7 is now on the male coupling/shell side) . Capacitance measured from female coupling/shell to female fuel tube with nothing else connected. Internal arcing occurred between 500 and the 1000 volt megohmmeter settings when taking resistance measurements.

43

000128

WL/MIS 97-097

APPENDIX

PHASE I TESTS

Date: March 3

Test: 1

Test Conducted: Dry testing was conducted on nine o-rings and a Wiggins coupling. The o-rings were individually sandwiched between an ASTM 150 electrode and an aluminum base plate. Resistance measurements were also made on Wiggins coupling T9/T10.

Conditions:

Test Voltage: 10 and 250 Volts

O-ring Materials: #1-6 Nitrile, #7 Fluorosilicon, #8 Fluorocarbon, #9 Nitrile

Results: O-rings #2 and #6 were static dissipative (10E6 through 10E9 ohms). O-rings 1, 3,4 and 5 were conductive (less than 10E6 ohms) at 10 volts. The resistance of the fluorosilicon o-ring was greater than 10E10 ohms. The fluorocarbon o-rings resistance was greater than 10E12 ohms. The nitrile o-ring resistance was 10E7ohms at 10 volts and less than 50,000 ohms at 250 volts. The Wiggins coupling resistance measured from male shell to aluminum fuel tube at 10 volts was 10E8 ohms, at 250 volts the resistance was less than 50,000 ohms. The results can be found in Table 3 of the main report.

Comments: The volumetric resistance measurement made did not duplicate the compressive environment of an o-ring installed in a Wiggins coupling but was measured to determine the relative difference between the various o-ring materials. Visual identification of the o-ring materials was not apparent. The resistances were also measured with the o-rings installed in a Wiggins coupling. A resistance measurement of 250 volts on Wiggins coupling T9/T1 O broke down the inner anodized layer of the male shell of the Wiggins coupling.

Note: There was concern that nylon ferrules used to isolate the streaming current measurement section field might affect the streaming current measurement.

Date: March 4

Test: 2

Tests Conducted: Resistance between the fuel line and a metal, Teflon cushioned loop clamp, DG26, was measured. Capacitance was measured with the fuel line grounded.

Conditions:

Capacitance: Measured at 1khz and 1 volt rms

Results: The loop clamp resistance measured was greater than 10E12 ohms, capacitance was 44.7 picofarads.

Date: March 4

Test: 3

Tests Conducted: Measured the voltage potential on an electrically isolated Teflon cushioned loop clamp with fuel impinging on its surface at a low flow rate.

Conditions:

Nozzle: 0.040 inch orifice

Distance from nozzle to clamp: 1.75 inches

Fuel Pressure: 15 psig

Fuel Temperature: between 69 and 80°F

000130

Fuel Conductivity: 7 pS/m at 69°F
Fuel: Jet-A from JFK
Target: Teflon cushioned loop clamp (DG 26)
Initial Resistance: greater than 10E12 ohms
Final Resistance: greater than 10E12 ohms
Initial Capacitance: 74 picofarads (clamp, test wiring, charge plate monitor)

Results: The voltage stabilized at -87 volts after 12 minutes of spraying. Streaming current was -0.1 nanoamps.

Comments: Resistance and capacitance of the DG26 Teflon cushioned loop clamp changed insignificantly during the test.

During this initial wet test sequence, significant charging (greater than 5kvolt) of the Lexan viewing window of the test chamber and sample holding stand was observed. Aluminum foil was placed around the holding stand and wire mesh was added to the lower 1/2 of the Lexan window where fuel splashing was most prevalent. The wire mesh and the section of fuel tube to which the test clamp was connected were grounded to the same point and the voltage signal line from the target item was rerouted through the viewing window well above the area where splashing occurred. This rerouting of the voltage line increased the capacitance of the target, line and charge plate monitor from 74 pF to 86 pF. An unstable streaming current measurement was also noted during this preliminary wet test. The input cable to the electrometer was sensitive to movement when low currents were measured. The cable was immobilized and all instrumentation was grounded.

Date: March 4
Test: 4

Test Conducted: Measured the voltage on an electrically isolated Teflon cushioned loop clamp with fuel impinging on its surface at a higher flow rate.

Conditions:

Nozzle: 0.040 inch orifice
Distance from nozzle to clamp: 1.75 inches
Fuel Pressure: 42 psig
Fuel Temperature: approximately 86°F
Fuel: Jet-A from JFK
Target: Teflon cushioned loop clamp (DG 26)
Initial Resistance: greater than 10E12 ohms
Final Resistance: greater than 10E12 ohms
Initial Capacitance: 86 picofarads (clamp, test wiring, charge plate monitor)

Results: The voltage on the clamp stabilized at -86 volts. The streaming current was -0.07 nanoamps.

Comments: Resistance and capacitance of the DG26 Teflon cushioned loop clamp changed insignificantly when the fuel flow rate was increased.

Date: March 4
Test: 5

Tests Conducted: Measured the voltage on an electrically isolated, Teflon cushioned loop clamp with fuel impinging on its surface at an intermediate flow rate.

Conditions:

Nozzle: 0.040-inch orifice

000131

Distance from nozzle to clamp: 2 inches
Fuel Pressure: 25 psig
Fuel: Jet-A from JFK
Target: Teflon cushioned loop Clamp
Initial Capacitance: 86 picofarads
Final Capacitance: 85.5 picofarads
Resistance: greater than 10E1 2 ohms both before and after the spray test

Results: The voltage on the clamp stabilized at -101 volts. The streaming current was -0.15 nanoamps.

Comment: The resultant voltage observed on the Teflon cushioned loop clamp increased slightly as the fuel flow rate and pressure decreased. Also, the resistance and capacitance of the clamp changed very little before and after the test.

Date: March 5

Test: 6

Test Conducted: Measured the resistance and capacitance of Wiggins couplings, T1/T2, T3/T4, T5/T6, T7/T8, T9/T1 O, and T1 I/T1 2. Measured the resistance and capacitance of three additional loop clamps: red/black (TA4C44D28AF); white (WH29); and black (DG32).

Conditions: Test voltages for both resistance and capacitance measurements were the same as test 2 on March 4.

Results: See Table 4 of the main report.

Comments: Resistances for most Wiggins couplings were in the static dissipative range indicating that they were poor candidates for isolated conductor fuel spray testing. Capacitance values were generally greater than 2000 picofarads with the highest values correlating to those with the lowest male shell to fuel tube resistance. The white loop clamp was the only clamp tested with a high enough resistance to be considered for fuel spray testing.

Date: March 5

Test: 7

Test Conducted: Measured the voltage on an electrically isolated 2-inch Wiggins coupling (TI I/T12) with fuel impinging on its surface.

Conditions:

Nozzle: 0.040-inch orifice
Distance from nozzle to clamp: 1.75 inches
Fuel Pressure: 25 psig
Fuel Temperature: 8 1.3°F
Fuel Conductivity: 10 pS/m at 69°F
Fuel: Jet-A from JFK
Target: T1 I/T1 2 Wiggins coupling
Initial Resistance: 1E8 ohms
Final Resistance: 1E8 ohms
Initial Capacitance: 2606 picofarads
Final Capacitance: 2990 picofarads

Results: The streaming current was -0.22 nanoamps. There was no voltage buildup on the Wiggins coupling.

000132

Comments: The low resistance to ground of the outer surfaces of the fuel wetted Wiggins coupling were insufficient to provide electrical isolation of the outer portion of the coupling and therefore insufficient to allow the coupling to retain a charge.

Date: March 5

Test: 8

Tests Conducted: Measured the voltage on an electrically isolated 2-inch T1 I/T12 Wiggins coupling with fuel impinging on its surface.

Conditions:

Nozzle: 0.040-inch orifice
Distance from nozzle to clamp: 1.75 inches
Fuel Pressure: 42 psig
Fuel Temperature: 83°F
Fuel: Jet-A from JFK
Target: T1 I/T12 Wiggins coupling

Results: The streaming current was -0.15 nanoamps. There was no voltage buildup on the Wiggins coupling.

Comments: The low resistance to ground of the outer surfaces of the fuel wetted Wiggins coupling were insufficient to provide electrical isolation of the outer portion of the coupling and therefore insufficient to allow the coupling to retain a charge.

Date: March 5

Test: 9

Tests Conducted: Measured the voltage on an electrically isolated 2-inch T7/T8 Wiggins coupling with fuel impinging on its surface.

Conditions:

Nozzle: 0.040-inch orifice
Distance from nozzle to clamp: 1.75 inches
Fuel Pressure: 42 psig
Fuel Temperature: 85°F
Fuel: Jet-A from JFK
Target: T7/T8 Wiggins Coupling
Initial Resistance: 1. 1E7 ohms
Final Resistance: 1.2E7 ohms
Initial Capacitance: 10380 picofarads
Final Capacitance: 10883 picofarads

Results: There was no voltage buildup on the Wiggins coupling. The streaming current was -0.14 nanoamps

Comments: The low resistance to ground of the outer surfaces of the fuel wetted Wiggins coupling were insufficient to provide electrical isolation of the outer portion of the coupling and therefore insufficient to allow the coupling to retain a charge.

Date: March 5

Test: 10

000133

Tests Conducted: Measured the voltage on an electrically isolated white loop clamp, WH29, with fuel impinging on its surface.

Conditions:

Nozzle: 0.040-inch orifice
Distance from nozzle to clamp: 1.75 inches
Fuel Pressure: 42 psig
Fuel Temperature: 84°F
Fuel: Jet-A from JFK
Target: White loop clamp, WH29
Initial Resistance: 1.4E10 ohms
Initial Capacitance: 73 picofarads

Results: There was -9 volt potential build upon the white loop clamp. The streaming current was -0.17 nanoamps.

Comments: Resistance to ground of the white loop clamp was much higher than that of the Wiggins couplings allowing for some charge to remain beyond what could decay through the clamps resistance and capacitance.

Date: March 5

Test: 11

Tests Conducted: Measured the streaming current and voltage on an electrically isolated Wiggins coupling (T7/T8) with isolated (taped) o-rings with fuel impinging on its surface.

Conditions:

Nozzle: 0.056-inch orifice
Distance from nozzle to clamp: 1.75 inches
Fuel Pressure: 42 psig
Fuel Temperature: between 80 and 83°F
Fuel: Jet-A from JFK
Fuel Conductivity: 17 pS/m at 68°F
Target: Wiggins coupling (T7/T8) with taped, electrically isolated o-rings
Initial Resistance: 2.4E9 ohms
Final Resistance: 7E8 ohms
Initial Capacitance: 447 picofarads
Final Capacitance: 520 picofarads

Results: The measured potential on the Wiggins coupling was -1 volt. The maximum streaming current was -0.16 nanoamps.

Comments: The resistance to ground of the outer surfaces of the Wiggins coupling (T7/T8) that were in contact with the fuel during the spraying process, were too low to provide good electrical isolation of the outer portion of the coupling.

Date: March 6

Test: 12

Tests Conducted: Dry resistance and capacitance testing conducted on an electrically isolated 1-inch Wiggins coupling (WL/PO sample coupling).

Conditions: Test voltages for both resistance and capacitance measurements same as test 2 on March 4.

000134

Results: See Table 5 of the main report,

Comments: Raised the male shell to fuel tube resistance of the coupling to greater than 1E10 ohms by inserting flouorcarbon O-rings. Individual O-ring resistance prior to installation in Wiggins coupling was greater than 1E 12 ohms. Female and male shell to tube capacitance ranged from 100-120 picofarads.

Date: March 6

Test: 13

Tests Conducted: Measured the streaming current and voltage on an electrically isolated, Teflon cushioned loop clamp (DG 26) with fuel impinging on its surface.

Conditions:

Nozzle: 0.040-inch orifice
Distance from nozzle to clamp: 2 inches
Fuel Pressure: 25 psig
Fuel Temperature: varied between 75 and 86.3°F
Fuel Conductivity: 9 pS/m at 70°F
Fuel: Jet-A from JFK
Target: Teflon cushioned loop clamp, DG 26
Initial Resistance: greater than 1E12 ohms
Final Resistance: See Test 15
Initial Capacitance: 91 picofarads
Final Capacitance: See Test 15

Results: The maximum streaming current was -0.27 nanoamps. The maximum voltage was -201 volts.

Comments: Significantly higher voltages were observed due to the increased resistance to ground properties of the clamp and Teflon cushioning.

Date: March 6

Test: 14

Tests Conducted: Measured the streaming current and voltage on an electrically isolated, Teflon cushioned loop clamp (DG 26) with fuel impinging on its surface at a high flow rate .

Conditions:

Nozzle: 0.040-inch orifice
Distance from nozzle to clamp: 2 inches
Fuel Pressure: 42 psig
Fuel Temperature: varied between 75 and 86.3°F
Fuel Conductivity: 9 pS/m at 70°F
Fuel: Jet-A from JFK
Target: Teflon cushioned loop clamp (DG 26)
Initial Resistance: Same as Test 13
Final Resistance: Same as Test 15
Initial Capacitance: Same as Test 13
Final Capacitance: Same as Test 15

Results: The maximum streaming current was -0.23 nanoamps. The maximum voltage was -276 volts.

Comments: Higher fuel flow contributed to higher resultant voltage on the Teflon cushioned clamp.

Date: March 6

Test: 15

Tests Conducted: Measured the streaming current and voltage on an electrically isolated, Teflon cushioned loop clamp (DG 26) with fuel impinging on its surface at a low flow rate.

Conditions:

Nozzle: 0.040-inch orifice
Distance from nozzle to clamp: 2 inches
Fuel Pressure: 15 psig
Fuel Temperature: varied between 92 and 99°F
Fuel Conductivity: 9 pS/m at 70°F
Fuel: Jet-A from JFK
Target: Teflon cushioned loop clamp (DG 26)
Initial Resistance: Same as Test 13
Final Resistance: greater than 1E12 ohms
Initial Capacitance: Same as Test 13
Final Capacitance: 91 picofarads

Results: The maximum streaming current was -0.56 nanoamps. The maximum voltage was -227 volts.

Comments: The cushion material was scanned with a field meter at the end of this test (approximately 5 minutes) to measure residual voltage. The maximum voltage that was observed with the field meter was approximately 60 volts.

The change in fuel flow rate due to a change in pressure did not significantly alter the voltage measured on the clamp.

Date: March 6

Test: 16

Tests Conducted: Measured the voltage on an electrically isolated, Teflon cushioned loop clamp (DG 26) using fuel flowing from a cracked orifice. Streaming current was also measured.

Conditions:

Nozzle: cracked orifice
Distance from nozzle to clamp: 2 inches
Fuel Pressure: 15 psig
Fuel Temperature: varied between 85 and 92.4°F
Fuel Conductivity: 9 pS/m at 70°F
Fuel: Jet-A from JFK
Target: Teflon cushioned loop clamp (DG 26)
Initial Resistance: greater than 1 E1 2 ohms
Final Resistance: not recorded
Initial Capacitance: 91 picofarads
Final Capacitance: not recorded

Results: The maximum streaming current varied between -0.38 and -0.54 nanoamps. The maximum voltage was -351 volts.

Comments: The Lexan cabinet cover voltage was measured to be less than 100 volts at the completion of this test.

The maximum achievable charge on the clamp was higher for fuel flowing from a cracked Orifice than for fuel flowing from a single holed orifice.

Date: March 6

Test: 17

Tests Conducted: Measured the voltage on an electrically isolated, Teflon cushioned loop clamp (DG 26) using fuel spraying from a cracked orifice and at a higher flow rate and pressure. Streaming current was also measured.

Conditions:

- Nozzle: cracked orifice
- Distance from nozzle to clamp: 2 inches
- Fuel Pressure: 42 psig
- Fuel Temperature: varied between 90 and 93.4°F
- Fuel Conductivity: 9 pS/m at 70°F
- Fuel: Jet-A from JFK
- Target Teflon cushioned loop clamp (DG 26)
- Initial Resistance: Same as Test 16
- Final Resistance: not recorded
- Initial Capacitance: Same as Test 16
- Final Capacitance: not recorded

Results: The maximum streaming current was -0.3 nanoamps. The maximum voltage on the clamp was -517 volts.

Comment: The maximum voltage achieved on the Teflon cushioned loop clamp increased as the fuel flow rate increased as a result of switching to a cracked orifice.

Date: March 6

Test: 18

Tests Conducted: Measured the voltage on an electrically isolated, Teflon cushioned loop clamp (DG 26) using fuel spraying from a cracked orifice. Also used high flow rate and greater clamp/orifice separation. Streaming current was also measured.

Conditions:

- Nozzle: cracked orifice
- Distance from nozzle to clamp: 5-6 inches
- Fuel Pressure: 42 psig
- Fuel Temperature: 83°F
- Fuel Conductivity: 9 pS/m at 70°F
- Fuel: Jet-A from JFK
- Target: Teflon cushioned loop clamp (DG 26)
- Initial Resistance: Same as Test 16
- Final Resistance: not recorded
- Initial Capacitance: Same as Test 16
- Final Capacitance: not recorded

Results: The maximum streaming current measured was -0.32 nanoamps. The maximum voltage on the clamp was -544 volts.

Comments: From the fuel that was sprayed (prior to running out) on the Teflon clamp, it appears that increases in the orifice to target distance further increases the voltage observed on the clamp.

000137

Date: March 6

Test: 19

Tests Conducted: Measured the voltage on an electrically isolated, Teflon cushioned loop clamp (DG 26) using fuel spraying from a cracked orifice. Streaming current was also measured. Repeat of test 18 with fuel supply refilled.

Conditions:

Nozzle: cracked orifice
Distance from nozzle to clamp: 5-6 inches
Fuel Pressure: 42 psig
Fuel Temperature: 83°F
Fuel Conductivity: 5 pS/m at 64°F
Fuel: Jet-A from JFK
Target: Teflon cushioned loop clamp (DG 26)
Initial Resistance: Same as Test 16
Final Resistance: not recorded
Initial Capacitance: Same as Test 16
Final Capacitance: not recorded

Results: The maximum voltage was -168 volts. Low streaming current.

Comments: Test conditions were similar to Test 18. The refueling process may have contributed to the different voltages observed between tests 18 and 19.

Date: March 6

Test: 20

Tests Conducted: Measured the voltage on an electrically isolated, Teflon cushioned loop clamp (DG 26) from fuel spraying on its surface from a 0.07-inch orifice.

Conditions:

Nozzle: 0.07-inch orifice
Distance from nozzle to clamp: 5-6 inches
Fuel Pressure: 42 psig
Fuel Temperature: 65°F
Fuel Conductivity: 5 pS/m at 64°F
Fuel: Jet-A from JFK
Target: Teflon cushioned loop clamp (DG 26)
Initial Resistance: Same as Test 16
Final Resistance: not recorded
Initial Capacitance: Same as Test 16
Final Capacitance: not recorded

Results: The maximum voltage measured on the clamp was -345 volts. Streaming current was insignificant.

Comments: Orifice style (0.07-inch vs. cracked) contributed to higher resultant voltage on the Teflon cushioned clamp.

Date: March 6

Test: 21

Tests Conducted: Measured the voltage on an electrically isolated, Teflon cushioned loop clamp (DG 26) after increasing the fuel temperature and changing to a 0.07 inch orifice.

Conditions:

Nozzle: 0.07-inch orifice
Distance from nozzle to clamp: 5-6 inches
Fuel Pressure: 42 psig
Fuel Temperature: 91°F
Fuel Conductivity: 5 pS/m at 64°F
Fuel: Jet-A from JFK
Target: Teflon cushioned loop clamp (DG 26)
Initial Resistance: Same as Test 16
Final Resistance: not recorded
Initial Capacitance: Same as Test 16
Final Capacitance: not recorded

Results: The maximum voltage measured on the clamp was 512 volts. Streaming current was insignificant.

Comments: Fuel temperature contributed significantly to the resultant voltage observed on the Teflon clamp.

Date: March 7

Test: 22

Tests Conducted: Dry resistance and capacitance testing conducted on an electrically isolated, 1 inch diameter Wiggins coupling (Supplied by WL/PO).

Conditions: Test voltages for both resistance and capacitance measurements same as prior test on March 4, capacitance measured at 1kHz and 1 volt rms. See Test 2.

Results: See Table 6 of the main report.

Comments: Raised the male and female shell to fuel tube resistance to 1E11 ohms by inserting two new O-rings that had the highest resistance that was readily available. Individual O-ring resistance prior to installation in Wiggins coupling was greater than 1E12 ohms. Female and male shell to tube capacitance ranged from 89-95 picofarads.

Date: March 7

Test: 23

Tests Conducted: Measured the voltage on an electrically isolated, Teflon cushioned loop clamp (DG 26) after further increasing the fuel temperature.

Conditions:

Nozzle: 0.07-inch orifice
Distance from nozzle to clamp: 5-6 inches
Fuel Pressure: 42 psig
Fuel Temperature: 106°F
Fuel Conductivity: 9 pS/m at 86°F
Fuel: Jet-A from JFK
Target: Teflon cushioned loop clamp (DG 26)
Initial Resistance: greater than 1E12 ohms

000139

Final Resistance: Same as Test 24
Initial Capacitance: 91 picofarads
Final Capacitance: Same as Test 24

Results: The maximum voltage measured on the clamp was -568 volts.

Comments: The resultant voltage observed on the Teflon cushioned loop clamp again increased as the fuel temperature was increased.

Date: March 7

Test: 24

Tests Conducted: Measured the voltage on an electrically isolated Teflon cushioned loop clamp (DG 26) with fuel spraying from an 0.07-inch orifice. In this test, the distance between the orifice and clamp was increased. All other variables remained as stated in Test 23.

Conditions:

Nozzle: 0.07-inch orifice
Distance from nozzle to clamp: 8 inches
Fuel Pressure: 42 psig
Fuel Temperature: 104°F
Fuel Conductivity: 9 pS/m at 86°F
Fuel: Jet-A from JFK
Target: Teflon cushioned loop clamp (DG 26)
Initial Resistance: Same as Test 23
Final Resistance: greater than 1E12 ohms at 100 volts
Initial Capacitance: Same as Test 23
Final Capacitance: 91 picofarads

Results: The maximum voltage measured on the clamp was -650 volts.

Comments: The resultant voltage observed on the Teflon cushioned loop clamp increased as the distance between the orifice and clamp increased. Also at the end of this run, the resistance from the clamp to ground was measured using 1000 volts. The resistance measured was approximately 8E12 ohms. The resistance could be lower during the test if the voltage on the clamp increases beyond 1000 volts.

Date: March 7

Test: 25

Tests Conducted: Measured fuel resistance of Jet A fuel from JFK and JP8 from WL/PO. Measurement made by submerging clamp and fuel tube in tested fuel. Test voltages varied from 25 volts to 500 volts. Conductivity of each fuel was also measured.

Results:

Resistance Jet A: 6E11 ohms at 100 volts, Conductivity: less than 10 pS/m
Resistance JP8: 1.5E10 ohms at 25 volts, 1.5E8 ohms at 100 volts, 1.5E8 ohms at 500 volts;
Conductivity: 150 pS/m

Comments: The resistance of the fuel appears to drop significantly with increased voltage. This may be significant in spray testing as voltage levels achieved increase.

Date: March 7

Test: 26

000140

Tests Conducted: Measured the voltage on an electrically isolated 1-inch Wiggins coupling, (O-ring resistance greater than 1E11 ohms) with fuel spraying from a 0.07-inch orifice.

Conditions:

Nozzle: 0.07-inch orifice
Distance from nozzle to clamp: 8 inches
Fuel Pressure: 42 psig
Fuel Temperature: 96°F
Fuel Conductivity: 9 pS/m
Fuel: Jet-A from JFK
Target: 1 inch dia. Wiggins Coupling (WL/PO sample)
Initial Resistance: 1.2E11 ohms
Final Resistance: Not Recorded
Initial Capacitance: 131 picofarads
Final Capacitance: Not Recorded

Results: The maximum voltage measured on the Wiggins coupling was -14 volts

Comments: The resultant voltage on the Wiggins coupling was minimal. The resistance to ground of the outer coupling shell was 1E11 ohms when installed in the test chamber before testing. This was low, but considerations should be made regarding the inner surfaces of the Wiggins coupling and breakdown of the anodized layer if two surface contact one another.

PHASE II

Date: April 7
Test: 27

Tests Conducted: Measured the resistance of the yellow epoxy chromate primer on the inner surface of the fuel catch tank. Also conducted tribocharging measurements of same surface.

Conditions:

Resistance Test Voltage: 100 volts
Coating Thickness: 0.0003-0.0008 inches
Tank Exterior: Anodized

Results: Resistance at 100 volts was greater than 1E12 ohms. Resistance was less than 50,000 ohms at 200 volts. Tribocharging produced minimal charging levels.

Comments: Minimal charge levels after the tribocharging test were credited to charge dissipation through very thin epoxy chromate primer coating layer. The relatively low breakdown voltage of 200 volts demonstrated this.

Date: April 8
Test: 28

Tests Conducted: Determined the maximum voltage that could be achieved by spraying low conductivity fuel into a catch tank. Fuel (low conductivity, approximately 5pS/m) was sprayed onto the surface of fuel (same conductivity) collected in the catch tank till an approximate depth of 4 inches was reached. Field meters were used to measure the voltage achieved on the fuel surface as well as a point removed from the fuel surface and near the top of the test chamber.

Conditions:

Nozzle: 5 hole, 0.07-inch diameter equivalent
Fuel: Jet A
Fuel Pressure: 25 psig
Fuel Temperature: 83°F
Fuel Conductivity: not measured, less than 10 pS/m
Fuel Flow Rate: 3900 ml/ 2min.
Target: Fuel surface (4-inch depth)
Meter settings, conversion factor: Fuel Surface meter, 10X scale (0- 10,000 volts), Output 0-1 volts; Air/Mist meter, 1X scale (0-1000 volts), Output 0-1 volts

Results: Minimal voltage levels were found on the surface of the fuel in the catch tank and in the remote space within the test chamber. The offset output voltage of the fuel surface field meter was 0.03 volts and remained near that value throughout the test. The offset voltage for the space field meter was 0.85 mV and also remained stable throughout the test.

Comments: The functionality of both meters was checked after the test with a charged material to verify full deflection of each field meter. Leads of both field meters were also switched to ensure that they were functioning properly.

Date: April 8

Test: 29

Tests Conducted: Determined the maximum voltage that could be achieved by spraying low conductivity fuel onto the surface of low conductivity fuel in the catch tank. Fuel was sprayed onto the surface of fuel collected in the catch tank. Field meters were used to measure the voltage achieved on the fuel surface as well as a point removed from the fuel surface but within the test chamber. Repeat of Test 28 with a cracked orifice.

Conditions:

Nozzle: cracked orifice
Fuel: Jet A
Fuel Pressure: 25 psig
Fuel Temperature: not recorded
Fuel Conductivity: not measured, less than 10 pS/m
Target: fuel surface

Results: No appreciable surface or space voltages were attained during the test.

Date: April 8

Test: 30

Tests Conducted: Determined the maximum voltage that could be achieved by spraying low conductivity fuel onto the surface of low conductivity fuel in the catch tank. Fuel was sprayed onto the surface of fuel collected in the catch tank. Field meters were used to measure the voltage achieved on the fuel surface as well as a point removed from the fuel surface but within the test chamber. Repeat of Test 29 with cracked orifice realigned.

Conditions:

Nozzle: cracked orifice
Fuel: Jet A
Fuel Pressure: 25 psig
Fuel Temperature: not recorded
Fuel Conductivity: not measured, less than 10 pS/m
Target: fuel surface

000142

Results: No appreciable surface or space voltages were attained during the test.

Date: April 8

Test: 31

Tests Conducted: Determined the maximum voltage that could be achieved by spraying low conductivity fuel onto the surface of low conductivity fuel in the catch tank. Fuel was sprayed onto the surface of fuel collected in the catch tank. Field meters were used to measure the voltage achieved on the fuel surface as well as a point removed from the fuel surface but within the test chamber. Repeat of Test 30 at 42 psig.

Conditions:

Nozzle: cracked orifice
Fuel: Jet A
Fuel Pressure: 42 psig
Fuel Temperature: not recorded
Fuel Conductivity: not measured, less than 10 pS/m
Target: fuel surface

Results: No appreciable surface or space voltages were attained during the test.

Date: April 9

Test: 32

Tests Conducted: Determined the maximum current and voltage that could be achieved by spraying low conductivity fuel onto an isolated epoxy chromate coated aluminum target plate.

Conditions:

Nozzle: 5 hole, 0.07-inch diameter equivalent
Fuel: Jet A
Fuel Pressure: 25 psig
Fuel Temperature: 96°F
Distance to Target from Nozzle: 24 inches
Target Angle: 45°, measured from horizontal
Fuel Conductivity: Approx. 5pS/m at 72°F
Target: 8 1/2X 12-inch epoxy chromate coated aluminum target plate (coated side facing fuel flow). Isolated from ground with Teflon sheeting.
Target Plate Resistance: much greater than 10E12 ohms
Target Plate Capacitance: 23 picofarads (alone), w/electrometer 377 picofarads, 60-63 picofarads in test chamber and wet with fuel

Results: The maximum charging current observed on the target plate varied between -0.29 and -0.40 nanoamps. The voltage after 12 minutes was 814 volts. A peak voltage of 860 volts was observed.

Comments: The higher capacitance value measured on the target plate when connected to the electrometer was due to the added input capacitance of the electrometer. The electrometer was not intended to be included in the overall system capacitance measurement.

Date: April 9

Test: 33

Tests Conducted: Determined the maximum current that could be achieved by spraying low conductivity fuel onto an epoxy chromate coated isolated target plate. A screen was introduced to "break up" the fuel in an attempt to increase the charging current on the target plate.

Conditions:

Nozzle: 5 hole, 0.07-inch diameter equivalent
Fuel: Jet A
Fuel Pressure: 25 psig
Fuel Temperature: Not recorded, see test 32
Distance to Target from Nozzle: 24 inches
Target Angle: 45°, measured from horizontal
Fuel Conductivity: See test 32
Screen: located 18.25 inches below the orifice, ungrounded
Target: 8 1/2X 12-inch epoxy chromate coated aluminum target plate (coated side facing fuel flow). Isolated from ground with Teflon sheeting.
Target Plate Resistance: See test 32
Target Plate Capacitance: See test 32

Results: The maximum current varied between -0.39 and 0.75 nanoamps.

Comments: A slight increase in charging current was observed due to the introduction of the screen.

Date: April 9

Test: 34

Tests Conducted: Determined the maximum current that could be achieved by spraying low conductivity fuel onto an epoxy chromate coated isolated target plate. Determined if the epoxy chromate coating on the target plate surface effects the target plate charging.

Conditions:

Nozzle: 5 hole, 0.07-inch diameter equivalent
Fuel: Jet A
Fuel Pressure: 25 psig
Fuel Temperature: Not recorded, see test 32
Distance to Target from Nozzle: 24 inches
Target Angle: 45°, measured from horizontal
Fuel Conductivity: See test 32
Screen: located 18.25 inches below the orifice, grounded
Target: 8 1/2X 12-inch epoxy chromate coated aluminum target plate (coated side facing away from fuel flow). Isolated from ground with Teflon sheeting.
Target Plate Resistance: See test 32
Target Plate Capacitance: See test 32

Results: The maximum target plate current varied between 0 and -0.40 nanoamps.

Comments: A decrease in charging current was observed with the bare side of the target plate facing the fuel flow.

Date: April 9

Test: 35

Tests Conducted: Determined the maximum current that could be achieved by spraying low conductivity fuel onto an epoxy chromate coated isolated target plate. Also, determined if the grounding of the spray breakup screen affects the current on the target plate.

Conditions:

Nozzle: 5 hole, 0.07-inch diameter equivalent
Fuel: Jet A
Fuel Pressure: 25 psig
Fuel Temperature: Not recorded, see test 32
Distance to Target from Nozzle: 24 inches
Target Angle: 45°, measured from horizontal
Fuel Conductivity: See test 32
Screen: located 18.25 inches below the orifice, ungrounded
Target: 8 1/2X 12-inch epoxy chromate coated aluminum target plate (coated side facing fuel flow). Isolated from ground with Teflon sheeting.
Target Plate Resistance: See test 32
Target Plate Capacitance: See test 32

Results: The maximum target plate current varied between 0 and -0.42 nanoamps.

Comments: The ground connection to the spray breakup screen had no influence on target plate charging current.

Date: April 9
Test: 36

Tests Conducted: Repeated Test 33 and determined if grounding the break-up screen impacted charging current.

Conditions:

Nozzle: 5 hole, 0.07-inch diameter equivalent
Fuel: Jet A
Fuel Pressure: 25 psig
Fuel Temperature: Not recorded, see test 32
Distance to Target from Nozzle: 24 inches
Target Angle: 45°, measured from horizontal
Fuel Conductivity: See test 32
Screen: located 18.25 inches below the orifice, ungrounded
Target: 8 1/2X 12-inch epoxy chromate coated aluminum target plate (coated side facing fuel flow). Isolated from ground with Teflon sheeting.
Target Plate Resistance: See test 32
Target Plate Capacitance: See test 32

Results: The maximum current varied between -0.38 and -0.70 nanoamps.

Comments: Optimum charging conditions from Tests 33 through 35 (9 April) were used to see if unbending the screen would lead to different results.

Date: April 9
Test: 37

Tests Conducted: Low conductivity fuel was sprayed onto an electrically isolated, epoxy chromate coated, aluminum plate. Determined if changing the angle of the target plate changes the current measured on the target plate.

Conditions:

Nozzle: 5 hole, 0.07-inch diameter equivalent
Fuel: Jet A

000145

Fuel Pressure: 25 psig
Fuel Temperature: 89°F
Distance to Target from Nozzle: 24 inches
Target: 8 1/2X 12-inch epoxy chromate coated aluminum target plate (coated side facing fuel flow). Isolated from ground with Teflon sheeting.
Target Angle: varied between 0° and 60°, measured from horizontal
Break up Screen Inserted and Grounded
Fuel Conductivity: 5pS/m at 72°F

Results: The maximum current achieved on the target plate was approximately -1.00 nanoamps at a plate angle of 45 degrees. Testing at 30 and 60 degrees also produced significant charging currents. The current as a function of target plate angle is plotted in Figure 7 of the main report.

Comments: Although the maximum charging currents observed were at 45 degrees, significant values were observed at 30 and 60 degrees.

Date: April 10
Test: 38

Tests Conducted: Low conductivity fuel was sprayed onto an electrically isolated, epoxy chromate coated aluminum target plate. Determined the impact of fuel temperature on the charging current observed on the target plate.

Conditions:

Nozzle: 5 hole, 0.07-inch diameter equivalent
Fuel: Jet A
Fuel Pressure: 25 psig
Fuel Temperature: Initial Temperature 58°F, increased to 115°F at conclusion of test
Distance to Target from Nozzle: 24 inches
Target: 8 1/2X 12-inch epoxy chromate coated aluminum target plate (coated side facing fuel flow). Isolated from ground with Teflon sheeting.
Target Angle: 30°, measured from horizontal
Fuel Conductivity: 6 pS/m at 83°F
No Screen here and ensuing tests in Phase II

Results:

Fuel Temp: 58°F, Target Plate Current: -170 picoamps
Fuel Temp: 71°F, Target Plate Current: -210 picoamps
Fuel Temp: 80°F, Target Plate Current: -260 picoamps
Fuel Temp: 90°F, Target Plate Current: -300 picoamps
Fuel Temp: 100°F, Target Plate Current: -390 picoamps
Fuel Temp: 115°F, Target Plate Current: -450 picoamps

The target plate current as a function of fuel temperature is plotted in Figure 5 of the main report.

Comments: The charging current on the target plate increased significantly with increasing fuel temperature.

Date: April 10
Test: 39

Tests Conducted: Low conductivity fuel was sprayed onto an electrically isolated, chromate coated, aluminum target plate. Determined the impact of target distance from the orifice on target plate charging current.

000146

Conditions:

Nozzle: 5 hole, 0.07-inch diameter equivalent
Fuel: Jet A
Fuel Pressure: 25 psig
Fuel Temperature: Relatively constant between 116 and 118°F
Distance to Target from Nozzle: 18 inches
Target: 8 1/2X 12-inch epoxy chromate coated aluminum target plate (coated side facing fuel flow). Isolated from ground with Teflon sheeting.
Target Angle: Varied from 0° to 60°, measured from horizontal
Fuel Conductivity: 6 pS/m at 83°F

Results: The maximum target plate current varied between -0.29 and -0.42 nanoamps. The charging current recorded at a target plate angle of 30° varied between -0.35 and -0.42 nanoamps. Target plate current as a function of target plate angle is plotted in figure 7 of the main report.

Comments: There was a slight decrease in target plate charging current as target distance decreased. There was a smaller contact area (fuel spray onto plate) as target distance decreased, which might result in a slightly lower charging current.

Date: April 10

Test: 40

Tests Conducted: Low conductivity fuel was sprayed onto an electrically isolated, chromate coated, aluminum target plate. Determined the impact of further decreasing target distance from the orifice on target plate charging current.

Conditions:

Nozzle: 5 hole, 0.07-inch diameter equivalent
Fuel: Jet A
Fuel Pressure: 25 psig
Fuel Temperature: Relatively constant between 110 and 115°F
Distance to Target from Nozzle: 12 inches
Target: 8 1/2X 12-inch epoxy chromate coated aluminum target plate (coated side facing fuel flow). Isolated from ground with Teflon sheeting.
Target Angle: varied from 0 to 60°, measured from horizontal
Fuel Conductivity: not measured, less than 10 pS/m

Results: The maximum target plate current varied between -0.23 and -0.44 nanoamps. The charging current recorded at a target plate angle of 30° varied between -0.32 and -0.44 nanoamps. Target plate current as a function of target plate angle is plotted in figure 7 of the main report.

Comments: No appreciable difference in charging current was observed for target plate distances of 12 and 18 inches.

Date: April 10

Test: 41

Tests Conducted: Low conductivity fuel was sprayed onto an electrically isolated, chromate coated, aluminum target plate. Determined the impact of further decreasing target distance from the orifice on target plate charging current.

Conditions:

Nozzle: 5 hole, 0.07-inch diameter equivalent

000147

Fuel: Jet A
Fuel Pressure: 25 psig
Fuel Temperature: Relatively constant between 111 and 114°F
Distance to Target from Nozzle: 6 inches
Target Angle: Varied from 0 to 60°, measured from horizontal
Target: 8 1/2X 12-inch epoxy chromate coated aluminum target plate (coated side facing fuel flow). Isolated from ground with Teflon sheeting.
Fuel Conductivity: Not measured, less than 10 pS/m

Results: The maximum target plate current varied between -0.22 and -0.43 nanoamps. The charging current recorded at a target plate angle of 30° varied between -0.27 and -0.37 nanoamps. Target plate current as a function of target plate angle is plotted in figure 7 of the main report.

Comments: There was a slight drop in charging current between that observed at a 12 inch target distance and that at 6 inches.

Date: April 10

Test: 42

Tests Conducted: : Low conductivity fuel was sprayed onto an electrically isolated, chromate coated, aluminum target plate. A slotted orifice was used with a fine mesh insert to provide better break up of the spray. Determined the relationship between target plate current and target plate angle.

Conditions:

Nozzle: 0.086 X 0.640 inch slot, 0.055 square inch open area, mesh insert
Fuel: Jet A
Fuel Pressure: 25 psig
Fuel Bulk Temperature: 100 to 110°F
Distance to Target from Orifice: 24 inches
Target Angle: Varied between 30° and 45°, measured from horizontal
Target: 8 1/2X 12-inch epoxy chromate coated aluminum target plate (coated side facing fuel flow). Isolated from ground with Teflon sheeting.
Fuel Conductivity: 5 pS/m
Screen: See results.

Results: Using a target angle of 30° and no screen the charging current varied between -0.4 and -0.5 nanoamps. When the screen was added and the target angle was increased to 45° the charging current was -1.5 nanoamps with peaks greater than -2.5 nanoamps.

Comments: The addition of the screen again contributed to the larger charging current observed (See Test 33, April 9).

Date: April 11

Test: 43

Tests Conducted: Measured individual Viton O-ring resistances (4 samples). Conducted dry resistance and capacitance testing on T7/T8 Wiggins coupling with Viton o-rings installed.

Conditions: Test voltage used for resistance testing was 100 volts. Test voltage for resistance and capacitance measurements of assembled coupling were the same as those from Phase I, Test 1.

Results: Individual Viton O-ring resistance: All four o-rings were much greater than 1E12 ohms.

Assembled coupling T7/T8: Female to Male Resistance, 1.6 ohms

Male Resistance to Fuel Tube, Approx. 2E11 ohms at 10 volts
Female Resistance to Fuel Tube, Approx. 2E11 ohms at 10 volts
Tube to Tube resistance, Approx. 9E11 ohms at 10 volts
Female to Tube Capacitance, 199 picofarads Q=20. 1, D=O.05,
G=O.062
Male to Tube Capacitance, 199picoFarads Q=20. 1, D=O.05, G=0.062

Comments: Raised the male and female shell to fuel tube resistance to 2E11 ohms by inserting different o-rings. Individual o-ring resistance prior to installation in Wiggins coupling was greater than 1E12 ohms. This again suggests that increasing the contact area between the o-ring and the walls of both the Wiggins coupling outer shells and the fuel tubes decreases the overall resistance.

Date: April 11

Test: 44

Tests Conducted: Low conductivity fuel was sprayed onto an electrically isolated, chromate coated, aluminum target plate. Monitored current flow from the fuel catch tank and target plate voltage with and without the screen placed in the fuel flow.

Conditions:

Nozzle: 0.086 X 0.640-inch slot, 0.055 square inch open area, mesh insert
Fuel Pressure: 25 psig
Fuel Bulk Temperature: 103 to 108°F
Distance to Target from Orifice: 24 inches (same as prior day)
Target Angle: 30°, measured from horizontal
Target: 8 1/2X 12-inch epoxy chromate coated aluminum target plate (coated side facing fuel flow). Isolated from ground with Teflon sheeting.
Fuel Conductivity: 31pS/m at 72°F
Fuel: Jet-A with Stadis-450
Screen: Varied, both in and out depending on test sequence, installed 14 inches below orifice

Results: The maximum fuel tank current with the screen installed was between -6.9 and -7.6 nanoamps and with the screen removed the maximum current was -3.5 nanoamps. The maximum target plate voltage achieved during this sequence was +1080 volts.

Comments: Tank current was measured to determine if there was a relationship between charge generated at the target plate/fuel surface interface and that collected in the fuel collection tank. This relationship might be better understood through measurement of the current observed in the target plate and the fuel collection tank. This test focused on the tank current. The ensuing test will focus on target plate current keeping all test conditions constant. As was the case in prior tests with the target plate, the insertion of the screen increased current levels observed in the fuel collection tank.

Also of significance was the change in target plate current polarity from negative to positive with the change in fuel conductivity from 5 pS/m to 31 pS/m.

Date: April 11

Test: 45

Tests Conducted: Fuel with a higher conductivity (approximately 31 pS/m) was sprayed onto an electrically isolated, chromate coated, aluminum target plate. Monitored current flow in the target plate and tank voltage with and without the screen placed in the fuel flow. Also varied the target plate angle to determine impact of target plate angle on target plate current and tank voltage.

Conditions:

Nozzle: 0.086 X 0.640-inch slot, 0.055 square inch open area, mesh insert
Fuel Pressure: 25 psig
Fuel Bulk Temperature: 105 to 111°F
Distance to Target from Orifice: 24 inches (same as prior day)
Target Angle: Varied between 0 and 60°, measured from horizontal
Target: 8 1/2X 12-inch epoxy chromate coated aluminum target plate (coated side facing fuel flow). Isolated from ground with Teflon sheeting.
Fuel Conductivity: 3 lpS/m at 72°F
Fuel: Jet-A with Stadis-450
Screen: Varied, both in and out depending on test sequence, installed 14 inches below orifice

Results: The target plate maximum current varied between +1.0 and +6.7 nanoamps and tank voltage varied between -90 and -300 volts with the highest values for each reached with the screen inserted in the fuel flow. 30,45 and 60 degree target plate angles again produced the highest target plate currents and tank voltages while 0 and 15 degree angles produced the lowest. Similar results but lower magnitudes of target plate current and tank voltage were observed without the screen in place. The target plate current as a function of target plate angle is plotted in figure 6 of the main report.

Comments: Similar correlation between target plate/tank current and voltage with respect to target plate angle and the use of the screen were achieved with the higher conductivity fuel to those found earlier with lower conductivity (-5pS/m) fuel. Fuel with a conductivity of approximately 31 pS/m produced higher overall target plate currents and voltages than the 5pS/m fuel. There was a slight increase (3-4 degrees) in fuel temperature for this test sequence as opposed to the prior test and some of the increase in target plate current and voltage may be attributed to this increase.

Date: April 11

Test: 46

Tests Conducted: Fuel with a higher conductivity (approximately 94 pS/m) was sprayed onto an electrically isolated, chromate coated, aluminum target plate. Monitored current flow on the target plate and voltage in the fuel tank, with and without, the screen placed in the fuel flow. Also varied the target plate angle to determine the impact of the angle on target plate current and tank voltage.

Conditions:

Nozzle: 0.086 X 0.640-inch slot, 0.055 square inch open area, mesh inserted
Fuel Pressure: 25 psig
Fuel Bulk Temperature: 113 to 120°F
Distance to Target from Orifice: 24 inches
Target Angle: varied between 0 and 60°, measured from horizontal
Target: 8 1/2X 12-inch epoxy chromate coated aluminum target plate (coated side facing fuel flow). Isolated from ground with Teflon sheeting.
Fuel Conductivity: 94 pS/m at 72°F
Fuel: Jet-A with Stadis-450
Screen: Varied, both in and out depending on test sequence, installed 14 inches below orifice.
Screen resistance was measured when in place and not grounded with a ground line. Resistance was 6 kohms.

Results: Initial testing was conducted with a target plate angle of 30 degrees, the screen removed and a fuel temperature of 117 degrees F. Tank current was -5 nanoamps. The screen was replaced and tank current increased to -11 nanoamps. Instrumentation was adjusted to measure both tank current and target plate voltage again at 30 degrees (target plate angle) and with the screen in the fuel flow. Tank current remained at -5 nanoamps and target plate voltage was 430 volts.

With flow continuing, a sequence of tests were run with the screen in the flow, fuel temperature at 117-118 degrees F, and varying target plate angles. Target plate current varied between -2.5 and +12.0 nanoamps. Negative target plate currents were achieved when target plate angle was perpendicular (zero degrees) or nearly perpendicular (15 degrees) to the fuel flow. Tank voltage varied from -40 volts at a target plate angle of zero degrees to -359 volts at a target plate angle of 60 degrees.

The screen was removed and the above sequence repeated under the same conditions. Target plate current varied between +5 and +13 nanoamps. Tank voltage varied from -39 volts at a target plate angle of zero degrees to -317 volts at a target plate angle of 60 degrees. Although a negative target plate current was not achieved in this test sequence, the relative change in current between target plate angles was similar.

For the first time a measurement of tank current and target plate voltage were measured concurrently. With the screen in, the voltage on the target plate reached +1000 volts. The current on the tank during this time decreased in magnitude from the start of the test, until settling out at about -8 nanoamps at the time the target plate voltage reached +1000 volts. Then the target plate was grounded and tank current was measured at -19 nanoamps.

Comments: Similar correlations between target plate/tank current and voltage with respect to target plate angle and the use of the screen were achieved with the higher conductivity fuel to those found earlier with lower conductivity (-3 pS/m fuel). Fuel with a conductivity of approximately 94 pS/m did produce higher overall target plate currents while target plate voltages remained similar, peaking at +1000 volts. This suggested that fuel resistance was beginning to play a role in the charging process. Higher charging current with little increase in voltage emphasized this point. Fuel temperature again was slightly higher (3-4 degrees) for this test sequence as opposed to the prior test and some of the increase in target plate current may be attributed to this increase.

Also in this sequence, target plate current fluctuated with respect to target plate angle such that current went from positive values at 30, 45 and 60 degrees to negative values at 0 and 15 degrees. The concept of residence time was considered here in addition to the effect of higher fuel conductivity. As target plate angle decreased, fuel "resided" on the grounded surface of the target plate longer than the steeper target plate angles. There were several contributors to the overall target plate current when the target plate was perpendicular to the flow. They include the effect of frictional charging (fuel contacting the target plate), the time the fuel resided on the target plate and the fuel flowing over the edges of the target plate. Charged fuel from the orifice also may contribute to target plate current more significantly when target plate angle was zero or nearly flat.

Date: April 17

Test: Test 47

Tests Conducted: Sprayed fuel onto an electrically isolated, chromate coated, aluminum target plate. Measured current and voltage on the target plate to determine the equivalent resistance during fuel flow and contact with the target plate.

Conditions:

Nozzle: 0.086 X 0.640-inch slot, 0.055 square inch open area, mesh inserted

Fuel Pressure: 25 psig

Fuel Bulk Temperature: Varied between 112 and 118°F

Distance to Target from Orifice: 24 inches

Target Angle: 60°, measured from horizontal

Target: 8 1/2X 12-inch epoxy chromate coated aluminum target plate (coated side facing fuel flow). Isolated from ground with Teflon sheeting.

Fuel Conductivity: 94 pS/m at 72°F

Fuel: Jet-A with Stadis-450

Screen: Varied, both in and out depending on test sequence, installed 14 inches below orifice

Results: With the screen in the fuel flow path, the target plate current was approximately -6.25 nanoamps. The target plate voltage was approximately -570 volts with an initial peak or “spike” of -850 volts. The calculated resistance was 1 E11 ohms. With the screen removed, the target plate current was +3 nanoamps and the target plate voltage was +700 volts. In this case the calculated resistance was 2.3E11 ohms.

Comments: Tests conducted on April 17 were done using fuel that had been idle since April 11. Initial target current and voltage were very erratic. A multitude of factors may have contributed to the erratic readings initially. Consistency of fuel flow from the orifice, mixing of fuel that was idle for several days and air in the fuel line all may have contributed. The final calculated resistance (after stabilized current and voltage) of 2.3E11 ohms was low enough to influence charge dissipation rate at the fuel/target plate interface. There was some concern however that the +3 nanoamps current used in the calculation was not the maximum current that could be achieved under these test conditions. Values similar to those obtained on April 11 were expected. No measurements of both target plate current and voltage WITHOUT the screen were taken on April 11. Using the current and voltage values obtained on April 11, WITH the screen, the resistance calculated, at a target plate angle of 60 degrees was 7.6E10 ohms.

Date: April 18

Test: 48

Tests conducted: Determined the impact of noise in test area on charging current measurements.

Comments: A review of the current measurement waveforms stored on the Lecroy 93141 Oscilloscope on 17 April revealed 60 cycle noise in the current waveforms. The 60 cycle noise was found to occur if the electrometer input cable was connected external to the test cabinet. Very little 60 cycle noise was observed if the electrometer input cable alligator clip was positioned internal to the test cabinet.

The effect, if any, of the 60 cycle noise on previous data collected by the electrometer was examined by connecting the electrometer in series with a 1E9 ohm resistor connected to a function generator. The function generator was set for a 5 VDC offset, including a 1 VRMS sine wave output to simulate noise. The frequency was varied from 0 through 20 Megahertz. The output of the electrometer was examined and it was found that it correctly obtained a DC offset corresponding to the 5 nanoamp DC current that should have been obtained.

Date: April 21

Test: 49

Tests Conducted: Fuel was sprayed onto an electrically isolated, epoxy chromate coated, aluminum target plate. Measured current (shielded electrometer alligator clamp) and voltage on the target plate to determine the equivalent resistance during fuel flow and contact with the target plate.

Conditions:

- Nozzle: 0.086 X 0.640-inch slot, 0.055 square inch open area
- Fuel Pressure: 25 psig
- Fuel Bulk Temperature: 94°F
- Distance to Target from Orifice: 24 inches
- Target Angle: 60°, measured from horizontal
- Target: 8 1/2X 12-inch epoxy chromate coated aluminum target plate (coated side facing fuel flow). Isolated from ground with Teflon sheeting.
- Fuel Conductivity: 94pS/m at 72°F (initial), 140 pS/m at 94°F (final)
- Fuel: Jet-A with Stadis-450
- Break up Screen: removed
- Target Plate Isolation: greater than 1E12 ohms
- Fuel Catch Tank Isolation: greater than 1E12 ohms

Target Plate Capacitance: 54 picofarads (including wiring and charged target plate monitor)

Results: The current measured on the target plate was approximately +1.2 nanoamps. The maximum tank current varied between -5.3 and -6.4 nanoamps. The target plate voltage reached a maximum of 630 volts. The calculated resistance of the isolated target plate to ground during the test was 5.25×10^{11} ohms.

Comments: Tests conducted on April 21 were done using aged fuel that had first been placed in the test apparatus on April 11. The observed charging current was much lower than expected. This may have been due to substantial fluctuations in the relative humidity (0.8 to 11.7 %RH) observed in the test chamber as well as a much lower fuel temperature and changes in fuel properties over time.

Date: April 22

Test: 50

Tests Conducted: Fuel (JP-8) was sprayed onto an electrically isolated, epoxy chromate coated, aluminum target plate. The Teflon sheeting used to isolate the target plate prior to this date was removed. The target plate was then electrically bonded to the target plate rotation bar that extended through the test chamber to the outside environment on both ends. The charging current and voltage on the target plate were measured during fuel flow from the orifice onto the target plate as well as the current in the fuel catch tank. Voltage decay rate from the target plate was also recorded. Direct electrical resistance measurements between the target plate and ground were made immediately after the fuel flow was stopped to see how they compared to the calculated measurements made using the dynamic target plate current and voltage. Voltage was increased during these resistance measurements to see if the resistance measurements were voltage sensitive.

Conditions:

Nozzle: 0.086 X 0.640-inch slot, 0.055 square inch open area, mesh insert

Fuel Pressure: 25 psig

Fuel Bulk Temperature: 92 to 113°F

Distance to Target from Orifice: 24 inches

Target Angle: 60°, measured from horizontal

Target: 8 1/2X 12-inch epoxy chromate coated aluminum target plate (coated side facing fuel flow). Mounted to isolated rotational bar and Teflon sheeting removed.

Fuel Conductivity: 145 pS/m at 69°F (before test), 225 pS/m at 72°F (after 1st test), 275 pS/m at 95°F (after 2nd test)

Fuel: JP-8

Break up Screen: removed

Target plate/rotation bar capacitance (installed): 61 picofarads at 60° target plate angle

Target plate/ rotation bar resistance (installed): much greater than 1×10^{12} ohms at 100 volts

Results: Two separate fuel flow tests were conducted. The maximum tank current varied between -10 and -18.5 nanoamps. The target plate voltage varied between +775 and +1132 volts. The maximum target plate current varied between +9.2 and +12.6 nanoamps. The target plate voltage decayed by one half, from 1090 to 538 volts, in five minutes.

The resistance measured between the target plate and ground after the fuel flow was stopped was much greater than 1×10^{12} ohms at 100 volts, 6.5×10^{12} ohms at 200 volts and 1.5×10^{12} ohms at 1000 volts. The calculated resistance after the first run was 2.2×10^{11} ohms and 8.8×10^{10} ohms after the second run.

Comments: The target plate was attached directly to the rotating bar and the Teflon isolation sheeting was removed in an attempt to eliminate all parallel resistance paths associated with fuel that coated the sheets and contacted the grounded rotating bar. Assuming all other variables remain constant elimination of this resistance path should lead to increased charging currents and voltages. At the same time, new fuel, JP-8, was introduced during this test sequence. It was difficult to determine whether the JP-8 or the elimination

of the resistance path associated with the Teflon sheeting was the major player in the increased charging current and voltage observed on the target plate. The calculated resistance after the second run was the lowest value observed to date. This further emphasizes that the high currents and voltages observed were offset by the reduced resistance of the fuel and parallel resistive paths that continue to exist in the system (fuel falling to the collection tank and fuel flowing from the orifice).

The fuel resistance was sensitive to voltage. As the target plate voltage increased, the resistance decreased requiring an increased charging source or current to produce a voltage.

Noise was a problem during the first test on 22 April. By removing the Teflon sheeting from the target plate and bonding the target plate to the rotating bar the target plate and bar become the isolated conductor. Portions of the bar were outside the test chamber and subjected to ambient noise in the test facility. The exposed areas were shielded after the first run and the repeatability of the readings improved during the second run.

Date: April 23

Test: 51

Tests Conducted: Fuel (JP-8) was sprayed onto an electrically isolated, epoxy chromate coated, aluminum target plate (bonded to the rotating bar electrically). The charging current and voltage on the target plate were measured with fuel flowing from the orifice onto the target plate.

Conditions:

Nozzle: 0.086 X 0.640-inch slot, 0.055 square inch open area, mesh insert

Fuel Pressure: 25 psig

Fuel Bulk Temperature: 106 to 108°F

Distance to Target from Orifice: 24 inches

Target: 8 1/2X 12-inch epoxy chromate coated aluminum target plate (coated side facing fuel flow). Mounted to isolated rotational bar and Teflon sheeting removed.

Fuel Conductivity: 357 pS/m at 72°F; 429 pS/m at 82°F; 544 pS/m at 108°F

Fuel: JP8+100

Break up Screen: removed

Results: For the first run, the target plate current peaked at 6 nanoamps but decreased to 1 nanoamp as the spray pattern became inconsistent. Target plate voltage peaked at 500 volts, but decreased to 300 volts when the spray pattern narrowed. In the second run, the target plate current peaked at 6 nanoamps then decreased to 3.3 nanoamps as the flow again fluctuated and narrowed. The target plate voltage peaked at near 500 volts in the second run and diminished to about 420 volts when the flow narrowed. The collection tank current was measured in the second run also while target plate voltage was recorded. Tank current peaked at -6.2 nanoamps and decreased to -2.0 nanoamps when the flow decreased.

Comments: No explanation can be given for the change in flow from the orifice during this test sequence. The fuel (JP8+100) had a much higher conductivity but should not have affected the flow pattern. A change in flow did produce a change in target plate current and voltage. Since the surface area of the target plate contacted by the flow decreased significantly, the contact surface area was another factor to consider when trying to achieve maximum current and voltage on the target plate. The air/fuel volume between the orifice and the target plate also changed with a change in flow pattern possibly creating more or less charge within the stream prior to contact with the target plate. This may also contribute to changes in the current and voltage values measured on the target plate. The fuel contact point on the target plate also changed slightly during this test sequence from the lower portion of the target plate to the upper portion. This did not appear to significantly change the current or voltage although concurrent changes in flow rate influenced any significant change that might have occurred. The relative humidity also fluctuated as the flow changed and the target current and voltage decreased. The nitrogen flow was not

adjusted during this time frame so it appears that the flow pattern and changes in it might impact chamber humidity. Changes in the number of airborne fuel particles or the influx of moist air from the fuel line might have caused the change in relative humidity.

Date: April 23

Test: 52

Tests Conducted: Measured the amount of charge present in fuel exiting the spray orifice. Fuel was collected in an electrically isolated, conductive container and charge was measured with an electrometer. Also measured the target plate and collection tank currents.

Conditions:

Nozzle: 0.086 X 0.640-inch slot, 0.055 square inch open area, mesh insert
Fuel Pressure: 25 psig
Fuel Bulk Temperature: 115-122°F (initial), 108°F (final).
Fuel Conductivity: same fuel as test 21
Break up Screen: removed
Fuel: JP8+100

Results: The test was run twice. The first test, ran for 13.3 seconds, resulted in a charge accumulation of -20 nanocoulombs and 810 ml of fuel being sprayed. The second test, ran for 10.6 seconds, resulted in a charge accumulation of -18.8 nanocoulombs. The calculated current was between -1.48 and -1.77 nanoamps. Target plate and collection tank currents were also measured. The tank current (with target plate grounded) was -9.6 nanoamps and the target plate current (with tank grounded) was +5.0 nanoamps.

Comments: The test showed that the fuel flow from the orifice was not electrically neutral and had a negative current value. This was of significance when trying to determine where charge was located in the overall test system. It was also important in determining whether fuel flowing from an orifice was charged prior to contact with an isolated conductor and how that charge impacts the overall charge generated at the fuel/target plate interface. When the current from the orifice, target plate, and collection tank were added a net current still remained. Charge flow may exist at other points within the test chamber (i.e. misting, larger mobile particles, etc.). Fuel temperature varied 14 degrees from the start of the test to the finish and as mentioned prior, significant changes in current and voltage can occur with changing fuel temperature.

Date: April 24

Test: 53

Tests Conducted: Rerun the tests of April 23 and analyze currents generated in the test chamber (i.e. orifice, target plate and collection tank) while keeping fuel temperature as stable as possible. Changed to the 5 hole orifice to obtain better flow pattern repeatability.

Conditions:

Nozzle: 5 hole, 0.07-inch diameter equivalent
Fuel Pressure: 25 psig
Fuel Bulk Temperature: 105 to 108°F.
Fuel Conductivity: 474 pS/m at 66°F; 666 pS/m at 107°F
Break up Screen: removed
Fuel: JP8+100

Results: Currents were measured at the orifice, target plate and within the collection tank with and without the drain plug in place. Fuel temperature was held constant between 106 and 110°F. The orifice current was calculated using the fuel collection and charge measurement technique described on April 23. Two charge measurements were made at the orifice. For each measurement the charge was collected for

100 seconds. The two measurements were -12.8 nanocoulombs and -14.8 nanocoulombs, resulting in calculated currents of 0.128 nanoamps and 0.148 nanoamps. The other currents were measured directly using the electrometer. The target plate current was +1.843 nanoamps. The tank current was -1.705 nanoamps with the plug and -1.804 nanoamps without the plug. A target plate voltage of +360 volts was also measured.

Comments: Adding the resultant currents from the orifice, target plate and collection tank produced a net current in the test system of near zero. Temperature was kept nearly constant throughout the test and the 5-hole orifice was used to minimize current fluctuations. Orifice current was much lower for this test sequence than the prior test. This was due to the use of the 5-hole orifice, which produced a more repeatable flow pattern, but less current. This was consistent with prior days testing where maximum charging and current were achieved with the slotted orifice. Since a "balance" in current was achieved, this suggests that losses due to misting and splashing fuel outside the collection tank were minimal for this test.

Date: April 30

Test: 54

Tests Conducted: Fuel was "dripped" onto the surface of an electrically isolated, 4 inch X 3.5-inch aluminum target plate. The resultant voltage on the target plate was recorded.

Conditions:

Nozzle: 5 hole, 0.07-inch diameter equivalent, mesh insert

Distance to Target from Orifice: 14-15 inches

Target Angle: Approx 40°, measured from horizontal

Target: 4 inch X 3.5 inch aluminum plate

Fuel Pressure: 25 psig

Fuel Bulk Temperature: 70-85°F

Fuel Conductivity: unknown, same fuel as test 53

Break up Screen: removed

Fuel: JP8+100

Target plate Capacitance: 2.5 picofarads (without charge target plate), 54 picofarads (with charge target plate)

Target plate Resistance: much greater than 1E12 ohms at 10 and 1000 volts

Results: Maximum voltage achieved was 420 volts

Comments: This "drip" test was done as an attempt to eliminate the continuous fuel flow path from the orifice to the target plate and from the target plate to the collection tank. These steady streams of fuel were thought to be resistive paths that allow charge to flow from the isolated target plate. Removal of these paths through dripping might allow for higher voltage levels to be achieved. Because dripping fuel was the charge generation source, maximum levels might take longer to achieve. The aluminum target plate was isolated during this drip test with Teflon rods. Although only 420 volts were measured in this test, several observations were made that might have limited the voltage level. First, the fuel temperature was only 70 degrees F. Temperature severely impacts charging current and hence, voltage. Second, there appeared to be a coating of fuel from the sample to the Teflon rods to ground. Using a high conductivity, low resistivity fuel could allow substantial charge drain through this fuel coating. The voltage signal line also had a substantial amount of fuel on it that also could have provided a low resistance path to ground. Third, the ambient relative humidity was high and may have impacted the accuracy of the voltage measurements made using the charge plate monitor. Its accuracy was dependent upon electrical isolation of the 6 inch X 6-inch conductive plate used to collect charge during the test process.

Date: May 2

Test: 55

000156

Tests Conducted: Measured the charge obtained using a low conductivity, clay filtered, fuel dripping onto an isolated 4 inch X 3.5-inch aluminum target plate.

Conditions:

Nozzle: glass burette
Fuel Pressure: gravity fed
Fuel Temperature: 58°F
Fuel Conductivity: 2 pS/m at 58°F
Target: 4 inch X 3.5-inch aluminum plate
Distance to Target: 15 inches
Fuel: Clay treated Jet-A

Results: No measurable charging.

Comments: Several variables were changed in this drip test that might provide insight as to why no appreciable charging was observed during testing. The fuel used in this test was extremely low in conductivity and void of many of the additives present in the fuel used for the preliminary drip test. These additives might contribute significantly to charge generation. In prior tests, low conductivity fuel provided little charge generation as compared to the 32 and 94 pS/m fuels. The temperature of the fuel was well below what appeared to be necessary for maximum charge generation (see prior testing). Dripping was done from a glass burette which may function as a charge generator to artificially charge the fuel prior to dripping. Charging of the fuel while in the glass burette could offset charging that occurred through dripping.

Date: May 2

Test: 56

Tests Conducted: Low conductivity, clay filtered fuel was sprayed onto an electrically isolated, epoxy chromate coated, aluminum target plate. Measured the maximum voltage obtained on the target plate.

Conditions:

Nozzle: 5 hole, 0.07-inch diameter equivalent
Fuel Pressure: 25 psig
Fuel Temperature: 88°F
Target: 4 inch X 3.5-inch aluminum target plate
Distance to Target from Nozzle: 14-15 inches
Target Angle: 60°, measured from horizontal
Break up Screen: not used
Fuel Conductivity: 2 pS/m at 58°F
Fuel: clay treated Jet-A

Results: The maximum voltage measured was 8 volts.

Comments: Clay filtered, low conductivity fuel appeared to be very resistive to charge generation when it contacts the target plate. Temperature again was low (88 degrees F) as compared to earlier tests (110-120 degrees F) where charge generation was greatest.

Date: May 2

Test: 57

Tests Conducted: Measured the resistance between two 1 X 2-inch conductive plates immersed in a glass beaker filled with clay filtered, low conductivity fuel.

Conditions:

Fuel Temperature: 70°F
Fuel Conductivity: 2 pS/m at 58°F
Fuel: clay treated Jet-A
Plate position/size: Parallel and facing each other, 1 X 2 X 1/16-inch (approximately)
Plate separation: 2.25 inches

Results:

~1E13 ohms at 10 volts
2.5E12 ohms at 50 volts
1.7E12 ohms at 100 volts
1.3E12 ohms at 200 volts
1.0E12 ohms at 500 volts
1.0E12 ohms at 1000 volts

Comments: The fuel resistance decreased with increased voltage potential between the conductive plates by as much as one magnitude. A resistance of 1E12 ohms was high in terms of allowing for substantial charge dissipation during the charging process. The impact of resistance would be minimal in the overall voltage achieved during charge generation testing.

Date: May 5

Test: 58

Tests Conducted: Measured the voltage obtained by using a low conductivity, clay filtered, fuel dripping onto an isolated 4 inch X 3.5 inch aluminum target plate. Corrosion inhibitor, anti-icing, and MDA additives were independently added to the fuel to evaluate their effect on the charging potential.

Conditions:

Nozzle: glass burette
Fuel Pressure: gravity feed
Fuel Temperature: 66°F
Target: 4 inch X 3.5-inch aluminum target plate
Distance to Target from Nozzle: 14-15 inches but stream breakup (into drip) approximately 4 inches above the target plate
Target Angle: 60°, measured from horizontal
Fuel Conductivity: 13 pS/m at 65°F
Fuel: clay treated Jet-A (3305) with MDA, anti-icing, or corrosion inhibitor additive added

Results: The maximum potential achieved with the clay treated Jet-A was +340 volts. The Jet-A with either MDA or corrosion inhibitor additive added had a charging potential of less than 30 volts. The maximum potential achieved when using Jet-A with DiEGME icing inhibitor added at ten times the normal concentration was +350 volts.

Comments: Clay treated Jet-A fuel with icing inhibitor showed a greater tendency to generate electrostatic charge than the Jet-A with MDA or corrosion inhibitor. Grounded aluminum foil was inserted around the burette orifice to try to neutralize the fuel upon exit from the burette and minimize any fuel tribocharging effect that might occur by flow through a glass burette. Again, fuel temperature was lower than what was measured during maximum charging conditions in prior tests.

Date: May 5

Test: 59

Tests Conducted: Repeated resistance measurements as conducted during test 57 between two 1 X 2-inch conductive plates immersed in a glass beaker filled with clay filtered fuel with various additives (corrosion

inhibitor, icing inhibitor, and MDA). Varied electrode spacing to determine impact on resistance measurements.

Conditions:

- Fuel Temperature: 65°F
- Fuel Conductivity: 2 pS/m at 58°F (from 2 May), otherwise as stated in tables below
- Fuel: clay treated JP-8
- Plate position: Parallel and facing each other, 1 X 2 X 1/16 inch (approximately)
- Plate separation: Approximately 2.0 inches

Results:

3 inch electrode spacing (approximately) (Note: MDA spacing between 2.5-2.75 inches)

Test Voltage	3305 Baseline Fuel 2 pS/m at 64.5F (OHMS)	Corrosion Inhibitor 1pS/m at 64.5F (OHMS)	Icing Inhibitor 13 pS/m at 64.5F (OHMS)	MDA 1 pS/m at 64.5F (OHMS)
10	>>1E13	>>1E13	1.5E12	>>1E13
50	3.0E12	>>1E13	4.5E11	>>1E13
100	2.0E12	>>1E13	4.2E11	>>1E13
500	1.1E12	1.5E13	3.7E11	1.0E13
1000	1.0E12	1.0E13	3.5E11	8.0E12

2inch electrode spacing (approximately)

Test Voltage	3305 Baseline Fuel 2 pS/m at 64.5F (OHMS)	Corrosion Inhibitor 1pS/m at 64.5F (OHMS)	Icing Inhibitor 13 pS/m at 64.5F (OHMS)	MDA 1 pS/m at 64.5F (OHMS)
10	>>1E13	>>1E13	9.0E11	>>1E13
50	1.5E12	>>1E13	4.0E11	>>1E13
100	1.5E12	>>1E13	3.5E11	>>1E13
500	6.0E11	1.5E13	3.0E11	1.0E13
1000	4.8E11	1.0E13	2.8E11	8.0E12

1 inch electrode spacing (approximately)

Test Voltage	3305 Baseline Fuel 2 pS/m at 64.5F (OHMS)	Corrosion Inhibitor 1pS/m at 64.5F (OHMS)	Icing Inhibitor 13 pS/m at 64.5F (OHMS)	MDA 1 pS/m at 64.5F (OHMS)
10	5.0E11	>>1E13	4.8E11	>>1E13
50	2.8E11	>>1E13	2.6E11	>>1E13
100	1.7E11	>>1E13	2.4E11	>>1E13
500	1.5E11	9.0E12	2.0E11	7.0E12
1000	1.2E11	7.0E12	1.8E11	6.5E12

Comments: All fuel samples tested showed decreased resistance as the test voltage was increased. In addition, resistance also decreased with decreases in electrode spacing. Note that the fuel with the largest tendency to charge the target plate in the prior test was that with the lowest resistance.

Date: May 6

Test: 60

Tests Conducted: Repeated resistance measurements as conducted during tests 57 and 59 between two 1 X 2 inch conductive plates immersed in a glass beaker filled with clay filtered fuel with BHT antioxidant additive. Varied electrode spacing to determine impact on resistance measurements.

Conditions:

Fuel Temperature: 86°F
Fuel Conductivity: 10 pS/m at 86°F
Fuel: clay treated Jet-A with BHT antioxidant added at 25 mg/l
Plate position: Parallel and facing each other, 1 X 2 X 1/16 inch (approximately)
Plate separation: Approximately 2.0 inches

Results:

3 inch electrode spacing (approximately)

Test Voltage	3305 Baseline Fuel 1 pS/m at 80°F (OHMS)	BHT Antioxidant 10 pS/m at 86°F (OHMS)
10	>>1E13	>>1E13
50	>>1E13	>>1E13
100	>>1E13	>>1E13
500	>>1E13	9.0E12
1000	8.0E12	7.0E12

2 inch electrode spacing (approximately)

Test Voltage	3305 Baseline Fuel 1 pS/m at 80°F (OHMS)	BHT Antioxidant 10 pS/m at 86°F (OHMS)
10	>>1E13	>>1E13
50	>>1E13	>>1E13
100	>>1E13	>>1E13
500	6.0E12	1.0E13
1000	4.5E12	8.0E12

1 inch electrode spacing (approximately)

Test Voltage	3305 Baseline Fuel 1 pS/m at 80°F (OHMS)	BHT Antioxidant 10 pS/m at 86°F (OHMS)
10	>>1E13	>>1E13
50	>>1E13	>>1E13
100	>>1E13	>>1E13
500	1.0E12*	6.0E12
1000	3.5E11*	5.0E12

*Note: Fluctuating measurement

Comments: As was found in test 59 all fuel samples that showed decreased resistance also showed increased voltage. In addition, resistance also decreased with decreased electrode spacing.

Date: May 6

Test: 61

Tests Conducted: Measured the charge obtained using a low conductivity, clay filtered, fuel dripping onto an isolated 4 inch X 3.5 inch aluminum target plate. The test was conducted with the BHT additive in the fuel to determine its effect on charging.

Conditions:

Nozzle: glass burette
Fuel Pressure: gravity feed
Fuel Temperature: 86°F
Target: 4 inch X 3.5-inch aluminum target plate
Distance to Target from Nozzle: stream breakup approximately 4 inches above the target plate
Target Angle: 60°, measured from horizontal
Fuel Conductivity: 10 pS/m at 86°F
Fuel: clay treated Jet-A with BHT additive

Results: The maximum potential achieved after five minutes was 4 volts.

Comments: The BHT additive did not show a tendency to generate charge on the target plate.

Date: May 7

Test: 62

Tests Conducted: Measured the maximum potential achieved by dripping fuel on three different targets: 1) Bare loop clamps mounted to an epoxy coated fuel tube with Teflon isolation sheeting; 2) Wiggins coupling ferrule mounted to an epoxy coated fuel tube; and 3) 4 inch X 3.5 inch aluminum target plate. The test fuel had various concentrations of Stadis-450 that produced various conductivities. Dripping was categorized in two ways, with and without streaming.

Conditions:

Nozzle: glass burette
Fuel Pressure: gravity feed
Fuel Temperature: various, as stated prior to each test
Targets: 1) Bare loop clamps mounted to an epoxy coated fuel tube with Teflon isolation sheeting;
2) Epoxy coated fuel tube, 3 ft X 1.75 inches with a Wiggins coupling ferrule mounted;
3) 4 inch X 3.5 inch aluminum target plate.
Distance to Target from Nozzle: not documented
Target Angle: 30°, measured from horizontal
Fuel Conductivity: Varied, depending on test from 27 to 360 pS/m
Fuel: Clay treated Jet-A diluted with Jet-A containing Stadis-450, added in various concentrations depending on test

Results: The initial fuel used for testing had a conductivity of 27 pS/m at 60°F. Standard drip testing onto the 4 X 3.5 inch bare aluminum target plate produced a voltage of 24 volts in 7 minutes. The same fuel dripped onto the painted portion of a 1.75 inch diameter 3 inch long fuel tube, with a Wiggins ferrule installed on the end produced a voltage of +12 volts.

The next fuel had a conductivity of 51 pS/m at 64°F. This fuel when tested on the bare 4 inch X 3.5 inch aluminum target plate produced a voltage of +38 volts with a dripping flow and + 48 volts with a near streaming flow.

Fuel with a conductivity of 74 pS/m at 64°F was then dripped onto the loop clamps using various drip rates and produced voltages that ranged from -3 to -13 volts. The same fuel was then used on the aluminum target plate and voltages between -2 and +5 volts were achieved. Target plate angle was varied to greater than 80°F but produced no appreciable change in resultant voltage.

Stadis-450 was added to the fuel to bring the conductivity up to 161 pS/m at 65°F. The fuel was dripped using a near streaming pattern onto the 4 inch X 3.5 inch aluminum target plate. The resultant voltage was +55 volts after 5 minutes. The same fuel and drip rate/pattern was then used on the painted tube end

of the Wiggins ferrule/fuel tube assembly. Using a streaming drip pattern, a maximum voltage of +68 volts was achieved after two and a half minutes.

Finally, a high conductivity fuel (360 pS/m) with water mixed in produced a maximum voltage of +67 volts after 4 minutes.

Comments: The addition of Stadis-450 to the Jet-A fuel produced a maximum voltage of +68 volts during this test sequence. As has been the case in prior days testing, fuel conductivity had an impact on the amount of charge produced. As the concentration of Stadis-450 in the fuel was increased to produce higher conductivities, the amount of charge increased for a given target. The addition of water did not have a major impact on the voltage produced.

Date: May 7

Test: 63

Tests Conducted: Determined the dry resistance and capacitance of Wiggins coupling, T7/T8, with Viton o-rings. The breakdown voltage was determined by applying a test voltage to the outer shell and monitoring current flow in the attached grounded fuel tube.

Conditions:

Capacitance: Measured at 1 kHz, 1 VRMS

Resistance: Test voltage varied

Test Surface: Plexiglas

Ambient Humidity: 21.6%

Temperature: 74.4°F

Results: Individual resistance measurements of the Viton o-rings used in Wiggins coupling T7/T8 were made first. All measurements were greater than 1E12 ohms measured at 10 volts using a 5 lb, 2 ½ inch diameter test electrode. Dry resistance and capacitance measurements were made of the assembled T7/T8 coupling. Resistance and capacitance values were made to/from the same points on the coupling as in prior dry testing using the same supply voltages and were as follows:

Female/Male Resistance: 2.1 ohms

Male Resistance to Tube: 7E11 ohms

Female Resistance to Tube: 4.5E11 ohms

Tube to Tube Resistance: 2.5E11 to 8E11 ohms (various tube orientations, fully expanded and compressed) Note that with tubes fully compressed and in contact, resistance was 5E11 ohms, indicating that the anodized layer on mating surfaces of the Wiggins coupling was at least 1E11 ohms at 10 volts.

Capacitance with both fuel tube ends grounded (expanded tubes and loose clamping force):

Female to Tube, 338 picofarads; Male to Tube, 1018 picofarads

Capacitance with both fuel tube ends grounded (expanded tubes and tight clamping force):

Female to Tube, 196 picofarads; Male to Tube, 196 picofarads

Capacitance with both fuel tube ends grounded (contacting tubes and tight clamping force):

Female to Tube, 195 picofarads; Male to Tube, 195 picofarads

Capacitance with grounded female shell only (expanded tubes): 95 picofarads (½ of prior)

Breakdown voltage testing was then conducted by applying a test voltage to the fuel tube under the female coupling shell and grounding the female shell. Voltage was applied to the fuel tube and the resultant voltage was observed on the female shell using a charge plate monitor. At +1 kV the voltage decreased to near zero. This suggested that a low resistive path had developed between the female shell and the fuel tube before any audible arc had been achieved. Resistance was measured to verify the short and it was present. The Megohmmeter was connected between the female shell and the fuel tube and various coupling orientations were tried to alleviate the short circuit. During each attempt the resistance was

measured by applying an increasing test voltage until 1000 volts was achieved at which time the power supply would be reapplied and voltages greater than 1000 volts could be applied. A short circuit continued to develop between 500 and 1000 volts for different configurations of the Wiggins coupling. Various set ups were tried to increase resistance. Clamping force was minimized, the internal locking ring was removed as well as the internal split rings and retainer ring. A resistance of 6E10 ohms was finally achieved at 1000 volts with only the o-rings, outer shells and inner fuel tubes remaining. With this configuration, breakdown voltages of between 3500 and 5700 volts were achieved. The different breakdown voltages were achieved by angling the two fuel tubes and decreasing the spacing between the end of the tube and any of the inner wall surfaces of the male or female shells. The final breakdown voltage test was done with only the retainer ring in place internally. A resultant breakdown voltage of 1250 volts was observed.

Comments: It was nearly impossible to configure the T7/T8 Wiggins coupling in such a way to produce breakdown voltage or arc externally or internally that exceeded 1000 volts. This was due to continuous contact between anodized surfaces internal to the coupling and breakdown of that anodized layer at fairly low voltage levels (less than 1000 volts). This was not readily obvious during dry testing when test voltages of 100 volts and less were used to measure resistance between these surfaces. When all internal components of the coupling had been removed, higher breakdown voltages were achieved.

Date: May 8

Test: 64

Tests Conducted Evaluated the maximum potential achievable on a painted fuel tube by dripping Jet-A fuel with Stadis-450 added.

Conditions:

Nozzle: glass burette

Fuel Pressure: gravity feed

Fuel Temperature: 62°F

Distance to Target from Nozzle: 8 inches

Target: Painted fuel tube, 3 ft X 1.75 inches with Wiggins coupling ferrule mounted on one end

Fuel Conductivity: 160 pS/m at 62°F

Fuel: Jet-A with Stadis-450 additive added to bring the conductivity to approximately 150 pS/m at room temperature.

Results: The potential varied between -2 and +1 volts,

Comments: Fuel temperature and Stadis-450 additive contributed to the minimal charge generation observed. Stadis-450 on prior days testing produced approximately 60 volts. Any residues from other fuels from prior tests on the target surface could have interacted with the new fuel and impacted the charge generation process.

Date: May 8

Test: 65

Tests Conducted: Evaluated the effect of aging clay treated fuel on the maximum potential achievable by dripping the fuel onto a painted fuel tube.

Conditions:

Nozzle: glass burette

Fuel Pressure: gravity feed

Fuel Temperature: 65°F

Distance to Target from Nozzle: 8 inches

Target: Painted fuel tube, 3 ft X 1.75 inches with Wiggins coupling ferrule mounted on one end

Fuel Conductivity: 2 pS/m at 65°F
Fuel: Clay treated Jet-A that has been aged for two weeks,

Results: The potential as a result of a slow drip was -6 volts. Increasing the flow to a slow stream resulted in a potential of +3 volts.

Comments: Similar results were observed during this test as those on May 2 (test 55) using clay treated Jet-A on a 4 X 3.5 inch target plate. Charging was minimal when the conductivity was low.

Date: May 8

Test: 66

Tests Conducted: Evaluated the effect of anti-icing additive on the maximum potential achievable by dripping the fuel onto a painted fuel tube.

Conditions:

Nozzle: glass burette
Fuel Pressure: gravity feed
Distance to Target from Nozzle: 8 inches
Target: Painted fuel tube, 3 ft X 1.75 inches with Wiggins coupling ferrule mounted on one end
Fuel: Jet-A treated with anti-icing inhibitor
Fuel Temperature: Not recorded
Fuel Conductivity: Not recorded

Results: Using a streaming drip pattern, the potential after 2 minutes was +30 volts, after 3 minutes the potential was +34 volts.

Comments: Anti-icing inhibitor from prior testing increased the overall fuel conductivity and showed a greater tendency to charge. Although the magnitude of charge was less than prior testing on the 4 X 3.5-inch aluminum target plate, measurable voltages were observed.

Date: May 8

Test: 67

Tests Conducted: Evaluated the effect of clay treated fuel with Stadis-450 by spraying through a slotted orifice onto a fuel tube with a Wiggins coupling ferrule mounted on one end.

Conditions:

Nozzle: 0.086 X 0.640-inch slot, 0.055 square inch open area
Fuel Pressure: 35 and 25 psig
Distance to Target: 24 inches
Target: Painted fuel tube, 3 ft X 1.75 inches with Wiggins coupling ferrule mounted on one end
Fuel Temperature: 84°F
Fuel Conductivity: 50 pS/m at 84°F
Fuel: Clay treated Jet-A treated with Stadis-450

Results: At 35 psig the potential was -113 volts, at 25 psig the potential fell to -10 volts.

Comments: Fuel flow rate influenced the magnitude of voltage seen during charge generation testing. This effect was observed during prior phase I testing. As stated prior, the target must be clean and free from impurities or residues from prior tests. These residues may influence the charge generation process and minimize charge levels observed. High internal humidity was also observed in the test chamber (21 %) which can also influence the charging process.

Date: May 8

Test: 68

Test Conducted: Wiggins coupling T7/T8 was retested for breakdown voltage with both Viton and Teflon o-rings installed. The supply voltage was applied between the outer female housing (shell) to the inner fuel tube (T7).

Conditions:

Coupling Capacitance (from T7 tube to female shell): 77 picofarads (with Viton o-rings), 36 picofarads (with Teflon o-rings)

Test Surface: Plexiglas

Results: Internal arcing was observed at +1080 volts when the Viton o-rings were installed in Wiggins coupling T7/T8. When Teflon o-rings were installed, the breakdown occurred between 500 and 1000 volts using the Megohmmeter as the power supply.

Comments: As observed earlier, the inner surfaces of the Wiggins coupling nearly always contact one another. The anodized coating on these inner surfaces was voltage sensitive and breaks down between 500 and 1000 volts. This occurred in both tests during this sequence.

Date: May 9

Test: 69

Tests Conducted: Used fuel similar in conductivity to fuel used in prior testing to achieve maximum charging (April 11, Test 44). The fuel was sprayed onto a loop clamp isolated with Teflon cushioning. This test was done to produce maximum voltage on aircraft hardware (loop clamp) using the most favorable conditions found throughout Phase I and 11 tests.

Conditions:

Nozzle: 0.086 X 0.640-inch slot, 0.055 square inch open area, mesh insert

Fuel Pressure: 25 psig

Distance to Target: 24 inches

Target: Teflon cushioned clamp on a chromate coated aluminum fuel tube

Fuel Temperature: 118°F and 1000 volts

Clamp Resistance: greater than 1E12 ohms at 10 volts

Capacitance (clamp, wiring, charge plate monitor): 85 picofarads

Internal Test Chamber Humidity: Start, 25%, Finish, 3.7%

Fuel Conductivity: Varied between 24 and 30 pS/m at 102°F

Fuel: Clay treated Jet-A treated with Stadis-450

Fuel Resistance (with 1 X 2 inch electrodes): 6E11 ohms at 10 volts

Results: The resultant voltage observed after 5 minutes of fuel flow was +34 volts.

Comments: The resultant voltage was substantially lower than that achieved with comparable fuel earlier in Phase II. Several variables that have been explained throughout this report may have contributed to the lower voltage levels. One may be the lower resistive fuel and wet clamp/Teflon/tube interface that would provide for charge dissipation through that junction to ground. The measured resistance of 6E11 ohms would provide a sufficient y low resistive path for charge to flow. Second, slightly elevated moisture content in the test chamber may have contributed to lower charging levels. The test chamber may not have been pressurized or sealed adequately to ensure that the nitrogen purge was sufficient to keep out moisture. Clamp positioning may have influenced the charging process also. Finally, even though the fuel conductivity was similar to the prior tests, it was not the same base fuel and other properties of the fuel were different. Other factors such as impurities, including additives, in the fuel or molecular structure may be altered when dynamically moved through the fuel lines as opposed to the static condition

under which the conductivity was measured.

Analysis of Hot Stamped Wiring
(Failure Analysis)

27 October 1997

Evaluation Report
(43491HRD/NTSB)

Report No. WL/MLS 97-101

AUTHOR

George A. Slenski
Materials Integrity Branch (WL/MLSA)
2179 12th Street
Wright-Patterson Air Force Base, Ohio 45433-7718

REQUESTER

Robert L. Swaim
National Transportation Safety Board
490 L'Enfant Plaza, East SW
Washington DC 20594

DISTRIBUTION STATEMENT F: Further dissemination only as directed
by National Transportation Safety Board (NTSB) (27 October 1997)
or DoD higher authority.

000167

ACKNOWLEDGMENTS

As is usual for this type of investigation the efforts of others are critical to its success. The author would like to thank Mr. John Ziegenhagen and Mr. Richard Reibel of the University of Dayton Research Institute for expert photography.

TABLE OF CONTENTS

	Page
LISTOFFIGURES.	iv
PURPOSE.	1
FACTUAL DATA	1
SUMMARY OF FINDINGS.	2

LIST OF FIGURES

Figure		Page
1	Scavenge pump relay with connector wiring attached.	4
2	Typical example of hot stamp markings on relay connector wiring. Note depth penetration of the mark. A close-up of the seven mark is shown at the top.	4
3	Note the lack of hot stamp penetration into the insulation of the top wire sample. This was stamped using a current generation machine.	5
4	Crack found to propagate from a hot stamp mark. Optical inspection revealed the conductor was exposed.	5
5	Cross section of the wire showing three layer construction and depth penetration of the hot stamp mark. Note thickness of layers and total thickness at bottom right. Considerable thickness variability was noted in the inner white layer. Also note deformation in the inner layer at the mark sites.	
6	Perpendicular cross section showing depth penetration of the hot stamp marks. Note that all three insulation layers were penetrated (0.07 mm insulation was remaining at the mark site) and the inner white layer was deformed by the stamping process.	7
7	Lateral cross section showing multiple hot stamp sites. Note variability of depth penetration from right to left. Also note close-up of upper left mark showing that the mark penetrated all three insulation layers .	

Figure		Page
8	Lateral cross section of a different wire than from Figure 9. Again note depth variability of the mark from right to left. The inset image shows a close-up of a single mark site. Note all three insulation layers were again penetrated.	9
9	FTIR spectrum of the outer white insulation layer	10
10	FTIR spectrum of the middle amber or brown insulation layer.	10
11	FTIR spectrum of the inner white insulation layer.	11

Analysis of Hot Stamped Wiring

PURPOSE

Examine submitted wire for electrical or mechanical damage.

FACTUAL DATA

The National Transportation Safety Board (NTSB) requested analysis of a scavenge pump relay with an attached connector and wire bundle removed from 747 aircraft N93119 wreckage (Figure 1) . Submitted hardware was removed from the ocean and had been identified, inspected, and tagged by investigators. Findings concerning the relay are given in evaluation report WL/MLS 97-86. The connector wiring portion was inspected and the wire markings had deeply penetrated the insulation (Figure 2) . These marks were consistent with a hot stamp marking process. For comparison purposes a hot stamp marked wire in 1997 is shown next to a relay wire in Figure 3.

The relay wiring was reported to be 20-gauge BMS 1342A (Poly-X) insulation. Two markings were noted. One was marked using ink and consistent on all wires (w42/1/1/20) . The other was hot stamped and different for each wire (as an example: W 74-Q-06) . In at least one location, a crack was noted in a hot stamp mark (Figure 4) . Inspection with an optical microscope revealed the conductor was exposed. Exposed conductors were always associated with a crack. There was no evidence of arc tracking or thermal degradation from sustained current flow.

Sections of four wires were removed from the relay connector and cross sectioned to ascertain the depth of the hot stamp marks . Perpendicular and lateral cross sections are shown in Figures 5, 6, 7, and 8. The multiple insulation layers can be seen clearly in Figures 5 and 6. Three wrapped layers (white, amber, and semitransparent) were noted. An average thickness of each layer is given in Figure 5. The average total insulation thickness was 201 urn (Figure 5) . Considerable thickness variability was noted in the inner white layer (Figures 5 and 6) . Also note deformation in the inner layer at the mark sites in Figures 5 and 6. The insulation thickness was significantly reduced in the marked areas (Figures 5 and 6) .

Figures 7 and 8 show the uneven mark depth in the lateral cross sections and penetration into the inner layer insulation in close-up areas. The minimum insulation thickness found in a marked area was 28 urn (1.1 mils) as shown in Figures 7 and 8.

Each layer was chemically identified using FTIR. The outer white and inner white, semitransparent layers were nearly identical and the spectra most closely matched references for polyimide materials based on pyromellitic anhydride and an

aliphatic diamine. The FTIR spectra for the middle amber layer most closely matched references for polyimide materials based on pyromellitic anhydride and diaminodiphenyl ether. A spectrum for each layer is given in Figures 9, 10, and 11) .

SUMMARY OF FINDINGS

In many areas the hot stamp marking process penetrated all three layers of wire insulation.

There was considerable variability in the depth penetration of the hot stamp marks.

Cracks initiated from several hot stamp marks.

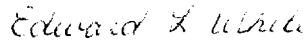
The mark sites did not exhibit any arc tracking or propagation damage typically associated with sustained current flow.

PREPARED BY



GEORGE A. SLENSKI
Structural Failure Analysis
Materials Integrity Branch
System Support Division
Materials Directorate

REVIEWED BY



EDWARD L. WHITE, Actg Team Lead
Electronic Failure Analysis
Materials Integrity Branch
Systems Support Division
Materials Directorate

PUBLICATION REVIEW: This report has been reviewed and approved.



FOR
GEORGE A. SLENSKI, Actg Branch Chief
Materials Integrity Branch
Systems Support Division
Materials Directorate

000174

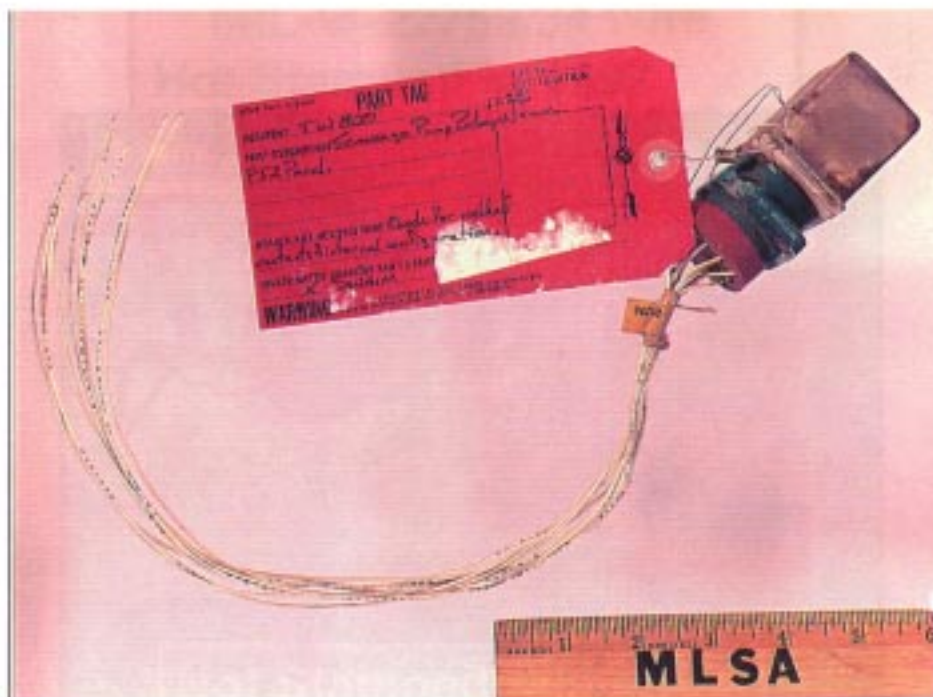


Figure 1. Scavenge pump relay with connector wiring attached.

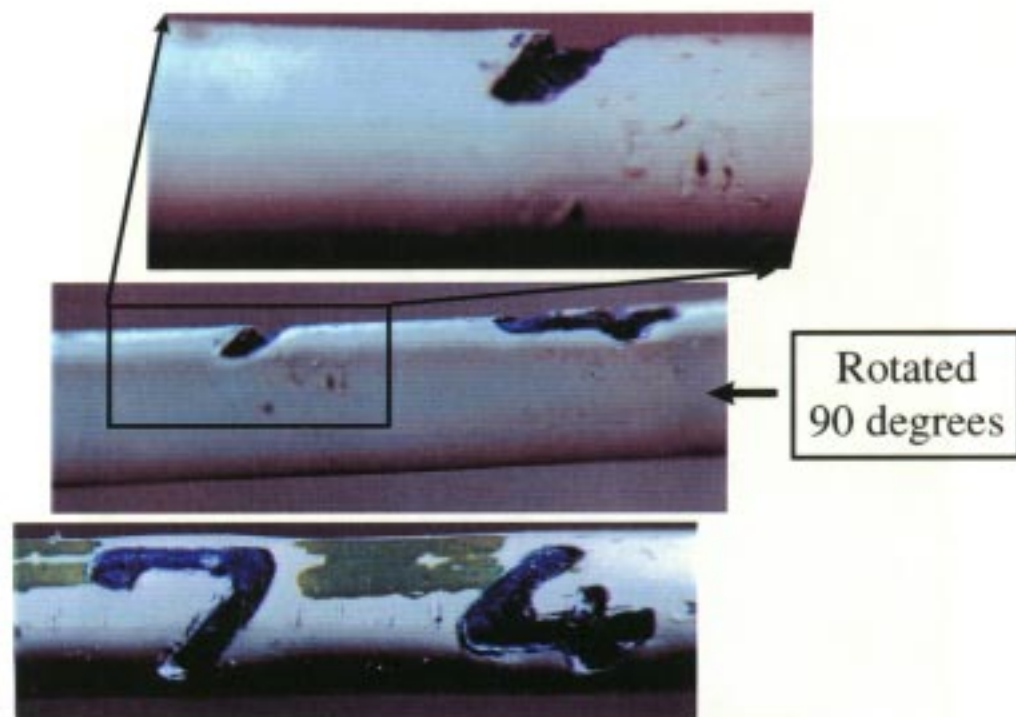


Figure 2. Typical example of hot stamp markings on relay connector wiring. Note depth penetration of the mark. A close-up of the seven mark is shown at the top.

Mag: 17X

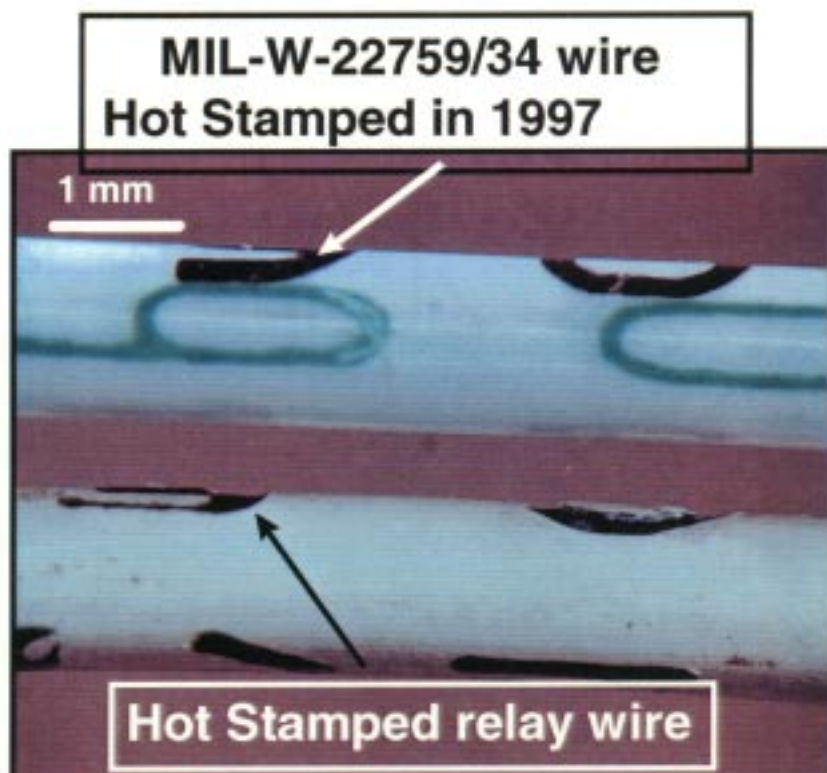


Figure 3. Note the lack of hot stamp penetration into the insulation of the top wire sample. This was stamped using a current generation machine.

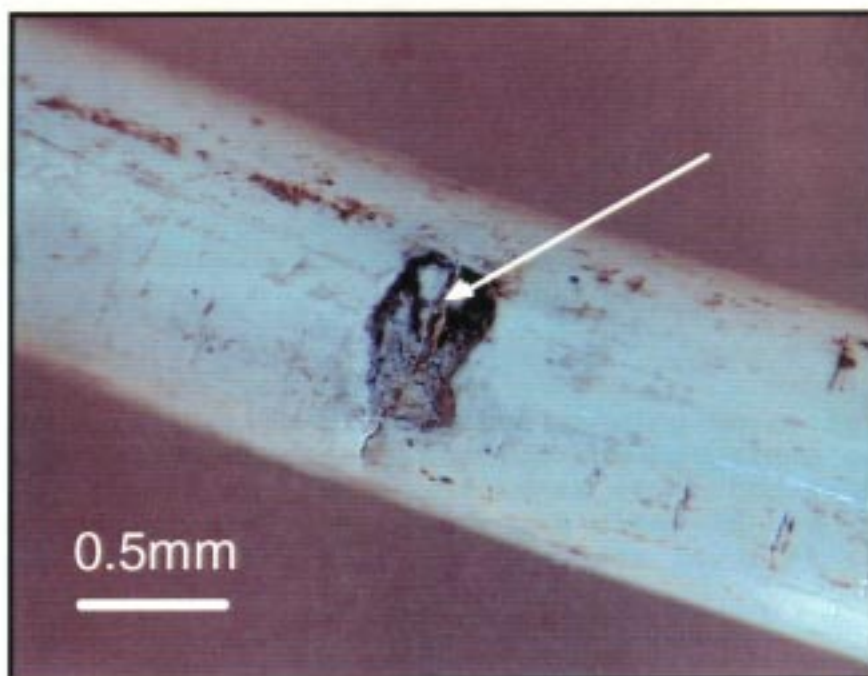


Figure 4. Crack found to propagate from a hot stamp mark. Optical inspection revealed the conductor was exposed.

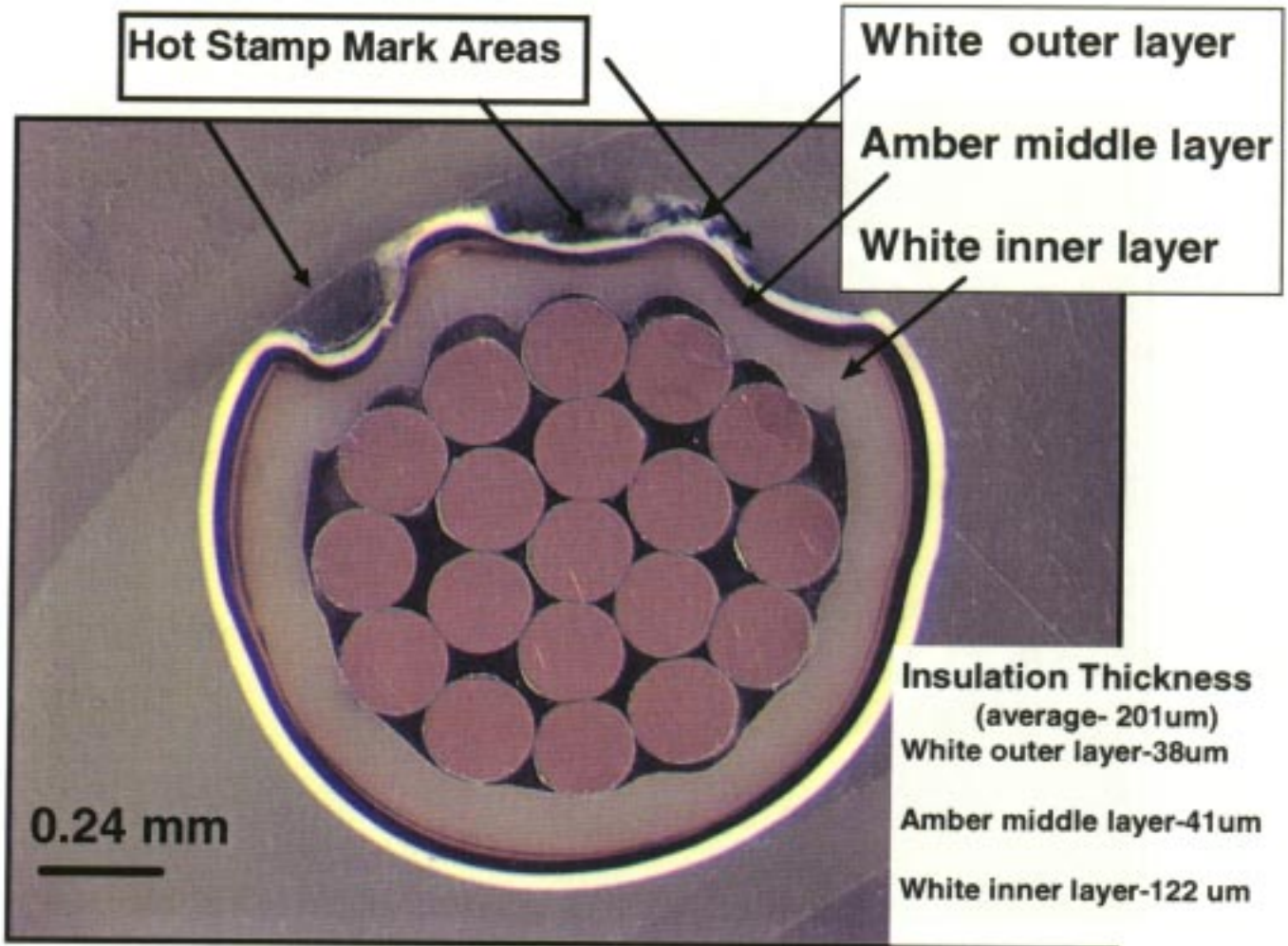


Figure 5. Cross section of the wire showing three layer construction and depth penetration of the hot stamp mark. Note thickness of layers and total thickness at bottom right. Considerable thickness variability was noted in the inner white layer. Also note deformation in the inner layer at the mark sites.

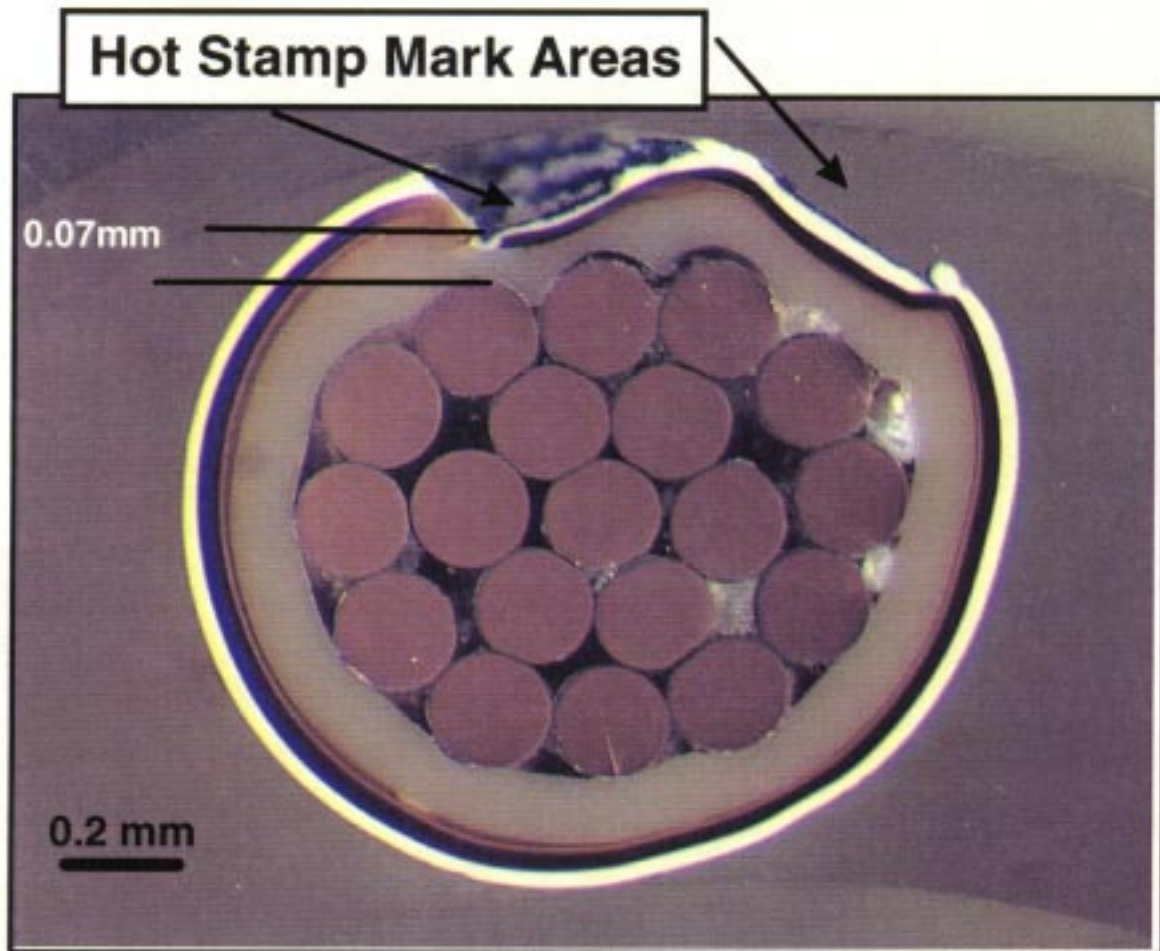


Figure 6. Perpendicular cross section showing depth penetration of the hot stamp marks. Note that all three insulation layers were penetrated (0.07 mm insulation was remaining at the mark site) and the inner white layer was deformed by the stamping process.

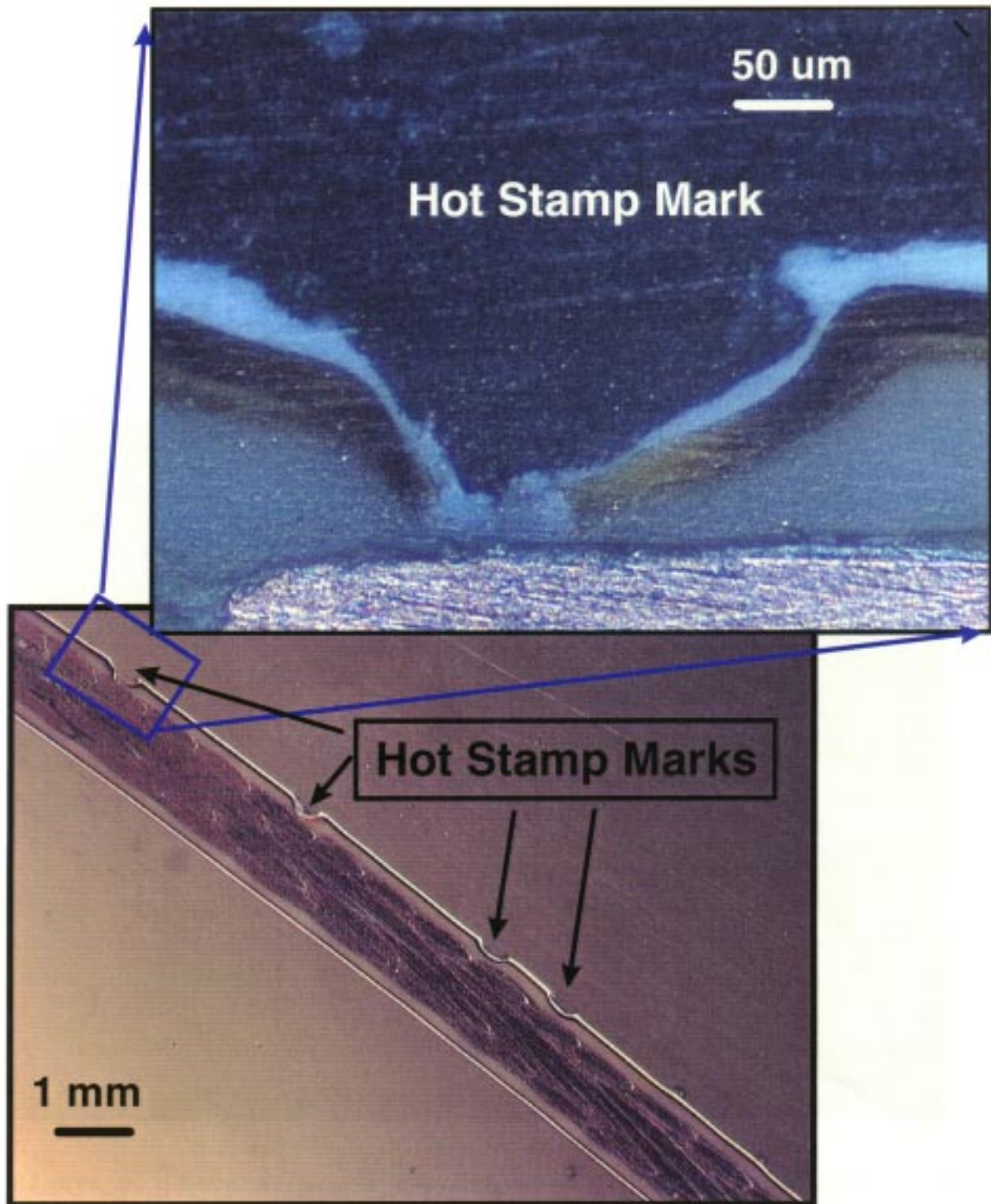


Figure 7. Lateral cross section showing multiple hot stamp sites. Note variability of depth penetration from right to left. Also note close-up of upper left mark showing that the mark penetrated all three insulation layers.

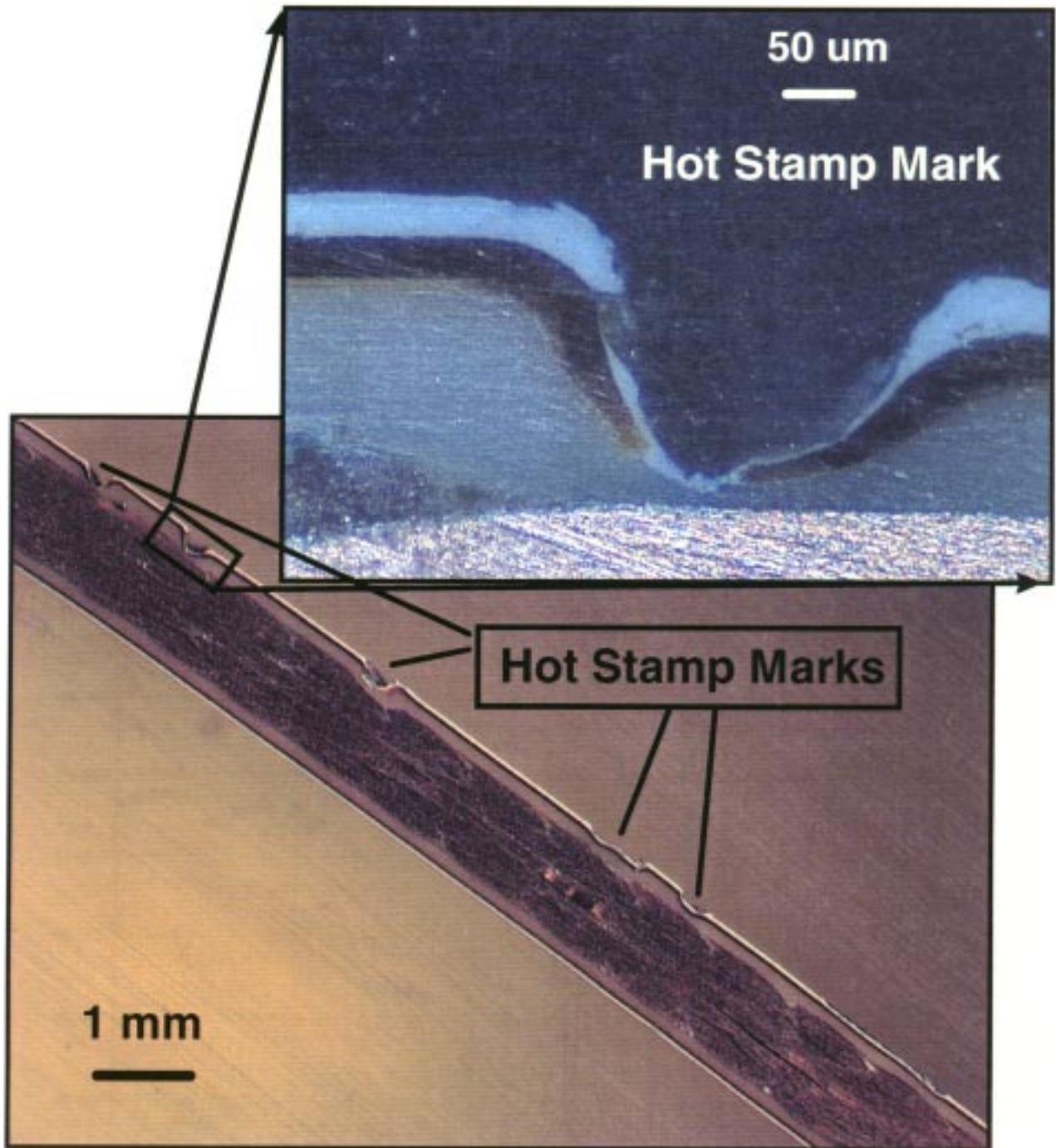


Figure 8. Lateral cross section of a different wire than from Figure 7. Again note depth variability of the mark from right to left. The inset image shows a close-up of a single mark site. Note all three insulation layers were again penetrated.

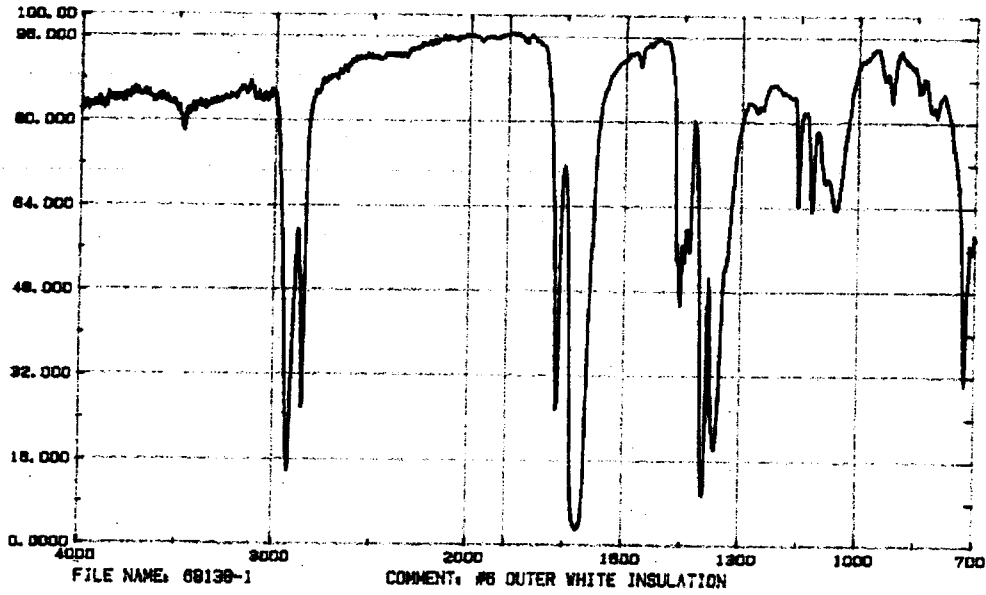


Figure 9. FTIR spectrum of the outer white insulation layer

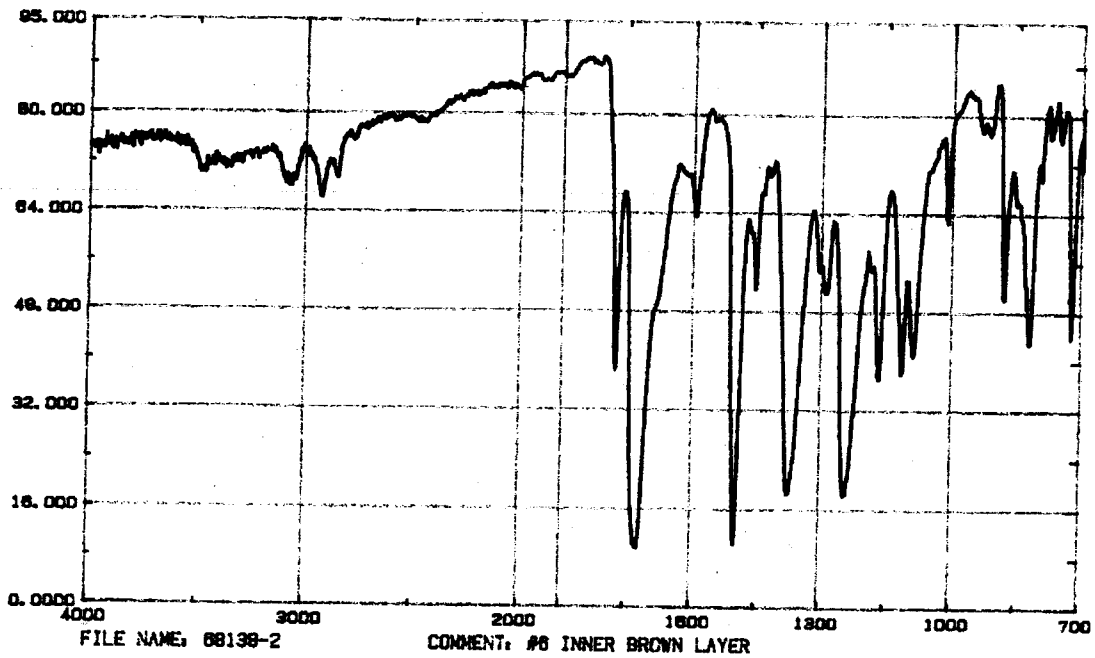


Figure 10. FTIR spectrum of the middle amber or brown insulation layer.

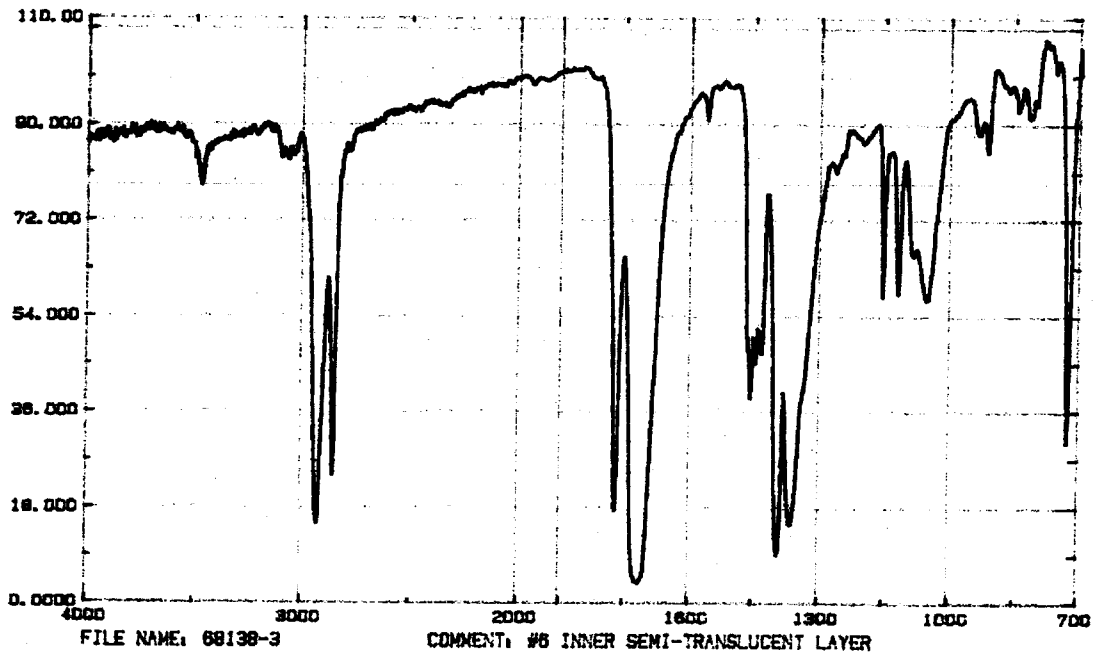


Figure 11. FTIR spectrum of the inner white insulation layer.

pages 183 - 339

were not available at time of printing